Feb 2008

Thesis for the
Doctor of Philosophy Award of a Research Degree
from University College London

Gee Wan Wong

The effects of prostate cancer-related Plexin-B1 mutations on protein function

Prostate Cancer Research Centre (PCRC)
University College London (UCL)
Professor John Masters, professor of experimental pathology
Dr Magali Williamson*, Ph.D

PCRC - UCL
Institute of Urology and Nephrology
67 Riding House Street
London W1W7EJ
00442076799597*

ProQuest LLC
789 East Eisenhower Parkway
P.O. Box 1346
Ann Arbor, MI 48106-1346

To Dad

Acknowledgement

I wish to thank University College London, Professor John Masters and Dr. Magali Williamson for funding, allowing and supervising the presented research work and for their support during the completion of the following thesis.

I would also like to thank my mother, brothers and my wife for their continueous support on my study.

And to Dr. Tharani Nitkunan, Dr. Izumi Oinuma, Miss Chun Zhou, Dr. Qin Wang, and Dr. Veronique Blanc, thank you, since you provided me with much desired and valuable friendships during my study.

Declaration that the work presented in this thesis is my own

I, Gee Wan Wong, confirm that the work presented in this thesis is my own. Where information has been derived from other sources, I confirm that this has been indicated in the thesis

---

Abstract

Semaphorin/Plexin signalling pathways modulate many biological processes such as neuronal axon pathfinding, angiogenesis, organogenesis, immune response, and cell migration. Given the fact that Semaphorins/Plexins have a strong influence on cytoskeleton structure through their interactions with receptor tyrosine kinases (RTKs) and Rho-like small GTPases, it has been suggested that they may also have a role in tumourigenesis. Recently we have identified a number of mutations in the gene *PLXNB1* which encodes the Sema4D receptor protein Plexin-B1 that are associated with prostate cancer metastasis. This study aims at elucidating the effects of three of the identified mutations in *PLXNB1*, A5359G (amino acid change: T1697A), A5653G (T1795A) and T5714C (L1815P). None of the mutations affected the Sema4D and PDZ-RhoGEF binding function of Plexin-B1 in coimmunoprecipitation assays. In addition, no influence on the Rho regulation function of Plexin-B1 from the mutations could be detected. However by GST-pull down assays we found that Plexin-B1LT5714C was defective in binding RacL61, a constitutively active Rac mutant. This Rac binding defect renders Plexin-B1T5714C unresponsive to the cell surface trafficking effect of RacL61. Moreover, Plexin-B1T5714C failed to sequester and inhibit Rac-GTP as evident from the fact that it could neither inhibit RacL61 mediated Pak phosphorylation nor inhibit the cell spreading process mediated by RacL61. Our results suggest that the prostate cancer related *PLXNB1* mutation T5714C has important effects on the functioning of Plexin-B1 by disrupting the interaction of Plexin-B1 with Rac.

List of figures

Chapter 1

Introduction

The invasion and metastasis of tumour cells is the major cause of death due to cancer. It represents dysregulation of a physiological programme for organ development, regeneration and maintenance. Cancer cells must be detached from adjacent cells; migrate among other cells (stromal cells for example) and break through the basement membrane in order to get into the circulation. At the distant site, cancer cells must be able to resist the apoptosis signals imposed on them by the environment and proliferate. These events are collectively known as the metastasis cascade. (Chambers et al., 2002). Metastasis results in greatly increased tumour burden in cancer patients and is the primary cause of death. Therefore, it is desirable to understand the process of metastasis at molecular level, so that better therapies can be developed to combat cancers.

Cell migration contributes significantly to the process of metastasis. Directional cell movement is largely controlled by extracellular signalling molecules. Semaphorins are one class of such molecules which take important roles in controlling cell migration. Semaphorins are secreted or transmembrane signalling molecules originally identified as axonal growth cues. In recent years, many more physiological functions for semaphorins have been discoveried. For instance, semaphorins are involved in phenomena as diverse as viral immunity to organogenesis (Section 1.1). From these various roles of semaphorins it is now clear that a majority of functions of semaphorins can be accounted for by their ability to either inhibit or induce directional cell motility.

Certain members of the semaphorin family have been implicated in cancer and its progression (Section 1.1.6). Likewise, some components of semaphorin signalling pathways have been associated with cancer progression as well. For example, Neuropilin-1, a co-receptor for some class 3 semaphorins, is

overexpressed in prostate cancer and promotes tumour angiogenesis and progression (Qi et al., 2003; Miao et al., 2000). We hypothesized that the function of the semaphoring signalling pathway in the control of cell migration could be harnessed by cancer cells during invasion and metastasis. In view of this, we investigated the possible involvement of other semaphorin signalling components in cancer metastasis by screening prostate cancer cell lines for mutations in the cytoplasmic domain of Plexin-A1, A3 and B1 (Wong et al., 2007). Plexins are single pass transmembrane receptors for semaphorins (Tamagnone et al., 1999). Plexins can be grouped into 4 subfamilies according to domain structure: Plexin-A, B, C, and D. They are functionally linked to various Rho-like small GTPases, which are key regulators of cell motility (Section 1.3). A missense mutation (A5359G) in the cytoplasmic domain of Plexin-B1 was found in LNCaP. Thirteen more mutations were found by SSCP analysis of the *PLXNB1* gene exons 22-29 in DNA microdissected from tumor tissue. The DNA we analysed came from 89 primary cancer samples, 9 bone metastases and 17 bone mestastases. Mutations were more frequent in prostate cancer metastasis then in primary tumors (Wong et al., 2007).

The aim of this project is to study the effects of the three most common mutations in the *PLXNB1* gene on the functions of the Plexin-B1 protein. The three mutations chosen for this study were A5359G, A5653G, and T5714C (with reference to Genebank sequence X87904). A5359G was the mutation found in LNCaP and causes a Thr1697Ala mutation in the Plexin-B1 protein. It is found in the prostate cancer cell line LNCaP. A5653G mutation causes a Thr to Ala mutation at position 1795 of the Plexin-B1 protein. A5653G was found in 9 of 26 (35%) metastases and 38 of 89 (43%) primary cancers. This mutation is predicted

to result in the loss of a conserved predicted serine/threonine kinase phosphorylation site. T5714C was found in three metastases and in two primary tumors and causes a Leu to Proline mutation at aa 1815 of Plexin-B1. Interestingly, all three of these mutations affect amino acid residues that are located within the putation Rac binding (Cdc42 Rac Interactive binding, CRIB) motif of Plexin-B1 (figure 1.1). The NMR structure of the Rac binding domain has recently been solved (Tong et al., 2008), and it was suggested that residue L1815 is on the GTPase interacting interface of Plexin-B1, hinting the importance of this residue (figure 1.2).

In the following sections, some general aspects about prostate cancer will be discussed. Then an overview of semaphorin functions in various physiological or pathological systems will be given. Following that a discussion of Semaphorin 4D (Sema4D) structure and function will be given. The intracellular signalling machinery associated with Plexin-B1 will be described in the last section of this chapter.

1.1 Prostate and prostate cancer

1.1.1 Anatomy and function of human prostate

The prostate is a gland in males that surrounds the neck of the bladder and the urethra. It is situated in the pelvic cavity behind the lower part of the pubic symphysis, above the deep layer of the triangular ligament, and rests upon the rectum (Figure 1.3A). The main function of the prostate is to produce seminal fluid.

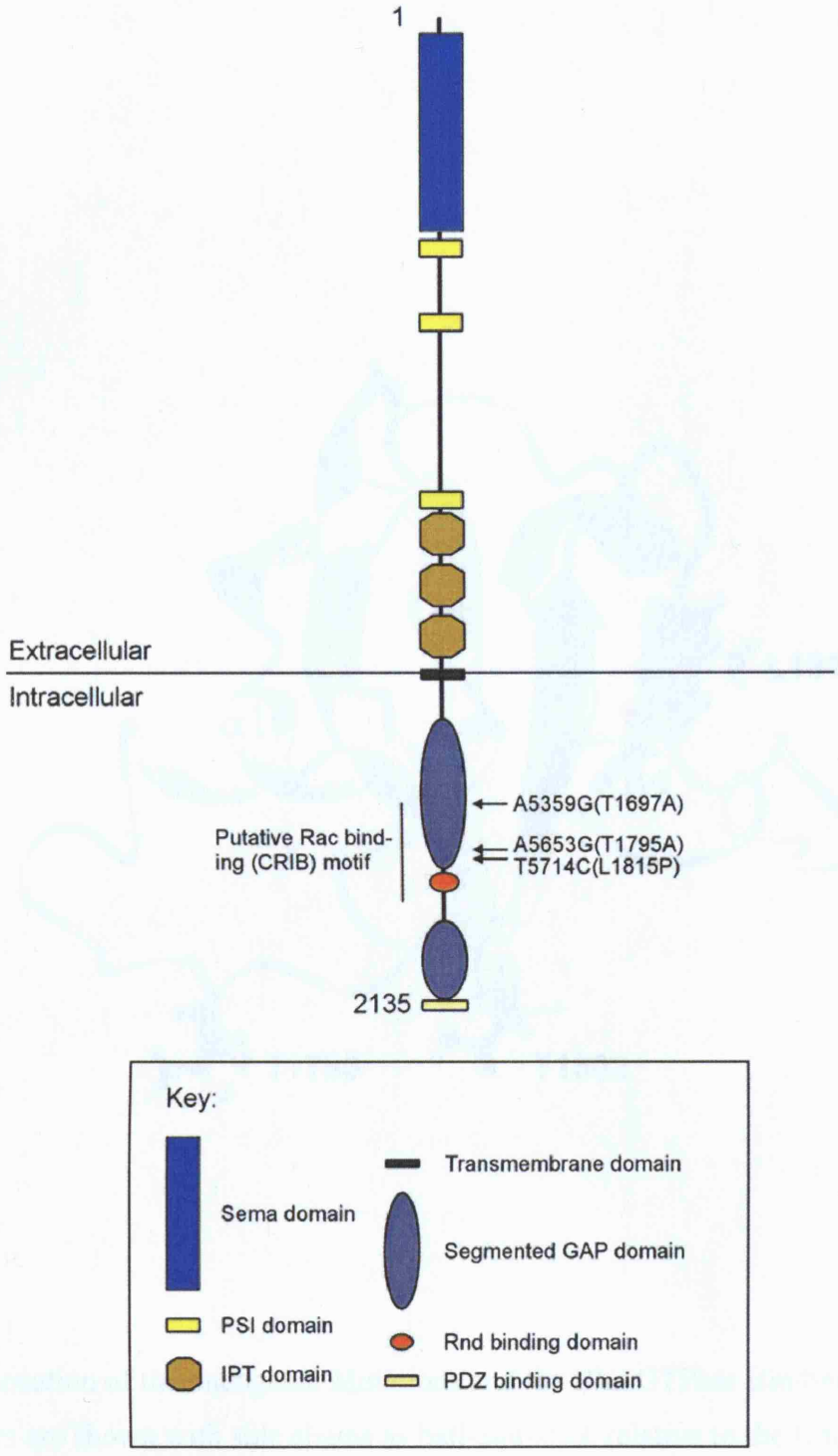

Figure 1.1 Domain structure of Plexin-B1 and the locations of mutations studied in this thesis. The domains were annotated according to the feature descriptions of RefSeq NP_002664 plexin B1 [Homo sapiens]. Reports about the Cdc42/Rac Interactive Binding (CRIB) motif mapped it to aa 1696-1910 (Vikis et al., 2000).

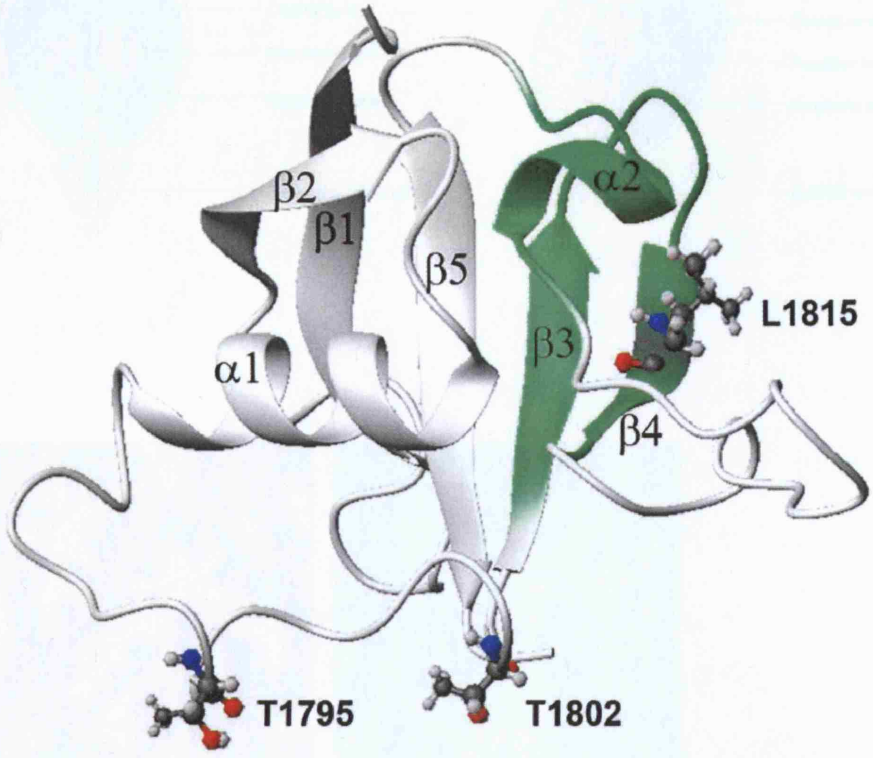

Figure 1.2. Location of the oncogenic Mutations and the Rho GTPase Binding Region. Mutation sites are shown with side chains as ball-and-stick relative to the Rho GTPase binding interface as determined by NMR (Tong et al., 2007). Two plexin Rho GTPase association motifs (PRAMs), residues 1805–1817 and 1834–1841, colored green, are brought together by the tertiary fold. Adapted from Tong et al., 2008.

A

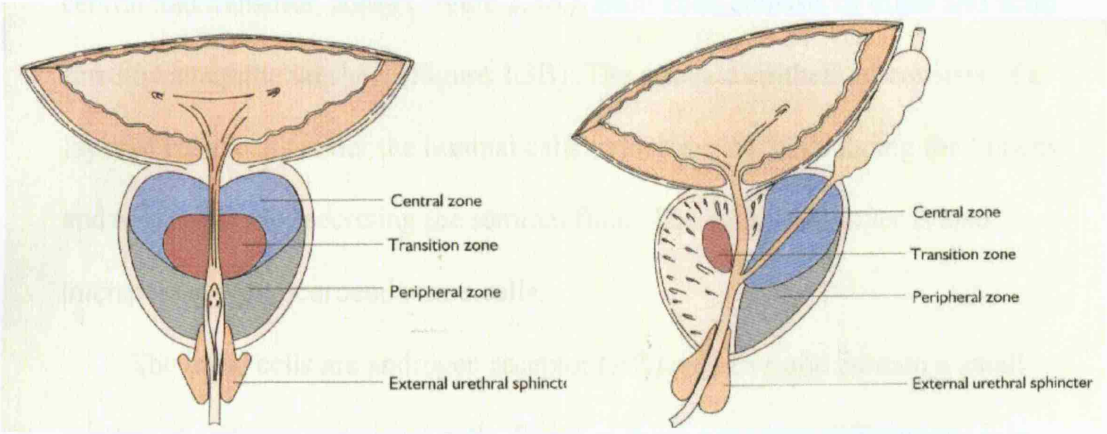

B

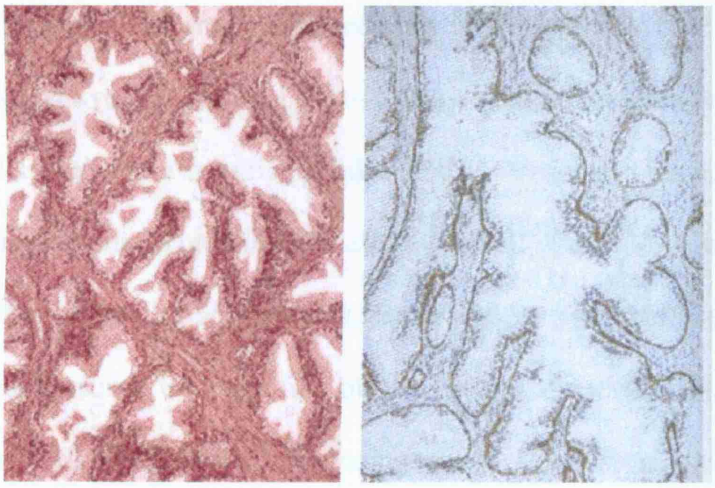

Figure 1.3 Anatomical and histological structure of the human prostate gland. (A) The prostate is situated in the pelvic cavity behind the lower part of the pubic symphysis, and surrounds the neck of the bladder and the urethra. It is divided into three zones: the peripheral zone (PZ), the transition zone (TZ), and the central zone (CZ). Left: anterior view. Right: sagittal view. (B) Paraffin section of the prostate showing the acini are lined with epithelial cells (left). The basal cell layer is more easily seen by immunohistochemical staining with anti-LP34 against cytokeratins of high molecular weight (right). Adapted from Kirby 2002.

Histologically, the prostate gland is divided into three zones: the peripheral, central and transition zones (Figure 1.3A). Each zone consists of ducts and acini lined by an epithelial sheet (Figure 1.3B). The prostate epithelium consists of a layer of basal cells under the luminal cells, which are the cells facing the lumens and responsible for secreting the seminal fluid. The basal cells layer is also interspersed with neuroendocrine cells.

The basal cells are androgen receptor (AR) negative and contain a small number of self-renewing stem cells. Some of these cells may differentiate into transit amplifying (TA) cells which are also AR negative. These TA cells divide, partially differentiate, and migrate from the basal to the luminal layer where they differentiate to form mature, secretory luminal cells that are nonproliferative and AR positive (Uzgare et al., 2004). Some cells differentiate into neuroendocrine cells that secrete specific peptides (e.g. bombesin, calcitonin, para-thyroid hormone related protein) (Arnold and Isaacs, 2002). The prostatic epithelium is surrounded by a fibromuscular stroma which mainly consists of AR-positive smooth muscle cells and fibroblasts. There is a basement membrane separating the basal cell layer and the surrounding stroma. These stromal cells take important roles in prostate development and maintenance by producing and secreting paracrine growth and survival factors for the epithelium in response to androgens. These andromedins diffuse into the epithelium where they bind to receptors on TA cells and regulate their survival and proliferation. Androgens stimulate the differentiation of luminal cells and regulate their production of secretory proteins such as PSA (prostate specific antigen).

1.1.2 Prostate cancer

Prostate cancer is the sixth most frequently diagnosed cancer in the world, the third most common cancer in men worldwide and the most common cancer in men in Europe, North America and some parts of Africa. In 2000, the number of new cases was 513,000 worldwide. The incidence of prostate cancer is steadily increasing, yet little is known about what causes this increase. It has been suggested that the increased use of PSA screening has increased the number of cases detected. Nevertheless there are several established risk factors for prostate cancer: age, ethnic origin, family history and IGF level. Dietary factors like lycopene, selenium and vitamin E may also play important roles (Gronberg, 2003).

The three zones of the prostate have different tendency to develop cancer, as evident from the fact that most cancers develop in the peripheral zone (68%). Less cases are from the transitional zone (24%) and even less in the central zone (8%) (McNeal et al., 1988). This difference in tendency to develop cancer may be due to their different phylogenetic origins. In primates, the gland is divided into two anatomically separated glands, the cranial prostate and the caudal prostate. They are fused in human to create a single gland but the different zonal pathological tendencies underscore their disparate origins (Kirby 2002).

1.1.2.1 Prostate carcinogenesis

The etiological agents that cause prostate cancer remain unknown. But it is believed that oxidative damage, dietary & environmental insults may lead to regenerative responses in the prostate epithelium which precede the development of prostate intraepithelial neoplasia (PIN). One of the possible causes of these

regenerative lesions, collectively referred as proliferative inflammatory atrophy (PIA), is heterocyclic amines (HCAs) generated from cooking red meats at high temperature (De Marzo et al., 2007). A current model of prostate cancer progression is shown in Figure 1.4. PIA may develop into prostatic intraepithelial neoplasia (PIN) if further genetics changes occur. High grade PIN is regarded as the precursor lesion of invasive adenocarcinoma (Gonzalgo and Isaacs, 2003).

1.1.2.2 Risk factors

The risk of prostate cancer increases with age. Prostate cancer is very rarely diagnosed in people aged younger than 50 years (<0.1% of all patients). The mean age of patients with prostate cancer is 72-74 years, and 85% of patients are diagnosed after age 65 years (Gronberg, 2003). However, with screening for prostate specific antigen (PSA) in recent years, asymptomatic, latent prostate cancer is actually more prevalent. For instance, in an autopsy study carried in Detroit, MI, USA on 600 men the rate of latent prostate cancer was high at all ages: 30% for men in their 30s, 50% for men in their 50s, and more than 75% for men older than 85 years (Sakr et al., 1993).

The incidence of prostate cancer varies widely between ethnic groups and countries. It is most prevalent in western developed regions like North America and Europe. The lowest rates are usually in Asia, especially Chinese people in Tianjin, China. The difference between ethnic groups can be accounted for by the differences in genetic susceptibility, exposure to unknown external risk factors or artificial reasons such as cancer registration and differences to health care. When Japanese people move from Japan (a country with low incidence) to the USA (high incidence), incidence of prostate cancer in the Japanese population

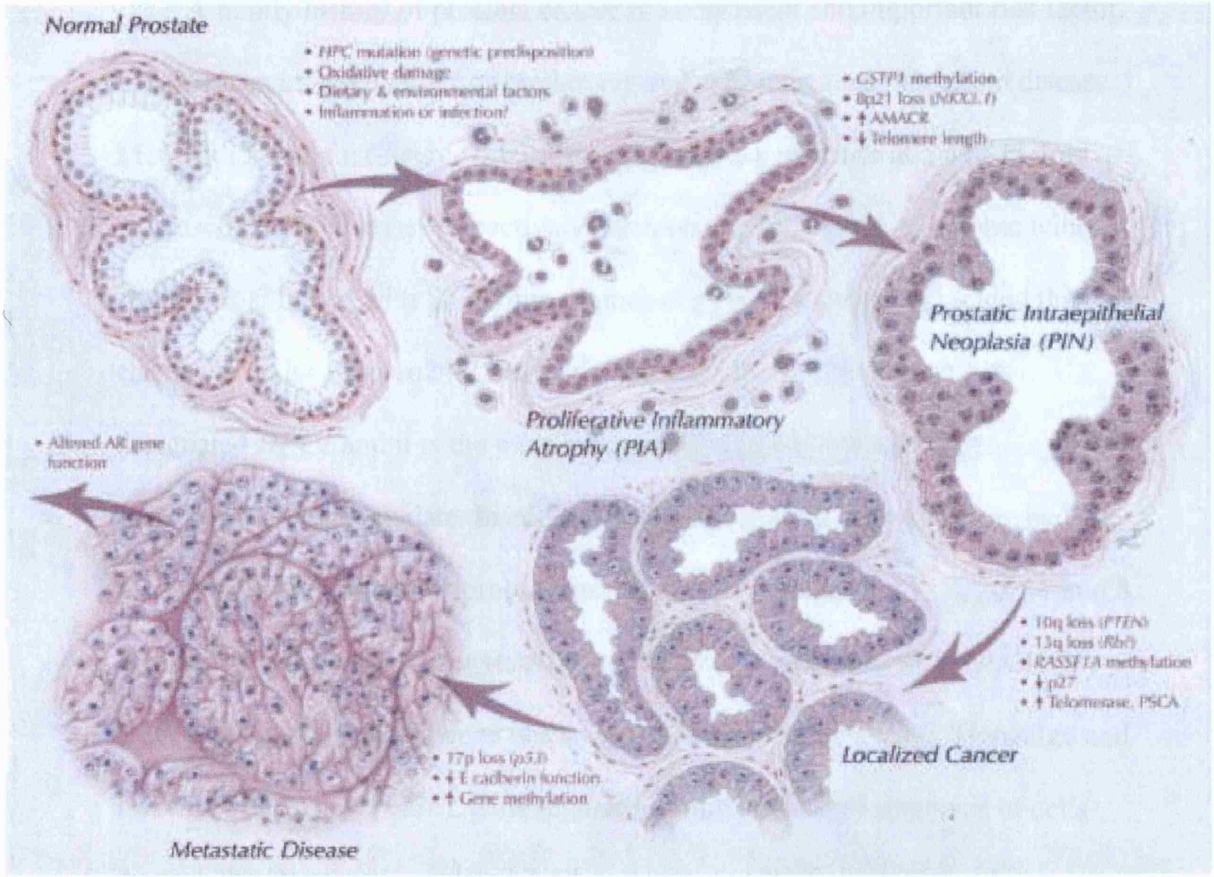

Figure 1.4 Contemporary model of prostate cancer progression. Genetic predisposition, oxidative damage and inflammatory changes are associated with earliest steps of prostate cancer development. Down-regulation of caretaker genes such as GSTP1 by aberrant promoter methylation may increase potential for neoplastic transformation. Chromosomal loss and telomere shortening may also contribute to genetic instability and progression to invasive disease. Further methylation changes, loss of tumor suppressor gene function and additional mutational events are associated with metastases and androgen independence. Adapted from Gonzalgo & Isaacs 2003.

increases. However, the increase is only to about 50% of the rate for white people and to 25% of that for African-American people in the USA, indicating that there are some genetic factors underlie the difference of incidence of the disease across ethnic group, in addition to the lifestyle differences (Gronberg, 2003).

A family history of prostate cancer is a consistent and important risk factor. Men with an affected father or brother are at 2-fold increased risk of the disease. Men with 2 or 3 first-degree relatives with prostate cancer are at 5 and 11-fold increased risk of disease, respectively (Steinberg et al., 1990). A genome wide scan for loci linked with family inheritance of prostate cancer has yielded the chromosome location 1q24-25 as a susceptibility locus. This region was designated *HPC1* and it is the most extensively studied prostate cancer predisposition locus to date. In addition to *HPC1*, linkage analysis suggested the other susceptibility loci for prostate cancer are on chromosome 1, X, 20, 17 and 8. The gene for 2'-5'-oligoadenylate (2-5A) dependent ribonuclease L (*RNASEL*) was mapped to be critical gene within 1q24-25 for prostate cancer (Gonzalgo and Isaacs, 2003). The *RNASEL* gene regulates proliferation and apoptosis of cells through the interferon-regulated 2-5A pathway and has been suggested as a tumour suppressor gene. Although mutation in RNASEL may only account for 6% of familial hereditable prostate cancer cases, the subset of families who met the criteria of HPC1 linkage had strong evidence of linkage. This may reflect the fact that prostate cancer is a complex disease and no single dominant genetic change exist in most of the cases (Gronberg, 2003).

Prostate cancer is associated with a western lifestyle which includes a high intake of meat, fat and dairy products. Some dietary components, for example α-linolenic acid (a polyunsaturated fatty acid in vegetables and dairy products) and

calcium, have been positively associated with prostate cancer. Asian people's low incidence is linked to high consumption of dietary phyto-oestrogens. Phyto-oestrogens are particularly rich in soybean products such as tofu and soymilk which are regular meal components for Asian people. In addition, frequent intake of tomato-based products is associated with a reduced risk of prostate cancer. The major component contributing to this effect is lycopene, a carotenoid and potent antioxidant. Selenium and vitamin E are also very good chemopreventive micronutrients for prostate cancer (Cheung et al., 2008).

Recently insulin growth factor (IGF)-1 was shown to be associated with prostate cancer (Monti et al., 2007). Thus, people in the highest quartile of IGF-1 plasma concentration had a 1.7-4.3 increased risk of prostate cancer compared with those in the lowest quartile. The IGF-1 may link the sedentary western lifestyle with prostate cancer. The model is that consumption of large amount of fat result in raised production of insulin that in turn increases production of IGF, thus explaining how IGF could be a risk factor for prostate cancer.

1.1.2.3 Gleason grading system

The Gleason score is the most widely used grading system for prostate cancer (DeMarzo et al., 2003). Unusually, the overall grade is not based on the highest grade within the tumour. In 1974, Gleason, Mellinger, and the Veterans' Administration Cooperative Study team showed that prognosis of prostate cancer was intermediate between that of the most predominant pattern of cancer and that of the second most predominant pattern. These predominant and second most prevalent patterns are identified and each is graded 1 (most differentiated) to 5 (least differentiated) and the two grades are added to give the Gleason sum score.

1.1.2.4 Treatment options

Whereas late stage prostate cancer needs active management, the decision on whether and how to treat early-stage prostate cancer has proven more challenging. Many patients diagnosed with prostate cancer are elderly and have comorbidities. For some of them the prostate cancer would not threaten their life and treatments which affect the quality of their life may not be justified. Management options for early-stage prostate cancer can be grouped into four broad categories: observation, surgery, radiotherapy, and hormone therapy.

Observation, or active surveillance, is probably the best option for patients with low-volume, less aggressive disease and with life expectancy of less than 10 years. During the observation period, regular PSA measurements are recommended and active treatment will be offered if disease progression occurs.

Radical prostatectomy is considered by many to be the best treatment for early prostate cancer. It involves the removal of the entire prostate. There is low risk of stress incontinence (2-3%) and a higher risk for erectile dysfunction (>50%) (Kirby, 2002).

External-beam radiotherapy is another good treatment for early localized prostate cancer. It involves daily treatment for 7-8 weeks. The survival rate is comparable to that of surgery, but with a slightly different side-effect profile.

The observation that the prostate is a hormone-responsive organ formed the basis for hormone therapy. It is done by either reduce serum testosterone or block the actions of this hormone. The agents used in prostate cancer hormone therapy include oestrogens, progestagens, gonadotropin-releasing hormone analogues, adrenal enzyme synthesis inhibitors, and antiandrogens .

1.2 Overview of Semaphorins

Semaphorins are a large family of secreted or membrane bound proteins. The earliest discovered members were found to be important in guiding axon growth. At least 30 semaphorins have been described. To avoid the confusion that may arise due to different names given to the same semaphorin family members by different researchers, an unified nomenclature system was installed in 1999 to divide them into eight classes based on domain organization and species of origin (Semaphorin Nomenclature Committee, 1999). Classes 1 and 2 semaphorins are invertebrate, classes 3-7 are vertebrate, and class V are viral. Semaphorins may be secreted (classes 2, 3, and V), transmembrane (classes 1, 4, 5, and 6), or membrane-anchored (class 7). A schematic explanation of the semaphorins is provided in Fig. 1.5.

All semaphorins possess a common 500-amino acid extracellular domain (Sema domain) which is critical for receptor binding and specificity. The Sema domain is also found in plexins and scatter factor receptors. Crystallization studies of the Sema domain suggested that it is well adapted to carry out protein-protein interactions. Nearly all semaphorins contain one or more copies of a small cysteine-rich domain located immediately C terminal to the Sema domain. This cystine-rich domain is either called MRS (MET-related sequence) or PSI (for a domain present in plexins, semaphorins and integrins). In addition, an immunoglobulin like domain is also present in most classes of semaphorin. Class 5 is unique as family members contain seven copies of a thrombospondin repeat (Gherardi et al., 2004). Their C termini are more divergent and may contain additional sequence motifs. For example, the C terminus of Class 6 semaphorins

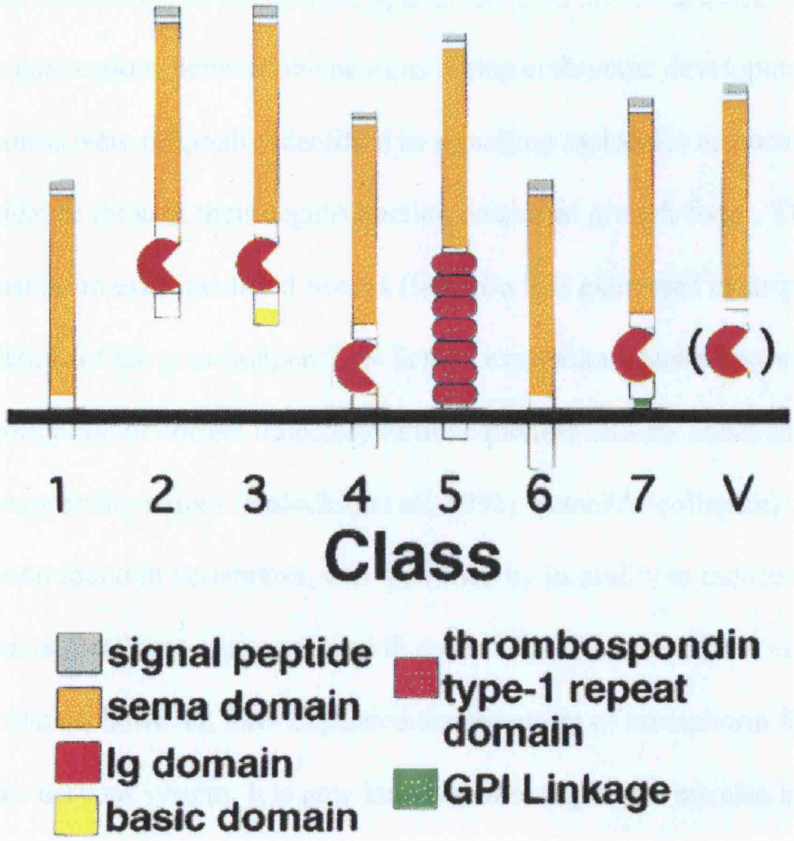

Figure 1.5 Classes of Semaphorin and their domain structures. Semaphorins are divided into eight classes according to their domain structure.

may contain a binding site for the Ena/Mena/VASP family of signal transducer, which is not present in other semaphorin members (Comoglio et al., 2004).

1.2.1 Semaphorins and nervous system development

The functioning of the nervous system relies on the formation of correct synaptic connections between the neurons during embryonic development. Semaphorins were originally identified as signalling molecules responsible for axon guidance through their negative action on axonal growth cones. Thus, the first semaphorin ever identified Sema I (fasciclin I) is expressed in stripes in the leg epidermis of the grasshopper. This Sema I expression pattern was important for the formation of correct trajectory of tibial pioneer sensory axons through the Sema I-expressing stripes (Kolodkin et al., 1992). Sema3A (collapsin) , the first semaphorin found in vertebrates, was identified by its ability to induce the retraction and collapse of axonal growth cones in chicken brain (Luo et al., 1993). Recent studies, however, have expanded the repertoire of semaphorin functions within the nervous system. It is now known that semaphorins are also involved in axonal fasciculation, dendritic guidance, and neuronal migration. In the adult nervous system, semaphorins may inhibit axon regeneration and guide adult neurogenesis (He et al., 2002). In this section I will briefly discuss the actions of semaphorins in various scenarios and the underlying molecular mechanisms using Sema3A, the best characterized semaphorin in the nervous system, as an example.

1.2.1.1 Axonal guidance

At the leading tip of a growing axon there is a highly motile structure called a growth cone which is sensitive to environmental cues. Stroma cells express

various signalling molecules which are either repulsive or attractive to growth cones so that regions permissive for axon growth are indicated. Repulsive signals from semaphorins tend to destabilize the cytoskeleton structure of growth cones and lead to their collapse. Attractive cues tend to stabilize growth cone cytoskeletal structure. The net effect of these 2 processes is to steer the growth cone towards regions permissive for axons (Dickson, 2002).

Sema3A is a repulsive cue for axons of sympathetic (Adams et al., 1997), motor (Shepherd et al., 1996; Varela-Echavarria et al., 1997), and sensory neurons from the trigeminal, facial, and vagal cranial ganglia (Kobayashi et al., 1997), as well as the olfactory sensory (Kobayashi et al., 1997), pontocerebellar mossy fibers (Rabacchi et al., 1999), and cortical neurons (Bagnard et al., 1998), plus a few other types of neurons from the hippocampus (Chedotal et al., 1998; Steup et al., 1999).

Growth cone turning is a complex process in which actin based motility is followed by a stable and directional microtubule advance (He et al., 2002). Axon guidance cues often induce asymmetrical filopodium extension by stabilizing or destabilizing the underlying actin cytoskeleton structure. Hence, more filopodia can be found on the side of attractive cues and less filopodia can be found on the side of repulsive cues. Microtubules form stable, cross-linked bundles in the axon shaft. Single microtubule filaments also emerge into the growth cone. These microtubules preferentially grow along the filopodial actin filaments, where they are captured and stabilized by an as yet unknown mechanism. Captured microtubules crosslink and fuse with axon shaft microtubules which result in growth of the growth cone towards attractive cues or away from repulsive cues. Given this growth cone turning model, a guidance cue might exert its effect at

various points. For example, it might promote the initiation, extension, stabilization, or retraction of filopodia by regulating actin dynamics, or it might influence the capture or stabilization of microtubules in certain regions of the growth cone.

Sema3A can regulate both actin and tubulin dynamics to reorganize the cytoskeleton for neuronal guidance. Sema3A-induced growth cone collapse occurs with disassembly of actin filaments (Fan et al., 1993; Fournier et al., 2000). How the semaphorin signal is transduced from the plasma membrane to the actin cytoskeleton is not clear, but most likely involves multiple signalling pathways. One of the consequences of Plexin-A1 activation by Sema3A is the tyrosine phosphorylation of the semaphorin receptor. The tyrosine kinase Fes phosphorylates Plexin-A1 upon ligand binding and dominant negative Fes was able to inhibit Sema3A-mediated dorsal root ganglion neurons growth cone collapse (Mitsui et al., 2002). Sema3A signalling also activates Glycogen synthase kinase-3 (GSK-3) associated with F-actin at the leading edge of neuronal growth cone. This GSK-3 activation is required for Sema3A-mediated growth cone collapse (Eickholt et al., 2002). Moreover, Rac1 has been implicated in Sema3A-mediated growth cone collapse. Rac1 is a member of the Rho family of small GTPases which are key components of the signal transduction pathway linking plasma membrane receptors to the actin cytoskeleton (Hall, 1998). Among them, Rac1 inhibition by dominant negative Rac1 or by an inhibitory peptide for Rac1 negates Sema3A-induced sensory neuron growth cone collapse (Jin and Strittmatter, 1997; Kuhn et al., 1999; Vastrik et al., 1999). Downstream of Rac1, LIM domain-containing kinase (LIM-kinase) is also necessary for Sema3A-induced growth cone collapse (Aizawa et al., 2001). LIM-kinase is a serine-

threonine kinase that phosphorylates cofilin and inhibits its actin-severing function. Another class of serine/threonine kinase, the collapsin-responsive mediator proteins (CRMPs) also are involved in actin dynamic control, although it is unclear how CRMPs act on the cytoskeleton (Goshima et al., 1995).

Genetic evidence suggested that the kinases Fyn and Cdk5 are involved in Sema3A-induced microtubule reorganization (Sasaki et al., 2002). In their system, Sasaki et al. found that Plexin-A2 can act as Sema3A receptor in the dorsal root ganglion neurons. Fyn is stably associated with Plexin-A2 and its activation facilitates the interaction between Plexin-A2 and Cdk5. Sema3A binding to Plexin-B2 leads to phosphorylation of Plexin-A2, Fyn, and Cdk5. Cdk5 then phosphorylates a microtubule associated protein, tau, resulting in destabilization of microtubules.

1.2.1.2 Axonal fasciculation

In a developing nervous system, axons travel in large bundles or fascicles and follow stereotyped pathways to reach their synaptic partners and will only segregate once they arrive at their target. When, where and how axons stay together or segregate is regulated by a balance of attractive and repulsive guidance cues from both the growing axons and their environment. Semaphorins have been involved in the regulation of those decision-making processes (He et al., 2002). Thus, in Sema3A deficient-mice peripheral projections of the trigeminal, facial, vagal, accessory, and glossopharyngeal nerves are highly defasciculated (Taniguchi et al., 1997; Kitsukawa et al., 1997). The defasciculation phenotype most likely arises because these axons are normally driven together into fascicles by the surrounding Sema3A protein.

1.2.1.3 Dendritic guidance

Like axons, neuronal dendrites form similar stereotyped networks in order to function. It was suggested that a Sema3A gradient can account for the projection of both dendrites and axons from the same cortical neuron (Polleux et al., 2000). Dendrites of cortical pyramidal neurons normally grow toward the cortical plate, whereas their axons grow away from it. Sema3A acts as a chemoattractant for the apical dendrites but as a chemorepellent for the axons of cortical pyramidal neurons.

How can the same semaphorin signal exert opposite effects on the axons and dendrites of the same neuron? Cytoplasmic levels of cGMP (cyclic GMP) may be the key (Song et al., 1998). The repulsion by Sema3A can be converted to attraction by increasing levels of cGMP. The local concentration of cGMP in an axon growth cone or a dendrite may be modulated by other signals which regulate guanylate cyclase or nitric oxide level. Electrical activity may also influence the level of cGMP through calcium-dependent pathways (He et al., 2002). In the case of cortical dendrites, it is interesting to find that a guanylate cyclase is specifically localized in the dendrites, suggesting that the cGMP level may be higher in dendrites than in axons (Polleux et al., 2000).

1.2.1.4 Neuronal migration

Sema3A guides neural crest cell migration during early development (Eickholt et al., 1999). It also guides the migration of GABAergic neurons in the developing neocortex (Tamamaki et al., 2003) as well as the migration of supporting cells in the central nervous system, such as oligodendroglial cells

(Spassky et al., 2002), glial cells (Tsai and Miller, 2002), and glial precursor cells (Sugimoto et al., 2001). Moreover, it is the main inhibitory factor for neural regeneration after spinal injury (de Winter et al., 2002a; de Winter et al., 2002b).

1.2.2 Semaphorins and immune system

Some semaphorins have roles in the immune system (Kikutani and Kumanogoh, 2003). Sema4D (CD100) is the best characterized semaphorin in the immune system and appears to serve several different functions. Firstly, Sema4D may promote B-cell activation. Sema4D-expressing transfectants promote the aggregation and survival of B-cells and also induce the shedding of CD23 from the surface of B-cells (Hall et al., 1996), so Sema4D is important for the mounting of a humoral immune response. Gene knock-out studies in mice support this role as Sema4D-deficient mice displayed reduced Ig production (Shi et al., 2000). Secondly, Sema4D seems to enhance T-cell function. In a study in which the expression of soluble Sema4D was increased, both Ab responses against T cell-dependent antigens and generation of antigen-specific T cells were enhanced (Watanabe et al., 2001). Thirdly, Sema4D may stimulate macrophages and monocytes and facilitate the formation of an inflammatory response. Recombinant soluble Sema4D can induce the production of pro-inflammatory cytokines IL-6 and IL-8 by human monocytes (Kikutani and Kumanogoh, 2003).

Whereas semaphorins signal through receptor complexes containing plexins outside the immune system (Tamagnone et al., 1999), Sema4D functioning in the immune system does not seem to require the participation of any plexin. Instead, the C-type lectin CD72 was found to be the functional receptor for Sema4D in the immune system (Kumanogoh et al., 2000). CD72 is a negative regulator of B-cell

activation. Through its cytoplasmic domain, CD72 recruits and activates Src-homology 2 (SH2)-domain-containing protein tyrosine phophatase 1 (SHP1), which dephosphorylates signalling proteins and inhibits the activation of immune cells (Adachi et al., 1998). Sema4D binding to CD72 induces dephosphorylation of CD72 and disassociation of SHP1 from CD72. Hence, Sema4D enhances B-cell by turning off the negative effect of CD72 on B-cell responses.

Sema4A, which is expressed in dendritic cells and B cells, enhances the *in vitro* activation and differentiation of T cells and the *in vivo* generation of antigen-specific T cells. Sema4A binds to Tim-2, a member of the family of T-cell immunoglobulin domain and mucin domain (Tim) proteins that is expressed on activated T cells (Kumanogoh et al., 2002).

The immuno-modulatory properties of some semaphorins are harnessed by some viruses to provide a survival advantage. The genomes of some Poxviruses, such as vaccinia virus, encode a semaphorin homolog protein A39R which strongly inhibits phagocytosis by dendritic cells and neutrophils (Walzer et al., 2005b). Moreover, A39R induces actin cytoskeleton rearrangement and inhibition of integrin-mediated migration in dendritic cells (Walzer et al., 2005a). Plexin-C1 (VESPR) is the cellular receptor for A39R (Comeau et al., 1998), and all of the above mentioned immunological activities of A39R seem to be dependent on Plexin-C1 signalling (Walzer et al., 2005a).

A39R may favour the spreading of the virus, since disruption of the neutrophil phagocytosis may prolong inflammation. Some cells involved in the inflammatory process, such as phagocytes, have been suggested to be vectors of vaccinia viruses propagation *in vivo*. In addition, the ability of A39R to interfere

with phagocytosis and migration of dendritic cells suggested that it may impede the antigen presentation function of dendritic cells.

1.2.3 Semaphorins and angiogenesis

Angiogenesis refers to the sprouting of new blood vessels from pre-existing ones. It is a process involving proliferation, survival, migration and differentiation of endothelial cells. Sema4D/Plexin-B1 signalling is associated with angiogenesis (Basile et al., 2004; Conrotto et al., 2005).

There is genetic evidence linking Semaphorins with vascular development. Plexin-D1 was found to be expressed only in vascular endothelium (van der et al., 2002). Plexin-D1 null mutant of zebrafish *out of bounds (obd)* exhibits defects in intersegmental vessel formation and patterning (Torres-Vazquez et al., 2004). Plexin-D1 knock-out mice had congenital heart disease and vascular patterning defects (Gitler et al., 2004). The cognate ligand of Plexin-D1, Sema3E, is highly expressed in developing somites, where it acts as a repulsive cue for plexin-D1-expressing endothelial cells of adjacent intersomitic vessels. Unlike other Class 3 semaphorins, Sema3E/Plexin-D1 mediated vascular patterning is independent of neuropilin (Gu et al., 2004).

Sema4D is a pro-angiogenic factor. It promotes the migration and *in vitro* tubulogenesis of porcine and human endothelial cells (EC). Sema4D also induces formation of blood vessels in gelatin implants or chicken chorioallantoic membrane (CAM), hence it has pro-angiogenic effect *in vivo* (Basile et al., 2004; Conrotto et al., 2005). Plexin-B1 is crucial in Sema4D induced angiogenesis, as Trk-A-Plexin-B1 chimera induced *in vitro* tubulogenesis when stimulated with NGF (Basile et al., 2004); and siRNA knock-down of Plexin-B1 antagonised the

pro-angiogenic effect of Sema4D (Conrotto et al., 2005). Consistent with these observations, Plexin-B1 is abundantly expressed in endothelial cells (Basile et al., 2004; Conrotto et al., 2005). Downstream events of Plexin-B1 in angiogenesis, however, are more controversial. In the porcine system, Sema4D stimulation of EC leads to activation of RhoA and formation of stress fibers. Met, a receptor tyrosine kinase shown to mediate increased cell migration induced by Sema4D, was found not to be involved in Sema4D mediated angiogenesis (Basile et al., 2004). On the other hand, Conrotto et al. have shown in their human endothelial cell culture system (HUVEC) that Met is essential for Sema4D mediated angiogenesis. RhoA did not seem to be activated upon Sema4D treatment in their system, since stress fiber dismantling occurred (Conrotto et al., 2005).

1.2.4 Semaphorins and organogenesis

Several class 3 semaphorins regulate branching morphogenesis in developing fetal lung. Lung explants of E11 mice have a few terminal buds originating from the lobar bronchi. The number of terminal buds increases with culture in serum-free medium. Recombinant Sema3A can inhibit branching morphogenesis and Neuropilin-1 is required for this inhibition (Ito et al., 2000). On the other hand, two of the other class 3 semaphorins, Sema3C and Sema3F, stimulate branching morphogenesis (Kagoshima and Ito, 2001). Sema3A, Sema3C and Sema3F have different expression patterns in the developing lung. During early development (E11.5-E13.5), Sema3A is expressed mainly in the distal mesenchyme, whereas Sema3C is expressed in the epithelium of the lobar bronchus. Sema3F expression is weak and diffuse in early stages, but at later stages its expression is confined to the terminal epithelium. Therefore, it seems

that while Sema3C and Sema3F are responsible for stimulating branching morphogenesis of the developing lung, Sema3A acts to limit the lung development (Kagoshima and Ito, 2001).

Sema6D is involved in cardiac morphogenesis (Toyofuku et al., 2004b; Toyofuku et al., 2004a). In vertebrate cardiac development, cardiogenic precursor cells first form a double layered straight tube. Myocardial and endocardial cells form the outer and inner layers respectively. This tubular structure then undergoes a complex series of morphogenetic events to form a curved S-shaped structure with segments for future atrium and ventricle. The ventricular segment of the tube undergoes two maturation processes: centripetal growth which leads to the formation of trabeculae (the fibrous tissue extending from the wall to the interior of the heart); and expansive growth, which leads to the formation of the outer compact layer and increase of ventricular volume (Lyons, 1996).

In heart development, Sema6D functions both as a ligand and a receptor for Plexin-A1, referred to as 'forward' and 'reverse' signalling, respectively. Forward signalling through Plexin-A1 is necessary for ventricular expansion, whereas Sema6D-mediated reverse signalling is needed for trabeculation. Thus, Plexin-A1 is co-expressed with its ligand Sema6D in a subset of proliferating non-motile myocardial cells in the compact layer. This simultaneous activation of both forward and reverse signalling induces the circumferential migration of myocardial cells and leads to expansion of the compact layer. A sub-population of the compact layer myocardial cells express only Sema6D, which transduces a 'reverse' signalling pathway through its own cytoplasmic tail. These cells acquire a highly motile phenotype and migrate to form the inner trabecular layer. Endocardium, the inner lining of the heart cavity, is separated from the

myocardium by a complex proteoglycan and glycosamino-glycan-rich matrix called 'cardiac jelly'. Endocardial cells express Plexin-A1 and they receive Sema6D signal released from myocardial cells which diffuses through the cardiac jelly. Sema6D can trigger differential migration in a sub-population of endocardial cells. Plexin-A1 forms a receptor complex with vascular endothelial growth factor receptor type 2 (VEGFR2) in the conotruncal segment. Concurrently Sema6D promotes the migration of cells from the conotruncal segment. On the other hand, cells from the ventricle segment express Off-track (OTK) as a co-receptor with Plexin-A1, and hence their migration was retarded when treated with Sema6D (Toyofuku et al., 2004b; Toyofuku et al., 2004a).

1.2.5 Semaphorins and cancer

There are several reports suggesting that some semaphorins are involved in cancer progression. Several small cell lung cancer cell (SCLC) and non-small cell lung cancer (NSCLC) lines have homozygous deletions in the chromosome region 3p21.3, where Sema3B and Sema3F are located. This region is also deleted in nearly 100% of SCLC cases, suggesting that these semaphorins have tumour suppressor activity (Roche et al., 2002; Sekido et al., 1996; Xiang et al., 1996; Muller et al., 2007; Nair et al., 2007; Futamura et al., 2007). On the other hand, overexpression of secreted semaphorins Sema3E and Sema3C is associated with increased invasive and metastatic behaviour or drug resistance of tumour cells (Yamada et al., 1997; Christensen et al., 1998; Christensen et al., 2005). These opposing effects on tumour progression may reflect the diversity of cellular signalling machinery employed by various semaphorins to transduce their signals. For instance, Sema4D receptor Plexin-B1 can associate with the oncogenic

receptor Met. Stimulation of Plexin-B1 with Sema4D triggers the activation of Met and leads to increase in cell mobility and invasive behaviour (Giordano et al., 2002). Plexin-B1 also associates with and activates the highly oncogenic receptor tyrosine kinase ErbB-2 (Swiercz et al., 2004). Class 3 semaphorins may negatively regulate VEGF signalling by sequestering the shared neuropilin co-receptors. Recently, we reported that Sema4D is overexpressed in >90% of primary prostate cancer samples, and mutations could be found in about 90% of prostate cancer metastatsis (Wong et al., 2007).

1.3 Semaphorin 4D

Within the semaphorin family, semaphorin 4D (Sema4D/CD100) is a unique member in the sense that its physiological function is best elucidated in the immune system. Sema4D was identified as a 150kDa dimer on activated T-cells using two monoclonal antibodies called BB18 and BD16 (Bougeret et al., 1992). The activated T-cell-specific antigen was assigned as CD100, without clear knowledge about its true identity. By expression cloning, Hall et al. established that CD100 is a semaphorin (Hall et al., 1996). At about the same time, mouse Sema4D was also cloned (Furuyama et al., 1996).

Sema4D is expressed broadly at the organ level. Sema4D's transcripts are abundant in skeletal muscle, peripheral blood lymphocytes, spleen, and thymus, and less abundantly in testes, brain, kidney, small intestine, prostate, heart, placenta, lung and pancreas, and are absent in colon or liver (Hall et al., 1996).

Sema4D was shown to be associated with CD45, a protein tyrosine phosphatase (PTP), and an unidentified serine kinase activity (Elhabazi et al., 1997; Herold et al., 1996). CD45 is responsible for regulating cell surface

Sema4D expression and shedding during T cell activation (Herold et al., 1996). Moreover, the PTP associated with Sema4D changes according to the activation and maturation states of B-cells. Hence, CD45 was the PTP associated with Sema4D in pre-B, activated B and pre-plasma cell. In plasma cells, another unidentified PTP was associated with Sema4D (Billard et al., 2000). The association between Sema4D and a serine kinase may suggest that there is a possibility of reverse signalling, as in the case of Sema6D in cardiogenesis.

Sema4D has at least two cell surface receptors, serving different purposes and expressed in different locations. Plexin-B1 is the Sema4D receptor widely expressed in adult tissues (Maestrini et al., 1996a), and mediates the effect of Sema4D on cell mobility (Tamagnone et al., 1999). CD72, on the other hand, is the lymphocyte receptor of Sema4D (Kumanogoh et al., 2000).

Sema4D is upregulated in HepG2 cells upon iron overload, presumably due to the oxidative stress exerted on the cells (Barisani et al., 2000). However, the Sema4D upregulation is not affected by vitamin E treatment, reducing the possibility that Sema4D expression is regulated through a redox mechanism. It is unclear whether this Sema4D upregulation has any physiological significance. In particular, Sema4D is not normally expressed in liver (Hall et al., 1996).

1.3.1 Cell surface processing

Although Sema4D belongs to the Class 4 transmembrane type semaphorin, several lines of evidence suggested that at least in the immune system it functions as a long range, soluble and diffusible factor. *In vivo* administration of recombinant soluble Sema4D-Fc enhanced the production of specific antibodies (Kumanogoh et al., 2000). Activated T and B lymphocytes release soluble

Sema4D (sSema4D). Serum levels of sSema4D positively correlate with antibody production (Wang et al., 2001). sSema4D can also inhibit the migration of monocytes (Delaire et al., 2001). Transgenic sSema4D overexpressing mice displayed the opposite phenotype to Sema4D knockout mice, and crossing them was sufficient to restore immune system function in the offspring (Watanabe et al., 2001). In other tissues, recombinant sSema4D induced invasive behaviour or inhibited cell adhesion through a Plexin-B1 dependent pathway (Giordano et al., 2002; Barberis et al., 2004).

Soluble Sema4D is shed into the culture medium through proteolytic cleavage (Herold et al., 1996). In Jurkat T cells cell surface Sema4D dimerizes, possibly through Cysteine 674, and is spontaneously cleaved near the transmembrane domain, which leads to the shedding of soluble Sema4D into the culture medium. The proteolytic cleavage is catalysed by MT1-MMP (Basile et al., 2007) and regulated by protein phosphorylation (Elhabazi et al., 2001). Whereas the cell surface Sema4D normally consists of a 300kDa homodimer, sSema4D is a homodimer of about 240kDa (Herold et al., 1996).

1.3.2 Structure

The crystal structure of the ligand-binding surface of Sema4D (residues 1-657) has been resolved at 2Å resolution (Love et al., 2003). The structure revealed that the sema domain is primarily composed of a seven-bladed β-propeller. The β-propeller is a common topology and is present in proteins with diverse functions. Interestingly, the closest structural homolog of the sema domain is the α subunit of the integrin αVβ3. The appearance of a sema domain in semaphorins, plexins, and the oncogenic receptors Met/Ron suggests it provides a common structural

scaffold which can be adapted to mediate a variety of protein-protein interactions (Gherardi et al., 2004).

1.3.3 Transgenic studies

Although Sema4D is widely expressed in various tissues, Sema4D-deficient mice only have functional defects in their immune system. While conventional B and T cells develop normally in Sema4D-deficient mice, the number of CD5+ B-1 cells was considerably decreased. This lack was reflected functionally when the *in vitro* proliferative responses and immunoglobulin production of B-cells isolated from Sema4D-deficient mice were compared with those of normal mice. Small resting B cells from Sema4D deficient mice displayed a delayed proliferative response when induced by anti-CD40 mAb and lipopolysaccharide (LPS) compared to those of wild-type mice. *In vivo*, the humoral immune response against a T cell-dependent antigen and *in vivo* priming of T cells were also defective. These results suggested that Sema4D performs an essential non-redundant role in the immune system, whereas in other tissues its function may be replaceable by other semaphorins (Shi et al., 2000).

Consistent with the knock-out study, transgenic mice expressing a truncated form of Sema4D (CD100-Tg mice) and hence had excessive soluble Sema4D in the circulation, presented the opposite phenotype to Sema4D-deficient mice. The number of CD5+ B-1 cells increased in CD100-Tg mice. *In vitro* proliferation and immunoglobin production by B cells isolated from CD100-Tg mice were also enhanced. T cell-dependent antigen and generation of antigen specific T cells were enhanced. Moreover, when CD-100Tg mice were crossed with CD-100

deficient mice, the resulting offspring had a normal immune response (Watanabe et al., 2001).

1.3.4 Neuronal action of Sema4D

Relative to its functions in the immune system, the role of Sema4D in the nervous system is newly discovered and poorly understood. Unlike Sema3A which can exert both neurotrophic and anti-neurotrophic effects on different types of neurons, only neurotrophic effects have been demonstrated for Sema4D so far. PC12 cells undergo neural differentiation, growing neurites upon stimulation with nerve growth factor (NGF). Sema4D increases the sensitivity of PC12 cells towards NGF, so that the cells responded to very low concentrations of NGF in the presence of 1nM Sema4D. Protein kinase C, phosphatidylinositol 3-kinase (PI3K), and voltage-dependent Ca^{2+} channel are implicated in this Sema4D-mediated neurotrophic effect (Fujioka et al., 2003). *In vivo*, it has been shown that Sema4D stimulates axonal outgrowth of embryonic dorsal root ganglion (DRG) neurons (Masuda et al., 2004).

Sema4D may be involved in neuroinflammatory diseases. T lymphocytes chronically activated by retrovirus infection can induce apoptosis and progressive collapse of process extensions of multipotent neural progenitors and immature oligodendrocytes. This action can be inhibited by neutralizing antibody against Sema4D, suggesting that activated T-lymphocytes infiltrating the CNS secret soluble Sema4D, which leads to demyelination and axonal degeneration (Giraudon et al., 2004).

1.3.5 Plexins

The first Plexin protein identified was an antigen specific for the *Xenopus* plexiform layers of the optic tectum (Takagi et al., 1987). Cloning and sequence analysis of the first plexin were done in mid-90's in Xenopus and mouse (Ohta et al., 1995; Kameyama et al., 1996a; Kameyama et al., 1996b). At about the same time, in a search for genes sharing significant homology with the proto-oncogenes *MET and RON*, Maestrini et al. identified *SEX* and three other related genes *SEP*, *OCT* and *NOV* (Maestrini et al., 1996b) which were later renamed as plexins. In 1999 Plexins were demonstrated to be single pass transmembrane receptors for semaphorins (Tamagnone et al., 1999). Class 3 semaphorins require co-receptors such as neuropilins in addition to plexins for signalling. Other semaphorins seem to use plexins exclusively as receptors. Plexins can be grouped into 4 subfamilies according to domain structure: Plexin-A, B, C, and D (Fig 1.6).

1.4 PlexinB1

Plexin-B1 is frequently mutated in prostate cancer metastases (Wong et al., 2007). Thirteen somatic mutations in the plexinB1 gene were found in 89% of prostate cancer metastases and 46% of primary tumors. This observation suggests that malfunction in the plexin-B1 signaling axis are advantageous for the cancer cell. Of the mutations identified, A5653G, which potentially changes the threonine at position 1795 to an alanine, was found in 64% of metastases. A5359G plexin-B1 mutant expressing cells display significantly enhanced anchorage independent growth ability when compared with wild type plexinB1 expressing cells. Our results suggested that aberrant plexinB1 function may play an important role in prostate cancer progression. The study described in this thesis

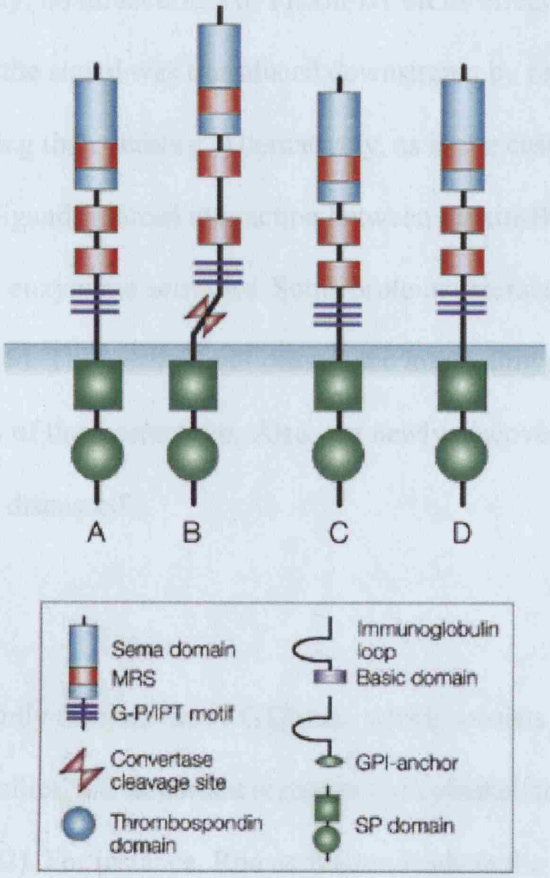

Figure 1.6 Classes of Plexins and their domain structures. Plexins are divided into four classes (A,B,C, and D) according to their domain structure. Adapted from Trusolino and Comoglio 2002.

will focus on effects of the plexin-B1 mutations at the molecular level. Therefore next section describes various aspects of Plexin-B1 molecular signaling.

1.4.1 Interaction partners of plexinB1

Until recently, no direct effect of Plexin-B1 on its effectors was identified. It was believed that the signal was transduced downstream by recruiting interacting partners and altering their activity. Alternatively, as in the case of non-receptor tyrosine kinases, ligand-induced interaction between Plexin-B1 and its effectors may activate their enzymatic activities. Some proteins interacting with Plexin-B1 have been identified. This section will discuss the interacting partners of Plexin-B1 and the effects of the interactions. Also, the newly discovered GAP activity of Plexin-B1 will be discussed.

1.4.1.1 Rac

The Rho family of monomeric GTPases, which consists of the Rho, Rac, and Cdc42 subfamilies, are important regulators of cytoskeleton function (Sahai and Marshall, 2002). For instance, Rho activation leads to the formation of actin stress fibers. Rac is involved in the regulation of lamellipodia (pleat-shaped protrusions at the cell periphery) and membrane ruffling whereas Cdc42 regulates the formation of thin finger-like cytoplasmic extensions known as filopodia. These proteins play an important role in the regulation of cell morphology, cell aggregation, tissue polarity, cytokinesis, cell motility, and also in smooth muscle contraction.

Two reports show the interaction between activated Rac and plexinB1 (Driessens et al., 2001; Vikis et al., 2000). In a yeast two-hybrid screen for

interacting partners of Rac, Plexin-B1was identified (Driessens et al., 2001). Plexin-B1 binds only to activated (GTP-bound form) of Rac (Driessens et al., 2000; Vikis et al., 2000). The Rac binding region in plexin-B1 was mapped to amino acid 1696 to 1910, within which the Cdc42/Rac interactive binding (CRIB) motif located. The motif between aa 1848-1890 is required but not sufficient for Rac binding (Vikis et al., 2000). On Rac, Y32, T35 and F37 are the amino acid residues important for plexin-B1 binding within the switch I region. Of note, Y40 is important for Rac to bind p21 activated kinases but not for plexin-B1, making it possible to construct Rac mutants that interact only with plexin-B1 or PAK (Vikis et al., 2002).

Overexpression of plexin-B1 has no observable effect on the cytoskeleton. However, recombinant plexin-B1, in which the extra-cellular domain was replaced with CD2, induces the formation of stress fibers upon crosslinking by addition of monoclonal antibody to CD2. The resultant crosslinking also leads to cell contraction. These phenotypes suggested that RhoA was activated in the cells with crosslinked CD2/plexin-B1 chimeric receptor. While Rac inhibition can block the formation of stress fiber formation and cell contraction induced by the chimeric receptor crosslinking, it remains to be explained why the Rac binding site on the receptor is not required for the RhoA activation phenotype (Driessens et al., 2001).

A bi-directional signalling model of Sema4D, plexin-B1, and GTP-Rac was suggested (Vikis et al., 2002). In this model, Sema4D inhibits p21-activated kinase (PAK) by enhancing the affinity of plexin-B1 toward GTP-Rac, which is required for PAK activation, hence promoting growth cone collapse. The binding

of GTP-Rac with plexin-B1 also facilitates the binding between Sema4D and plexin-B1 by enhancing the cell surface expression of plexin-B1.

1.4.1.2 PDZ-RhoGEF/LARG

The cycling between GTP-bound and GDP-bound forms of Rho family monomeric GTPase is regulated by three kinds of factors. Guanine nucleotide exchange factors (GEF) enhance the exchange of GTP for GDP. GTPase activating proteins (GAP) increase the low-intrinsic GTPase activity of the Rho family GTPase they interact with and hence act as negative regulators. Guanine nucleotide dissociation inhibitor (GDI) sequesters the GDP-bound form of Rho family GTPase and effectively reduces the pool of GTPase available for activation (Sahai and Marshall, 2002).

PDZ-RhoGEF was identified as a regulator of Rho activity similar to Dbl. It contains a tandem DH/PH domain closely related to those of Rho-specific GEFs, a PDZ domain, a proline-rich domain, and an area of homology to Lsc, p115-RhoGEF, and a *Drosophila* RhoGEF that was termed Lsc-homology (LH) domain. It was hence termed PDZ-RhoGEF (Fukuhara et al., 1999). Leukaemia-associated Rho guanine nucleotide exchange factor (LARG) was originally identified as a fusion partner of the MLL gene at 11q23 in human acute myeloid leukaemia (Kourlas et al., 2000). Both PDZ-RhoGEF and LARG activate RhoA by catalyzing the exchange of GTP for GDP. Moreover, both PDZ-RhoGEF and LARG interact with the activated alpha-subunits of G12/G13 and are thus believed to mediate G-protein coupled receptor(GPCR)-induced Rho activation (Fukuhara et al., 2000; Fukuhara et al., 1999). This suggested a means of cross-talk between GPCR and Plexin-B signalling.

Several lines of evidence suggest that stimulation of plexin-B1 leads to RhoA activation (Driessens et al., 2001; Swiercz et al., 2002). In Drosophila, Plexin-B directly interacts with RhoA and stimulates its activity upon ligand binding (Hu et al., 2001). Although Plexin-B1 does not interact directly with RhoA in mammalian cells, Sema4D binding to Plexin-B1 leads to stress fiber formation, which suggests RhoA activation (Driessens et al., 2001). Signals were transduced from plexin-B1 to RhoA through PDZ-RhoGEF (Driessens et al., 2002; Hirotani et al., 2002; Oinuma et al., 2003; Swiercz et al., 2002). Plexin-B1 interacts directly with PDZ-RhoGEF through its C-terminal PDZ domain-interacting motif (amino acid sequence motif TDL) (Driessens et al., 2002; Hirotani et al., 2002; Oinuma et al., 2003; Swiercz et al., 2002). This PDZ domain-interacting motif was only found in class B plexin.

The interaction between Leukemia-associated Rho GEF (LARG) and plexin B1 was identified using mass spectrometry (Aurandt et al., 2002). Like PDZ-RhoGEF, LARG interacts with plexin-B1 thought its PDZ domain (Hirotani et al., 2002).

1.4.1.3 Rnd1

Rnd1, Rnd2 and Rnd3 (also known as RhoE) are the members of a Rho GTPase subfamily with the characteristic property of very low intrinsic GTPase activity. Therefore, all members in this subfamily are constitutively in the GTP-bound form (Foster et al., 1996). Expression of Rnd1 in fibroblasts leads to loss of actin stress fibers and loss of cell substrate adhesion, which leads to cell retraction and rounding (Nobes et al., 1998). Rnd3 expression induced cell spreading in MDCK cells but did not affect the actin bundles in the periphery of the colonies.

Moreover, Rnd3 can enhance hepatocyte growth factor/scatter factor's effect on MDCK cells by increasing migration speed of the stimulated cells. Therefore, Rnd3 was shown to be able to antagonize some RhoA regulated responses such as stress fiber formation, but had no effect on others, such as peripheral actin bundle formation (Guasch et al., 1998).

Plexin-B1 directly interacts with Rnd1, Rnd2 and, to a lesser extent, Rnd3 (Oinuma et al., 2003). The Rnd1 binding site in the cytoplasmic domain of Plexin-B1 was located between amino acids 1724 and 1915. Hence, it overlaps substantially with the mapped Rac-GTP binding site (aa 1848-1890). In fact, mutations in the region which abolish interaction with Rac also affect Rnd1 binding. Stimulating COS-7 cells expressing both Plexin-B1 and Rnd1, or Rnd3, with Sema4D led to cell contraction and rounding, which suggests a role of Plexin-B1/Rnd1/Rnd3 signalling in regulating cell adhesion. The cell contraction phenotype induced by Plexin-B1/Rnd1 is dependent on RhoA, as inhibition of RhoA signalling by dominant negative construct or a chemical inhibitor prevented the cell rounding phenotype (Oinuma et al., 2003). In addition, Rnd1 seems to enhance the interaction between Plexin-B1 and PDZ-RhoGEF, thereby leading to cell contraction (Oinuma et al., 2003).

Recently, Plexin-B1 was shown to be a GAP for R-Ras (to be described in more detail in section 1.4.1.6), and Rnd is indispensable for this Plexin-B1 function. Plexin-B1 can interact with and induce the hydrolysis of GTP by R-Ras only in the presence of Rnd (Oinuma et al., 2004a). In their most recent report, Oinuma et al. reported that the C1 and C2 domain of Plexin-B1 cytoplasmic domain interact and hence the cytoplamic domain of Plexin-B1 is in a closed conformation . Rnd1 binding to Plexin-B1 seems to open up the closed

conformation of the Plexin-B1 cytoplasmic domain, so that a site for R-Ras interaction becomes accessible (Oinuma et al., 2004b).

Interestingly, while both RhoA stimulation and R-Ras inactivation by Plexin-B1 are dependent on Rnd, they are largely independent of each other. So mutations affecting the GAP activity of Plexin-B1 did not affect RhoA stimulation by Plexin-B1, nor did C-terminal deletion, which abolishes RhoA stimulation by Plexin-B1 affect Plexin-B1 GAP activity (Oinuma et al., 2004a).

1.4.1.4 Scatter factor receptor family

The scatter factor receptor includes two members: Met, which is the receptor for hepatocyte growth factor (HGF), and Ron, which is the receptor for macrophage stimulating protein (MSP). They are the primary transducers of signals for invasive growth, a biological program which instructs cells to dissociate, migrate, degrade the surrounding matrix, proliferate and survive. Both receptors have tyrosine kinase activity and have been implicated in the invasive growth of many cancer cell types (Gentile and Comoglio, 2004).

Met is a disulphide-linked heterodimer which consists of an extracellular alpha chain and a transmembrane beta chain. The cytoplasmic portion contains the catalytic domain and critical sites for the regulation of kinase activity. Mutations of the gene for the proto-oncogene protein c-MET are associated with papillary renal carcinoma and other neoplasias (Birchmeier et al., 2003).

Met stably interacts with Plexin-B1 and is an important signalling component of Sema4D/Plexin-B1. Thus, stimulation of Plexin-B1 by Sema4D in epithelial cells leads to Met/Ron activation and initiates classical scatter responses, including loss of cell-cell contact and increased migration. Plexin-B1

interacts with Met constitutively in a ligand independent manner. Upon stimulation by Sema4D, both Plexin-B1 and Met become phosphorylated. Their phosphorylation is dependent on the tyrosine kinase activity of Met. When the kinase activity of Met was inactivated by mutations, Sema4D failed to induce scatter (Giordano et al., 2002). This indicates that Sema4D depends largely, if not solely, on Met in transducing the invasive growth signal. In fact, Met is the only receptor kinase which signalling is associated with invasive behaviours. Interestingly, HGF and Sema4D signalling seems to converge on Met since HGF and Sema4D act synergistically to induce scatter. Sema4D plexin-B1 signalling can induce invasion, and this signalling process requires Met.

Both Met and Ron interact with Plexin-B1, and all members of the Plexin-B family interact with both Met and Ron. Similar to Met, Ron activation via Plexin-B1 by Sema4D increased the invasive ability of epithelial cells. Signalling through Met and Ron seems to be a Class B Plexin specific property, since Plexin-D1 and Plexin-A1 do not interact with Met and Ron (Conrotto et al., 2004).

1.4.1.5 ErbB-2

The ErbBs are typical receptor tyrosine kinases that are associated with cancer development. Within the ErbB family, ErbB-2 is the most potent oncoprotein but it has no known ligand. ErbB-2 preferentially forms heterodimer with other ErbBs and acts as an active component in the resultant receptor complex (Yarden and Sliwkowski, 2001).

To further elucidate the mechanism of RhoA activation by Plexin-B1, Swiercz et al. tried to detect Plexin-B1/PDZ-RhoGEF-mediated RhoA activation in the presence of a panel of pharmacological inhibitors. They found tyrphostin

AG1478, an inhibitor of receptor tyrosine kinases of the ErbB family, almost completely blocked Plexin-B1 mediated activation of RhoA. Further investigation using a dominant negative mutant established that ErbB-2 is the ErbB involved in Plexin-B1 mediated RhoA activation. Immunoprecipitation experiments suggested that Plexin-B1 and ErbB-2 form a stable complex, and binding of Sema4D to Plexin-B1 induced the phosphorylation of both Plexin-B1 and ErbB-2. Moreover, ErbB-2 seems to be important for axonal growth cone collapse in primary hippocampal neurons (Swiercz et al., 2004).

1.4.1.6 R-Ras

The Ras family of small GTPases includes four Ras proteins encoded by the *H-ras*, *N-ras* and *K-ras* genes (H-Ras, N-Ras, K-Ras4A and K-Ras4B), the R-Ras proteins (R-Ras, R-Ras2/TC21, R-Ras3/M-Ras), the Ral proteins (A and B), the Raps (1A, 1B, 2A and 2B), Rheb, Rin and Rit (Kinbara et al., 2003).

Due to their high sequence homology, Ras family members were once thought to be functionally redundant. However as analyses of their cellular function and regulation evolve, evidence supporting the notion that they serve distinct functions accumulates. Ras proteins are membrane localized through modification of their carboxy-terminal 25 amino acids, called the Hypervariable domain (HVR) (Hancock, 2003). Dependent on the sequence context in the HVR, Ras proteins have different modifications. The type of modification a Ras protein receives then in turn determines the microdomain on the plasma membrane to which it is directed. For instance, whereas K-Ras is farnesylated and localizes to the plasma membrane, H-Ras is palmitoylated and localizes to the lipid raft (Kinbara et al., 2003).

R-Ras has significant effects on cell adhesion. Constitutively active R-Ras can activate integrin, hence leading to increase of cell adhesiveness to fibronectin substrates (Zhang et al., 1996). R-Ras does not directly regulate integrin function but instead acts as an antagonist of the Ras/Raf suppression on integrin (Sethi et al., 1999; Kinbara et al., 2003). R-Ras mediated activation of integrin enhances migration and invasion of breast epithelial cells. This effect is dependent on collagen but not fibronectin, suggesting that R-Ras activates only certain types of integrin in this particular kind of cell (Keely et al., 1999).

It has been suggested that the Plexin-B1 cytoplasmic domain contains regions homologous to GAP, and hence Plexin-B1 may function by regulating the activities of some small GTPases (Rohm et al., 2000). However, direct biochemical evidence showing Plexin-B1 possesses GAP activity was lacking until Oinuma et al. demonstrated that Plexin-B1 can act as a GAP for R-Ras, but only in the presence of Rnd1 (Oinuma et al., 2004a). Plexin-B1 interacts directly with R-Ras only in the presence of Rnd1 and stimulates the intrinsic GTPase activity of R-Ras when stimulated by Sema4D. The Rnd1 binding region in Plexin-B1 divides the R-Ras GAP domain into C1 and C2 domains. Without Rnd1, C1 and C2 constantly bind to each other. Binding of Rnd1 disrupts this C1-C2 interaction and the receptor cytoplasmic domain adopts an active conformation (Oinuma et al., 2004b). The R-Ras GAP activity of Plexin-B1 is important for Sema4D induced neurite retraction in differentiated PC12 cells as well as growth cone collapse in hippocampal neurons (Oinuma et al., 2004a). It has been demonstrated previously that growth cone collapse mediated by Sema4D/Plexin-B1 signalling is dependent on RhoA activation through the action of PDZ-RhoGEF/LARG (Swiercz et al., 2002). In their supplementary data, Oinuma et al.,

showed that the inactivation of R-Ras and activation of RhoA involves different parts of the Plexin-B1 cytoplasmic domain and can be separated. Therefore, the interaction between the effect of R-Ras inactivation and RhoA activation on growth cone morphology awaits clarification.

There is evidence that Plexin-B1 signalling affects integrin functions. COS-7 cells expressing exogenous Plexin-B1 retract their cellular processes and become round-shaped ("cell collapse") upon Sema4D treatment. This phenotype is caused by disassembly of integrin-based focal adhesion and actin depolymerization induced by Plexin-B1 activation (Barberis et al., 2004). Given the facts that inhibition of R-Ras may inactivate Rac (Holly et al., 2005) and Plexin-B1 may sequester GTP-Rac from the cytosol (Vikis et al., 2002), Plexin-B1 has the potential to be a potent Rac inhibitor.

1.4.1.7 PYK2, PI3K and Src

PYK2 is an intracellular nonreceptor tyrosine kinase belonging to the focal adhesion protein tyrosine kinase (PTK) family. The family consists of the focal adhesion kinase (FAK) and the RAFTK/PYK2 kinase (also known as CAK-beta and CADTK). PYK2 is activated by a variety of extracellular signals that elevate intracellular calcium concentration and by stress signals. RAFTK/Pyk2 is expressed mainly in the central nervous system and in cells derived from hematopoietic lineages (Avraham et al., 2000).

Sema4D is a chemoattractant for porcine aortic endothelial cells (Basile et al., 2004). PYK2 was shown to be crucial for this chemotactic response (Basile et al., 2005). Upon stimulation by Sema4D, Plexin-B1 in endothelial cells rapidly recruits a protein kinase complex consisting of PYK2, PI3K and Src. This event

induces the autophosphorylation and activation of PYK2. Activated PYK2 phosphorylates Src. Src then phosphorylates PI3K. These event lead to the phosphorylation and activation of Akt and, at a cellular level, enhancement of cell movement. It is unclear how stimulation of Plexin-B1 by Sema4D brings about the activation of PYK2.

1.4.1.8 p190 GAP

Although there is much evidence suggesting that Plexin-B1 signalling activates RhoA (Section 1.4.2.2), some researchers discovered an alternative Plexin-B1 signalling pathway that inactivates RhoA (Barberis et al., 2005).

p190 is an ubiquitously expressed RhoA specific GTPase-activating protein (Ridley et al., 1993). p190 is also known as p190A, to distinguish it from an homologous protein p190B. p190A and p190B exhibit similar activities but are regulated by different upstream regulatory mechanisms (Burbelo et al., 1998).

Barberis et al. observed a transient downregulation of RhoA activity upon Sema4D treatment of epithelial and fibroblastic cells. Using siRNA, they were able to demonstrate p190GAP is essential for many Plexin-B1 signalling activities, including induction of cell collapse and neurite outgrowth. Interestingly, unlike Rac and PDZ-RhoGEF, the interaction between Plexin-B1 and p190 is induced by Sema4D binding (Barberis et al., 2005).

1.4.1.9 Summary of Plexin-B1-Rho GTPases signalling

A summary of Plexin-B1 signalling through Rho-GTPase is provided in figure 1.7. Please note that the signalling between Plexin-B1 and Met/Ron/ErbB-2 was not shown since they were not studied in details in this study.

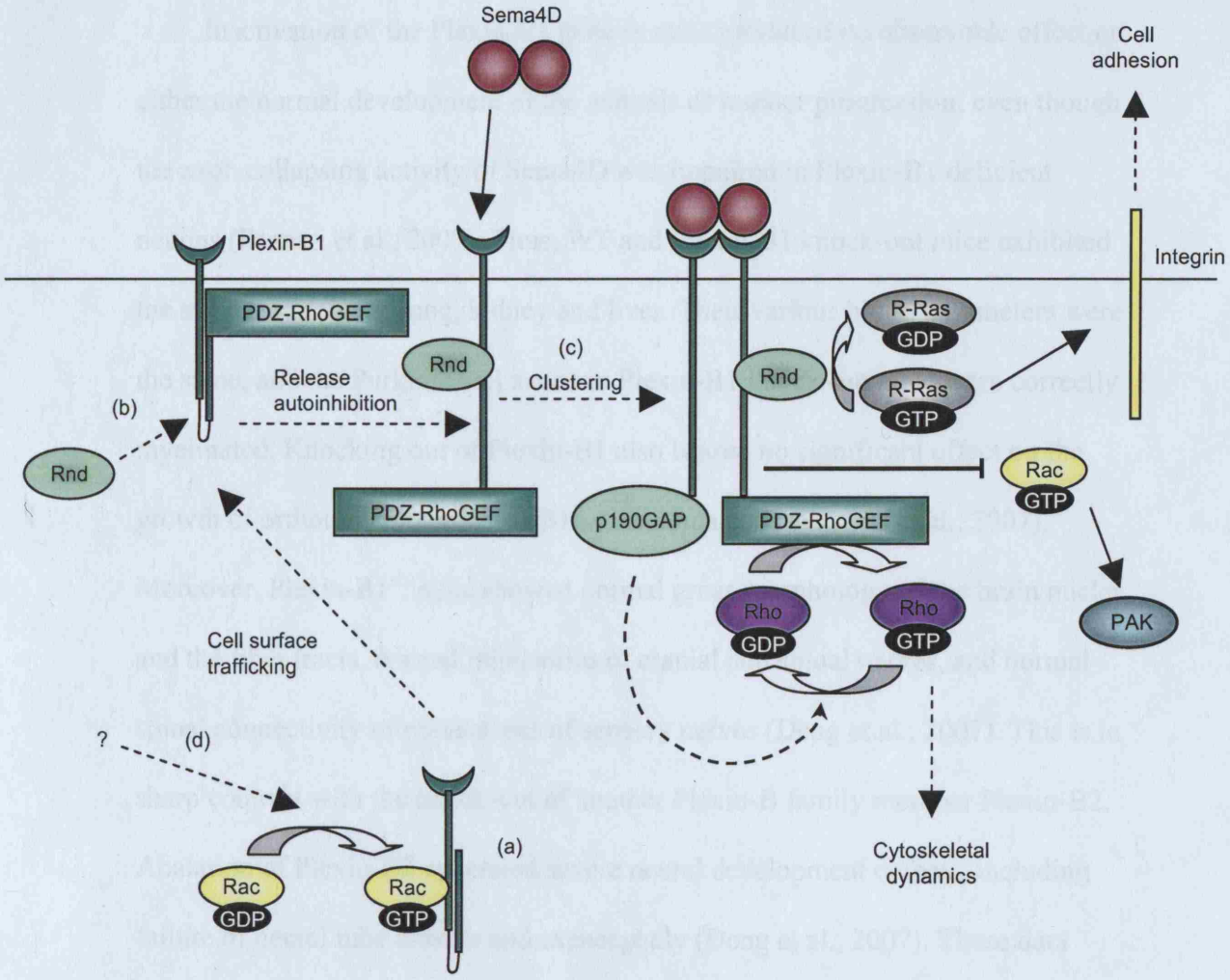

Figure 1.7 Model of Sema4D–plexin-B1 signalling in cell and growth-cone collapse. (a) In the absence of Rnd, the cytoplasmic region of plexin-B1 is closed owing to autoinhibitory intramolecular interactions. (b) Rnd1 binds to plexin-B1 and relieves the 'closed' conformation of the plexin-B1 cytoplasmic region. (c) In an 'open' conformation, plexin-B1 can induce several cytosolic signalling events induced to cluster by Sema4D: first, plexin-B1 sequesters active Rac1 away from its downstream targets, including p21-activated kinase (PAK); second, plexin-B1 functions as an Rnd1-dependent GAP for R-Ras. Inactivation of R-Ras suppresses integrin activation and, consequently, reduces cell adhesion; third, the C-terminal PDZ-binding motif of plexin-B1 binds to the RhoGEFs PDZ-RhoGEF and LARG. Sema4D–plexin-B1 interactions increase PDZ-RhoGEF and LARG activity, leading to RhoA activation and collapse responses. Interestingly, Rnd proteins can bind to and stimulate p190 RhoGAP, an event shown to antagonize RhoA activation. (d) Rac-GTP binding may regulate the sensitivity of the cell toward Sema4D by controlling the cell surface trafficking of Plexin-B1.

1.4.2 Knock-out studies

Inactivation of the Plexin-B1 gene in mice produced no observable effect on either the normal development of the animals or tumour progression, even though the axon collapsing activity of Sema4D was impaired in Plexin-B1 deficient neuons (Fazzari et al., 2007). Thus, WT and Plexin-B1 knock-out mice exhibited the same histology of lung, kidney and liver. Their various blood parameters were the same, and the Purkinje cell axons in Plexin-B1 knock-out mice were correctly myelinated. Knocking out of Plexin-B1 also beared no significant effect on the growth of orthotopically injected B16 melanoma cells (Fazzari et al., 2007). Moreover, Plexin-B1$^{-/-}$ mice showed normal gross morphology of the brain nuclei and the fiber tracts, normal trajectories of cranial and spinal nerves, and normal spinal connectivity of populations of sensory nerves (Deng et al., 2007). This is in sharp contrast with the knock-out of another Plexin-B family member Plexin-B2. Abalation of Plexin-B2 generated severe neural development defects, including failure of neural tube closure and exencephaly (Deng et al., 2007). These data suggested that Plexin-B1 is not essential for neural development, even though it is highly expressed in neural tissues during development. The true physiological function of Plexin-B1 remains to be discovered.

1.5 Hypothesis

Based on the distribution of Plexin-B1 mutations in primary and metastatic prostate cancer, we hypothesize that Plexin-B1 mutations play a role in prostate cancer progression. The effect of the mutations may be mediated by (1) altering the interactions between plexin-B1 and downstream signalling molecules e.g. PDZRhoGEF and, Rnd, leading to their aberrant activation or inactivation; (2)

interfering with the phosphorylation of plexin-B1 or Met/ErbB-2 which leads to inappropriate signalling from the receptors; (3) changing the binding properties of the receptor to the ligand Sema4D.

The aim of this project is to identify the effects of three mutations in the *PLXNB1* gene, A5359G, A5653G and T5714C, on the molecular functions of the Plexin-B1 protein.

Chapter 2

Materials and Methods

2.1 Cell culture

COS-7 cells were grown in DMEM medium (Invitrogen) supplemented with 8% Fetal Bovine Serum (FBS).

NIH-3T3 cells were grown in DMEM medium (Invitrogen) supplemented with 10% Newborn Claf serum (NCS).

HEK293T cells were grown in RPMI1640 medium (Invitrogen) supplemented with 8% FBS.

2.2 Plasmid constructs

The expression constructs for VSV-Plexin-B1WT and Sema4D-AP were kind gifts from Dr. L Tamagnone. The expression construct for PDZ-RhoGEF was from Dr. M.H. Driessen. The expression construct for RhoA was from Dr. J.M. Swiercz. The expression plasmids for RacL61 and RacN17 were kind gifts from Dr. KL Guan.

2.3 Transformation of E.coli

Subcloning Efficiency DH5α (Invitrogen cat. # 18265-017) or One Shot® OmniMax™-T1^R Chemically Competent *E.coli* cells (Invitrogen cat. # C8520-03) were used for transformation of intact plasmids or ligation mixtures respectively. 0.25μg of intact plasmid or the whole of a ligation mixture was mixed with 50μl of competent cells and incubated on ice for 20min. Afterwards the mixture was heat-shocked at 42°C for 1 minute and then incubated on ice for 2 minutes. 300μl of S.O.C. media (Invitrogen cat. # 15544-034) was then added and the cells were incubated at 37°C for one hour before plating on LB agar plates with 50μg/ml

Ampicillin (Sigma cat. # A2804). The plate was incubated at 37°C overnight until colonies appeared.

2.4 Miniprep of DNA

Purifications of DNA from 1-5ml culture of *E.coli* were done with QIAprep Spin miniprep kit (Qiagen cat. # 27104). All steps were performed at room temperature unless otherwise stated. Bacteria were collected by centrifugation (5000rpm for 5mins) then the pellet of bacterial cells was resuspended in 250µl Buffer P1 and transferred to a microcentrifuge tube. Next, 250µl of Buffer P2 was added and mixed thoroughly by inverting the tube 4–6 times. The mixture was allowed to stand for 5 minutes, before 350µl of Buffer N3 was added and mixed immediately by inverting the tube 4-6 times. The precipitate so formed was spun down (13000rpm for 10min) in a table-top microcentrifuge. The supernatants were applied into the QIAprep spin columns by decanting or pipetting. The spin columns were centrifuged for 30–60s at 13000rpm and the flow-through discarded. The spin columns were washed by adding 0.75 ml Buffer PE and centrifuged for 30–60s at 13000rpm. The flow-through was discarded and the spin column was centrifuged for an additional 1 min to remove residual wash buffer. The column was eluded by placing the column in a clean 1.5ml microcentrifuge tube and adding 50µl Buffer EB (10 mM Tris-Cl, pH 8.5) to the center of each QIAprep spin column, let stand for 1 min, and centrifuged for 1 min.

2.5 Maxiprep of DNA

Large scale purifications of DNA from 100 to 500ml culture of *E.coli* were done using QIAGEN Plasmid Maxi Kit (Qiagen cat. # 12163). For each

purification, a single colony was picked from a freshly streaked selective plate and inoculated into a starter culture of 2–5 ml LB medium containing the appropriate selective antibiotic. The starter culture was incubated for approximately 8 hours at 37°C with vigorous shaking at 300rpm. After the incubation, 0.5 ml of the starter culture was diluted 1/200 to 1/1000 (100ml and 500ml respectively) into selective LB medium. The culture was incubated at 37°C for 12-16 hours with vigorous shaking (250rpm). The bacterial cells were harvested by centrifugation at 6000g for 15min at 4°C. The bacterial pellet was resuspended in 10ml Buffer P1 (supplemented with RNase A provided with the kit). Then 10ml of Buffer P2 was added to the resuspended culture, mixed thoroughly by vigorously inverting the sealed tube 4-6 times, and incubated at room temperature for 5 minutes. 10ml of chilled Buffer P3 was added then and mixed immediately and thoroughly by vigorously inverting 4-6times. The mixture was incubated on ice for 20min. To remove the precipitate, the mixture was centrifuged at 20000g for 30min at 4°C. During the centrifugation, a QIAGEN-tip 500 was equilibrated with 10ml Buffer QBT, and allowed to empty by gravity flow. The supernatant from the centrifuged mixture was applied to the QIAGEN-tip 500 column and allowed to enter the resin by gravity flow. The QIAGEN-tip was washed with 2 x 30ml Buffer QC. The bound DNA was eluted into a 50ml centrifugation tube with 15ml Buffer QF. The eluded DNA was precipitated by adding 10.5ml isopropanol and centrifuged at 20000g for 15min at 4°C. The resultant DNA pellet was washed with 5ml 70% ethanol and spun down at 20000g for 5min at 4°C. The ethanol was then removed and the DNA pellet was let air-dried. The air-dried DNA pellet was redissolved in 0.5ml TE (Tris-EDTA pH 8) and the DNA concentration measured by spectrophotometry.

2.6 Agarose electrophoresis for DNA

The DNA from purifications, PCR or restriction digestions were analysed by agarose gel electrophoresis. One gram of agarose (BDH cat. # 443665WP) was mixed with 100ml 0.5X Tris-borate-EDTA (TBE; 90mM Tris-borate, 2mM EDTA, pH 8.3) buffer, heated at full power in microwave oven until the agarose was dissolved and then 2 μl of ethidium bromide (0.5μg/ml) was added. The gel was poured into the gel cast with combs *in situ* until set. The gel together with the gel cast was immersed in TBE in the electrophoresis unit (Electro-4Gel Tank, Thermo Electron Corporation). Samples were mixed with 1/5 sample volume of 6X DNA loading dye (0.25% bromophenol blue, 0.25% xylene cyanol FF, 30% glycerol in H_2O) before loading into wells. A lane of 1kb Plus DNA ladder (Invitrogen cat. # 10787-026) marker was also included in each gel (0.5μg per lane). The gel was run in 150V for one hour or until the separation of desired bands. The DNA in complex with ethdium bromide was visualized by using a UV transilluminator (Gene Genius, Bio Imaging System).

2.7 DNA sequencing

Sequencings were done to confirm the correct cloning or successful mutagenesis. Regions of interest on each individual plasmid were amplified by PCR using primers shown in Table 1. The PCR products were gel purified and sent to the DNA Analysis Facility of Ninewells Hospital in Dundee, together with the amplifying primers for sequencing. Concentration of each PCR product sent was 0.5ng/μl, whereas primers were sent at 5pmols/μl.

Table 1 Primers used in sequencing.

Primer name	Sequence	For sequencing of
pcdna3_884-903	5'-GACCCAAGCTTGGTACCGAG-3'	pVSVPlexinB1, VSV tag insertion
Plexin-B1_169_rv	5'-GGAACAGGAAGTTGGTAGCC -3'	
plxnB1_4647	5'-TGAGATGACCGATCTCACCA-3'	pVSVPlexinBl, xd/xf/xg mutagenesis
plxnB1_5534_rv	5'-GCTCCATCTGGGACCTTGT -3'	
pGEX_seq_fr	5'-GGGCTGGCAAGCCACGTTTGGTG -3'	pGEXB1cyto, 5' and 3' insert-vector junctions
pGEX_seq_rv	5'-CCGGGAGCTGCATGTGTCAGAGG -3'	
pcDNA3.1D_786	5'-CGTGTACGGTGGGAGGTCTA -3'	pTOPOMet, 5' and 3' insert-vector junctions
pcDNA3.1D_1070rv	5'-GTGATGATGACCGGTACGC -3'	

2.8 DNA purification from sliced agarose gel

Purification of DNA of a specific size was done by first running the DNA sample through an agarose gel, then the gel containing the desired DNA band was cut out. The DNA contained in the gel slice was extracted by using QIAquick PCR Purification Kit (Qiagen cat. # 28106). Three volumes of Buffer QG was added to one volume of gel. The gel was then incubated at 50°C for 10 min (or until the gel slice has completely dissolved). If the size of DNA fragment to be purified was <500 bp or >4 kb, one gel volume of isopropanol was added to the sample and mixed. A QIAquick spin column was placed in a provided 2ml collection tube. The sample was applied to the QIAquick column for DNA binding, and centrifuged for 1 min. The flow-through was discarded and the QIAquick column was placed back in the same collection tube. Then 0.75ml of Buffer PE was added to the QIAquick column and centrifuge for 1 min for washing. The flow-through was discarded and the QIAquick column was centrifuged for an additional 1 min at 13,000 rpm (~17,900*g*) to remove residual

wash buffer. The QIAquick column was then placed into a clean 1.5ml microcentrifuge tube. 50 µl of Buffer EB (10 mM Tris·Cl, pH 8.5) or H2O was added to the center of the QIAquick membrane and the column was centrifuged for 1min to elute the bind DNA. Alternatively, for increased DNA concentration, 30µl elution buffer was add to the center of the QIAquick membrane, the column let stand for 1min, and then centrifuged for 1min.

2.9 Lipofectamine transfection

For COS-7 cells, 5 x 10^5 cells were seeded into each well of a 6-well plate one day before transfection. The seeding cell density for HEK293T was 8 x 10^5 cells per well. For each transfection, 10µl of Lipofectamine2000 reagent was mixed with 250µl of OptMEM®I (Invitrogen) serum-free medium. In a separated tube, 0.4-4µg of plasmid was mixed with 250µl OptMEM®I according to experiment. The Lipofectamine mixture was added to the DNA mixture and incubated at room temperature for 15 minutes, before the final mixture was added directly into the growth medium in the 6-well plate. Six hours later the transfection growth medium was replaced with normal growth medium.

2.10 Insertion of VSV tag

A VSV tag was inserted near the N-terminus of Plexin-B1 to facilitate detection and immunoprecipitation. PCR products flanking the insertion site (between nucleotide 78 and 79 according to Genebank sequence X87904) were produced with pcDNA3-plexin-B1 as template. VSV tag sequence was added in the primers, so that the two PCR products' sequences overlap on the VSV sequence. The two PCR products were gel purified, annealed and extended in the

first two cycles of the following PCR reaction, and then primers flanking the whole final product were added. The scheme of the cloning strategy is depicted in Figure 3.1A. The Primer sequences are: 5'-GACCCAAGCTTGGTACCGAG-3'/5'-CTTACCCAGGCGGTTCATTTCGATATCAGTGTAAGTTGGTGGAAGGGGCTGGA-3' (PCR upstream of insertion); 5'-TACACTGATATCGAAATGAACCGCCTGGGTAAGGCATTCACTCCCAATGGCAC-3'/5'-ATTGTGTGTCCCCAGGCCGC-3' (PCR downstream of insertion) The VSV sequence in the primers are underlined. The PCR reactions were set according to the following table:

PCR component	Volume per reaction
10X Reaction Buffer	5μl
10mM dNTP	1μl
10μM Primer A	2μl (added after cycle 2)
10μM Primer B	2μl (added after cycle 2)
QuickSolution	3μl
Template PCR products	0.5μl each
Pfu Turbo DNA polymerase (Stratagene)	1μl
H_2O	35μl
Total:	50μl

The reactions were subjected to the following PCR condition in a Px2 Thermal cycler (Thermo Electron Corporation):

Cycling parameters		
95°C	1 min	
95°C	50s	30 cycles
60°C	50s	
68°C	1 min	
68°C	7 min	

The PCR product was digested with KpnI and SfiI and gel purified. pcDNAPlexin-B1 was digested with KpnI and SfiI and the larger fragment was gel purified. The digested PCR product and pcDNAPlexin-B1 large fragment were then ligated.

2.11 *In vitro* mutagenesis

pcDNA3-plexin-B1A5359G/ A5653G/T5714C were generated using QuickChange II XL *in vitro* mutagenesis kit (Stratagene cat. # 200522). The sequences of mutatagenesis primers used are : 5'-GTCCATCTGTCTGTAT**GCC**TTCGTGAGGGACTC-3'/5'-GAGTCCCTCACGAA**GGC**ATACAGACAGATGGAC-3' (A5359G); 5'-AGTGCCTCTC**GCC**CAGCGGCCAG-3'/5'-CTGGCCGCTG**GGC**GAGAGGCACT-3' (A5653G); 5'-GGCCGGGCAC**CCC**ATTCTTTCTGACGA-3'/5'-TCGTCAGAAAGAAT**GGG**GTGCCCGGCC-3' (T5714C). The changed codons are in bold. The following mutagenesis reaction was setup for each mutation:

10X reaction buffer 5μl

10ng/μl template DNA (pcDNA3-plexin-B1)	1μl
100ng/μl Primer 1	1.25μl
100ng/μl Primer 2	1.25μl
100mM dNTP	1μl
QuickSolution	3μl
Distilled water	36.5μl
Pfu Turbo DNA polymerase	1μl

PCR cycling parameters:

95°C	1minute	
95°C	50s	⎫
60°C	50s	⎬ 18cycles
68°C	12minutes	⎭
68°C	7minutes	

1μl (10U/μl) *DpnI* was added to the PCR reaction and the mixture was incubated at 37°C to digest the parental DNA template. 2μl of the reaction was then used to transform XL10-Gold Ultracompetent E.coli by first incubating on ice for 30 minutes, followed by 30s of heat shock at 42°C and allowing the cells to recover for 1 hour at 37°C. The cells were then plated on LB-agar plates containing 50μg/ml ampicillin. Colonies were picked and the plasmid DNA prepared by miniprep for screening.

2.12 Collection of total cell lysate and measurement of total protein concentration

To obtain total cell lysate for immunoprecipitation experiments or western analyses, cells were lysed with Cytobuster (Novagen cat.# 71009-4) protein extraction reagent or Modified Radioimmunoprecipitation (RIPA) buffer (50mM Tris pH 7.4, 1% NP-40, 0.25% sodium deoxycholate, 150mM NaCl, 1mM EDTA) supplemented with Complete Mini Protease Inhibitor Cocktail tablets (1 tablet per 10ml of extraction buffer)(Roche cat. # 11836153001). For each well in a 6-well plate, 300µl of extraction buffer was used. The cells were incubated with extraction buffer for 30 minutes at 4°C. The cell lysate was collected and cleared by centrifugation at top speed on a desktop centrifuge for 10 minutes at 4°C. After centrifugation the supernatant was obtained and the cell debris was disposed of.

The total protein concentrations of the lysates were measured with Modified Lowry Protein Assay Kit (PIERCE cat. # 23240). To setup the standard curve, BSA standards (Conc. of standard provided by kit : 2000 µg/ml) were prepared according to the following table:

Protein standard solution (µl)	Distilled water (µl)	Final Protein concentration (µg/ml)
0	200	0
5	195	50
10	190	100
20	180	200
30	170	300
40	160	400

Twenty μl of each sample was added with 180μl water to dilute it 10-fold. Then 1ml Modified Lowry reagent was added into each tube of sample or standards. The tubes were ticked before standing for 10mins at room temperature. While the tubes were standing 1X Folin & Ciocalteu's Phenol reagent was prepared from 2X using distilled water. After the 10 minute incubation, 100μl 1X Folin & Ciocalteu's Phenol reagent was added to each tube with rapid and immediate mixing. The reaction was incubated for 30 minutes at room temperature. The reactions were then transferred to plastic cuvets. Measurements of the absorbance of STANDARDS and SAMPLE tubes VS. Blank were made at wavelength 750nm. The measurements were completed within 30mins.

2.13 SDS-PAGE

SDS-PAGE gels were set according to the follow table (volume of component per gel):

	6%	8%	10%	12%	14%
1M Tris pH8.8	3.75ml	3.75ml	3.75ml	3.75ml	3.75ml
30% Acrylamide	2ml	2.67ml	3.33ml	4ml	4.67ml
H_2O	4.2ml	3.53ml	2.87ml	2.2ml	1.53ml
20% SDS	50μl	50μl	50μl	50μl	50μl
10% APS	100μl	100μl	100μl	100μl	100μl
TEMED	6μl	6μl	6μl	6μl	6μl

After mixing the components, 8ml gel solution was pour into an assembled PROTEAN II gel casting apparatus (Bio-Rad). When the separating gel was set, stacking gel was prepared as follows (components per gel):

1M Tris 6.8	375μl
30% Acrylamide	374μl
H_2O	2.24ml
20% SDS	15μl
10% APS	30μl
TEMED	5μl

The Comb for forming wells was pushed into the stacking gel before the stacking gel was set. Each cell lysate sample was added with one fifth volume of 6X SDS-loading buffer (60% glycerol, 300mM Tris pH 6.8, 12mM EDTA, 12% SDS, 864mM β-mercaptoethanol, 0.05% bromophenol blue), and heated at 95°C for 8 minutes before being loaded into the gel. Immunoprecipitation samples eluted with SDS-loading buffer were loaded directly into the gel. The gel was run at 80mA constant current until the dye front ran out from the gel.

2.14 Western analysis

The proteins in a SDS-PAGE gel were electroblotted onto a PVDF membrane (Sigma cat. # P2813) using Mini Trans-Blot cell (Bio-Rad cat. # 170-3836). Everything shown in the following figure was soaked in 1 X transfer buffer (12.5mM Tris, 100mM glycine) right before use. PVDF membrane was pre-wet in 100% methanol (15 seconds) then soaked in 1 X transfer buffer before use. The

gel and membrane was assembled and placed this way up on CLEAR HALF of the cassette:

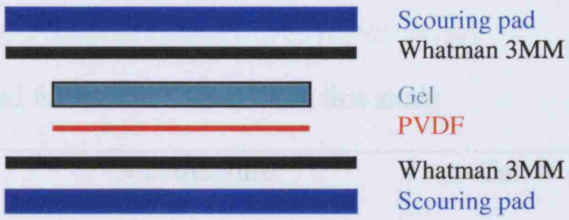

The cassette was placed into the western tank (placed on magnetic stirrer), so that the black half of the cassette is nearest the black electrode (cathode). The tank was topped up with 1 X transfer buffer. The electrodes were connected to powerpack and transfer done overnight at 20V at 4°C.

After the transfer, the membrane was taken off gel and stained with ponceau S (SIGMA) if cutting was necessary. Otherwise the membrane was directly put into blocking solution (5% marvel non-fat milk in 0.1% PBS-Tween) in a 50ml centrifugation tube and blocked for 1 hr at room temperature with gentle rocking and rolling. After the blocking step, the membrane was put into 5 ml of primary antibody solution (dilution according to Table 2 using 1% milk in 0.1% PBS-Tween) and incubated for 1 hr at room temperature. The membrane was then washed 4 times with 0.1% PBS-Tween. 5 ml of secondary antibody solution (HRP-conjugated Anti-Rabbit IgG sc-2004 or Anti-Mouse IgG sc-2005, Santa Cruz, 1/10000 dilution in 1% milk in 0.1% PBS-Tween) was then added and incubated for 1 hr. The membrane was washed 4 times with 0.1% PBS-Tween before 3ml of SuperSignal West Pico Chemiluminescent Substrate (PIERCE cat. # 34078) was added. After that the membrane was mounted between two sheets of

transparency and put into a Kodar BioMax cassette. Kodak® BioMax™ light films (Sigma cat. # Z370371)were exposed to the membrane for various periods of time. The films were developed by conventional means.

Table 2. Antibodies used for western analysis in this study

Against antigen	Manufacturer	Cat. #	Dilution
VSV tag	Sigma	V4888	1/3000
myc tag	Sigma	C3956	1/5000
Flag tag	Sigma	F7425	1/5000
Plexin-B1	Santa Cruz	sc-25642	1/1500
GST tag	Sigma	G7781	1/5000
V5 tag	Sigma	V8137	1/5000
Human IgG Fc	Jackson ImmunoResearch Laboratories	109-005-098	1/10000
PAK	Chemicon	AB3844	1/1000
Phospho-PAK1 (Thr423)	Cell Signalling	2601	1/1000
CD2	Abcam	ab33767	1/5000
Anti-Rabbit IgG-HRP	Santa Cruz	sc-2004	1/10000
Anti-mouse IgG-HRP	Santa Cruz	sc-2005	1/10000
ErbB-2	Upstate	06-562	1/5000
Phospho-erbB-2/HER-2 (Tyr1248)	Upstate	06-229	1/5000

2.15 Expression and purification of Sema4D-AP

One day before transfection, 6 x 10^6 COS-7 cells were seeded into each of four T175 tissue culture flasks. 48μg GST-Sema4D-AP expression plasmid per flask was transfected into the COS-7 cells by Lipofectamine2000 transfection reagent according to manufacturer's instruction. Four days after transfection, the supernatant was filtered through 0.2μm filter. The supernatant was stored at 4°C before further purification. Procedures hereafter were all carried out in 4°C unless otherwise stated. The storage buffer of a pre-packed glutathione sepharose 4B column from the GST purification modules (Amersham) was drained and washed with two bed volumes of PBS. The filtered supernatant was loaded into the prepacked glutathione column. After washing with ten bed volumes of PBS, the bound protein was eluted with 10mM glutathione, 50mM Tris-HCl pH 8.0. The fractions were analysed by Coomassie Blue staining in 8% SDS-PAGE gel.

2.16 Immunoprecipitation

8 x 10^5 HEK293T cells were seeded into each well of a 6-well plate one day before transfection. The HEK293T cells were transfected with 3μg pVSVPlexin-B1WT/mutant and 1μg Sema4D-Fc expression plasmid (or other expression construct according to experiment) per well with Lipofectamine2000. Twenty-four hours after transfection the cells were first washed with PBS then lysed on ice with 500μl CytoBuster protein extraction reagent (Novagen) supplemented with Complete Mini Protease inhibitor (1 tablet per 10ml, Roche cat. # 11836153001) per well for 30min. Lysate was cleared by centrifugation at 10,000g for 10mins at 4°C. 400μl of the lysate was used in each immunoprecipitation. The lysate was precleared by mixing with 20μl protein A agarose (Invitrogen cat. # 15918-014)

and rocked at 4°C for one hour. The pre-cleared lysate was collected by centrifugation at 8000g for 1 minute. Afterwards, 1μg of goat anti-Fc antibody (or 1μg of anti-VSV) was added into the lysate and incubated at 4°C for one hour. The antigen-antibody complex was precipitated by incubating with 40μl of protein A agarose with rocking at 4°C. The immune complexes were washed three times with the lysis buffer and eluted by boiling in 40μl 2X SDS-PAGE sample buffers.

2.17 In situ binding of Sema4D-AP with Plexin-B1

COS-7 cells were seeded on a 6-well plate at a cell density of 5 x 10^5 per well. The cells were transfected with expression plasmids for Plexin-B1 WT or mutant the next day by Lipofectamine2000. One day after transfection, the cell were washed with 1 ml HBAH (Hanks balanced salt solution with 20mM HEPES pH 7.0, 0.5mg/ml BSA, 0.1% (w/v) NaN_3) per well followed by treatment of 1ml HBAH containing 1000ng/ml Sema4D-AP per well for 90 minutes at room temperature. After the treatment, the cells were washed six times with ice-cold HBAH. For each wash, cells were incubated with HBAH for 5 min and gently swirled by a platform shaker. The last HBAH wash was aspirated and the cells were fixed with 1ml of acetone-formalin fixative (65% (v/v) acetone, 8% (v/v) formalin, 20mM HEPES pH 7.0) per well for 15 sec. The fixative was removed by aspiration and the cells washed twice with 1ml of HBS (150mM NaCl, 20mM HEPES pH 7.0). The last wash was left in the wells. The plate was then floated on a 65°C water bath for 100min to inactivate the endogenous alkaline phosphatase activities. The HBS was aspirated off after the incubation and the cells were first washed with 0.5ml BCIP/NBT (5-bromo-4-chloro-3-indolyl phosphate/nitro blue tetrazolium) solution (SIGMA cat. # B5655) and then incubated with 1ml

BCIP/NBT solution per well at room temperature under a shade of aluminum foil. The reaction was stopped by washing the plate with PBS when sufficient color was developed. Each well of cells were stored in 1 ml of PBS with 10mM EDTA at 4°C in the dark.

2.18 Inducing competence in and transforming BL21

BL21 strain of E.coli was obtained from Amersham. One single colony of *BL21* was inoculated into 5ml of LB medium and grown at 37°C overnight. 4ml of the overnight culture was inoculated into 400ml LB medium next morning and let grown until $OD_{590} > 0.375$. The culture was then divided into eight aliquots in 50ml pre-chilled tubes and left on ice for 10 minutes. The cells were then centrifuged at 1600g, 4°C for 7 minutes. The supernatant was removed before the cell pellets were resuspended in 10ml ice-cold $CaCl_2$ solution (60mM $CaCl_2$, 15% glycerol, 10mM PIPES). This washing step was repeated once more and then the resuspended cells were kept on ice for 30 minutes. The cells were then collected by centrifugation for 5 minutes at 4°C 1100g. The cell pellets were resuspended in 2ml ice-cold $CaCl_2$ solution. The cell solution was dispensed into 250µl aliquots and frozen at -70°C. To transform the competent *BL21*, 0.5µg of DNA was mixed with 250µl of thawed BL21 competent cells. The mixture was incubated on ice for 20 minutes, followed by heat shock at 42°C for 1 minute and then 300µl of S.O.C medium was added. The mixture was incubated at 37°C for 1 hour. 100µl of the transformation mixture was spread onto selective agar plates (ampicillin 50µg/ml) and incubated overnight at 37°C.

2.19 GST-B1cyto purification

The region on Plexin-B1 cDNA encoding the intracellular domain (aa 1512-2135, accession no. X87904) was amplified by PCR (primers used are shown in Table 3). The PCR product was cloned into pGEX-4T-3 (Amersham) by SalI and XhoI sites to produce pGEXB1cytoWT. Mutations were introduced into pGEXB1cytoWT by using QuickChange II XL *in vitro* mutagenesis kit (Stratagene) according to manufacturer's instruction.

To produce sepharose beads bound by the GST-B1cyto fusion proteins, pGEXB1cyto WT/mutants were transformed into BL21 strain of *E.Coli.*. When the *E.Coli.* cultures reached $OD_{600}\approx0.6$ expression of the fusion protein was induced with 0.1μM IPTG for 3 hours. After that cells were harvested by centrifugation and lysed with Cellytic B (Sigma) supplemented with 0.2mg/ml lysozyme (Sigma), 50μg/ml DNaseI (Sigma) and 1X Halt protease inhibitor cocktail (Pierce). GST fusion protein in the lysate was purified with Glutathione Sepharose 4B (Amersham). The bound proteins were analysed by Coomassie Blue staining in 8% SDS-PAGE gel.

To assess the binding of GST-B1cyto WT/mutants to Rac, HEK293T lysate expressing RacL61 or RacN17 was obtained. 20μl of GST-fusion protein coated sepharose beads were added into 30μg of lysate and incubated overnight at 4°C. The beads were then washed with lysis buffer and the bound protein was eluted with SDS-loading buffer followed by SDS-PGAE and western analysis.

Table 3. Primers used for pGEXB1cytoWT/xd/xf/xg cloning.

Primer sequence	Use	Remark
AAAAAAGTCGACAGGAGGAAGAGCAAGCAGGC	pGEXB1cytoWT cloning	Underlined: SalI site
AAACTCGAGCTATAGATCTGTGACCTTGT	pGEXB1cytoWT cloning	Underlined: XhoI site
GTCCATCTGTCTGTAT**G**CCTTCGTGAGGGACTC	pGEXB1cytoxd cloning	Bold: Mutation introduced
GAGTCCCTCACGAAGG**C**ATACAGACAGATGGAC	pGEXB1cytoxd cloning	Bold: Mutation introduced
AGTGCCTCTC**G**CCCAGCGGCCAG	pGEXB1cytoxf cloning	Bold: Mutation introduced
CTGGCCGCTGGG**C**GAGAGGCACT	pGEXB1cytoxf cloning	Bold: Mutation introduced
GGCCGGGCACC**C**CATTCTTTCTGACGA	pGEXB1cytoxg cloning	Bold: Mutation introduced
TCGTCAGAAAGAATG**G**GGTGCCCGGCC	pGEXB1cytoxg cloning	Bold: Mutation introduced

2.20 Immunocytochemistry

To prepare coverslips for immunocytochemistry experiments, the coverslips were first boiled in 1X TriGene disinfecting solution for half an hour with a microwave oven. The disinfecting solution was washed away by running the coverslips under cold tap water for one hour. After that the coverslips were rinsed with distilled water five times. The coverslips were then soaked in 100% ethanol for 5 minutes, before being spreaded on 3MM paper to dry. Dry coverslips were put into metal container and baked at 180°C for two hours.

One day before transfection, one coverslip was placed into each well of a 6-well plate. The coverslips were coated with fibronectin dependent on experiments. To coat the coverslips with fibronectin, 1 ml fibronectin solution (10μg/ml, Invitrogen cat. # 33016-015) was added into each well and incubated for overnight at 4°C. After aspiration of fibronectin solution the coverslips were incubated in 2% BSA in PBS for one hour at room temperature.

After cells were seeded onto the coverslip for an appropriate time and an appropriate treatment was given, cells were fixed by incubating in 4% paraformaldehyde for 10 minutes. The cell membrane was permeablized by incubating the cells with 0.1% Triton-X100 for 5 minutes. The cells were washed six times with PBS before before blocking with 2% BSA in PBS. After blocking the fixed cells were incubated with primary antibody solution for one hour with shaking. After washing with PBS three times the cells were incubated with secondary antibody solution supplemented with phalloidin-TRITC (1/10000, Sigma cat. # P1951) for one hour with shaking. After the incubation cells were washed six times with PBS before

mounting on to glass slides using mounting medium containing DAPI (Vector Laboratories cat. # H1200)

2.21 Cell spreading

Transfected COS-7 cells were plated on coverslips coated with 10μg/ml fibronectin for two hours. Unattached cells were washed away after 2 hours. Attached cells were fixed in 4% paraformaldehyde in PBS for 10 minutes, permeabilized with 0.1% Triton-X 100 in PBS for 5 minutes and then blocked for 20 miuntes with 2% BSA in PBS. The cells were then incubated with primary antibody (Santa Cruz anti-myc 4E10 1:2000) for one hour with shaking. After washing with PBS secondary antibody solution (Southern Biotech goat-anti-mouse FITC 1:200) supplemented with Phallodin-TRITC (Sigma 1:10000) was added. The incubation time for secondary antibody was one hour with shaking. After washing the coverslips six times with PBS, they were mounted on to glass slides with mounting medium (Vector Laboratories cat. # H1200). The stained cells were observed under a Nikon Diaphoto200 fluroscent microscope. Pictures were taken with a Nikon Digtal Camera DX1200 and captured with Nikon ACT-1 software. Transfected cells were identified be positive anti-myc staining. The number of transfected spread cells was counted verus transfected non-spread cells. The identities of the slides counted were blinded to the researcher. At least 200 cells were counted per slides.

2.22 Stress fiber formation assay

COS-7 cells were seeded onto coverslips without fibronectin coating at cell density of 2×10^5 one day before transfection. One day after transfeciton, cells were fixed in 4% paraformaldehyde in PBS for 10 minutes, permeabilized with 0.1%

Triton-X 100 in PBS for 5 minutes and then blocked for 20 miuntes with 2% BSA in PBS. The cells were then incubated with primary antibody (Santa Cruz anti-Plexin-B1 H-300, cat # sc-25642, 1:200) for one hour with shaking. After washing with PBS secondary antibody solution (Southern Biotech goat-anti-mouse FITC 1:200) supplemented with Phallodin-TRITC (Sigma 1:10000) was added. The incubation time for secondary antibody was one hour with shaking. After washing the coverslips six times with PBS, they were mounted on to glass slides with mounting medium with DAPI (Vector Laboratories cat. # H1200). The stained cells were observed under a Nikon Diaphoto200 fluroescent microscope. Pictures were taken with a Nikon Digital Camera DX1200 and captured with Nikon ACT-1 software. The number of cells possessing more than three straight actin bundles of at least 5μm long was counted. The identities of the slides counted were blinded to the researcher. At least 50 cells were counted per slides.

2.23 Alkaline phosphatase measurement

The alkaline phosphatase activity of the fractions were analysed with AP Assay Reagent A (Biogene). 50μl of the AP assay reagent A was added to a 1.5ml microfuge tube per sample to be assayed. Each sample was diluted 50-fold and 50μl of the diluted sample was mixed with the 50μl of AP Assay Reagent A. The reaction tube was mixed and incubated at 37°C until yellow colour is developed. The reaction time was recorded. The reaction was stopped by addition of 100μl 0.5N NaOH. The stopped reaction mix was diluted 5-fold with 800μl distilled water and OD_{405} was measured by a spectrophotometer.

2.24 Protease K treatment

HEK293 cells were transfected with 1 μg of VSV-plexin-B1 with or without 0.1 μg of myc-RacL61 expression constructs. Forty-eight hours posttransfection cells were washed in PBS and incubated in PBS with 0.02 mg/mL proteinase K for 30 minutes at 37°C. Cells were then washed with PBS (plus 1 mM PMSF), lysed in NP-40 buffer (20 mM Tris-Cl at pH 7.5, 100 mM NaCl, 1% NP-40) and subject to SDS-PAGE and Western blot with anti-B1cyto antibody (from Dr. K.L. Guan).

2.25 RhoA activity assay

One day before transfection, 2×10^6 COS-7 cells per dish were seeded in 100mm dishes with 5ml DMEM supplemented with 8% FBS and L-glutamine (culture medium). Then the cells were transfected by lipofectamine2000 with plasmids. Two days after transfection the cells were serum starved by culturing in DMEM supplemented with L-glutamine (serum starve medium) for 24 hours. Then the cells were treated with serum starved medium with or without 1000ng/ml Sema4D-AP for 15 minutes. Cells were lysed by 0.55ml/dish ice-cold 1X MLB (from Rho activation assay kit, Upstate, cat# 17-294) with protease inhibitors, scraped, and the lysates cleared by centrifugation (5 minutes, 14,000xg, 4°C). 0.5ml of each cell extract was aliquoted to a microfuge tube. 15μl of the GST-Rhotekin RBD (RhoA Assay Reagent), agarose was added into the cell extract. The reaction mixture was incubated for 45 minutes at 4°C with gentle agitation, after which the agarose beads were pelleted by brief centrifugation (10 seconds, 14,000xg, 4°C). The supernatant was removed and discarded. The beads were washed (add 0.5ml MLB, mix gently, pellet beads, remove MLB) 3 times with MLB. Care was taken to minimize loss of beads when MLB was removed. The agarose beads were then resuspended in 40μl of 2X

SDS sample buffer, added with 2μl of 1M dithiothreitol and boiled for 5 minutes. The condensate was collected by brief centrifugation. The pulldown proteins were analysed on western blotting analysis.

2.26 Silver staining of SDS-PAGE gel

Silver staining of SDS-PAGE gel was performed using SilverQuest silver staining kit from Invitrogen (cat# LC6070). All incubations were performed on a rotary shaker rotating at a speed of 1 revolution/sec at room temperature. 100 ml of each solution was used per gel. After electrophoresis, the SDS-PAGE gel was removed from the cassette and placed in a clean staining tray of appropriate size. The gel was first rinsed briefly with ultrapure water. Then it was fixed in 100 ml of fixative for 20 minutes with gentle rotation. The fixative solution was decanted and the gel was washed in 30% ethanol for 10 minutes. The ethanol was then decanted and 100 ml of sensitizing solution was added to the washed gel in the staining container and incubated for 10 minutes. The gel was washed in 100 ml of 30% ethanol for 10 minutes followed by 100 ml of ultrapure water for 10 minutes. The gel was incubated in 100 ml of staining solution for 15 minutes. The staining solution was decanted after staining was completed and the gel was washed with 100 ml of ultrapure water for 20-60 seconds. The gel was then incubated in 100 ml of developing solution for 4-8 minutes until bands started to appear and the desired band intensity was reached. Once the appropriate staining intensity was achieved, 10 ml of stopper solution was immediately added directly to the gel still immersed in developing solution. The gel was gently agitated for 10 minutes. The Stopper solution was decanted and the gel was washed with 100 ml of ultrapure water for 10 minutes.

Chapter 3

Effects of Plexin-B1 mutations on ligand binding

3.1 Introduction

Plexin-B1 is the cognate receptor for Sema4D outside the immune system (Tamagnone et al., 1999). It is responsible for the axon guidance function of Sema4D (Worzfeld et al., 2004; Oinuma et al., 2004a; Oinuma et al., 2004b). Unlike the case for Class 3 semaphorins, Plexin-B1 is fully capable of binding to Sema4D without the assistance of co-receptors (Tamagnone et al., 1999). The capacity of binding to Sema4D is therefore crucial to the functioning of Plexin-B1.

It is suggested that binding of Sema4D to Plexin-B1 leads to the dimerization of the receptor protein. Thus, the interaction between ectopically expressed Plexin-B1 carrying different tags increased upon Sema4D binding (Oinuma et al., 2004b). Moreover, cellular responses upon activation of Plexin-B1 could be mimicked by crosslinking CD2-Plexin-B1 by anti-CD2 antibody, giving support to the dimerization model (Driessens et al., 2001).

The aim of this part of the study was to investigate whether A5359G, A5653G, and T5714C mutations have any effect on the ligand binding capacity of Plexin-B1. To achieve this aim, firstly a DNA sequence encoding a VSV tag was cloned into the mammalian expression construct for Plexin-B1 WT. Expression constructs for VSV-tagged mutant Plexin-B1 were then generated from the WT construct by *in vitro* mutagenesis. A VSV tag was inserted to facilitate the detection and immunoprecipitation of the exogenously expressed Plexin-B1 proteins. Secondly, an expression construct for recombinant Sema4D was obtained from Dr. Tamagnone. Sema4D protein was produced and affinity purified taking advantage of the GST tag on the recombinant protein. Finally the interaction between Sema4D and Plexin-B1 mutants were tested with two techniques, namely coimmunoprecipitation and *in situ* staining with recombinant Alkaline phosphatase. The cloning and verification of

pTOTO-hMET/V5/His, a mammalian expression construct of human HGF receptor Met, were also described in this Chapter.

3.2 Results

3.2.1 Tagging of WT Plexin-B1 with VSV

I sought to examine the interaction between Plexin-B1 and its known binding partners by coimmunoprecipitation. The expression plasmid pcDNAPlexin-B1 was obtained from Dr. Alan Hall (Driessens et al., 2001). To facilitate carrying out of coimmunoprecipitation experiments, a VSV tag was inserted near the N-terminus of Plexin-B1 by a PCR cloning method. To avoid disturbing the membrane localizing signal which is located at the very N-terminus and to avoid disrupting the PDZ binding domain at 3' end, the VSV tag was inserted immediately C-terminal to the signal sequence but before the Sema domain (Fig. 3.1A). Briefly, the DNA sequence encoding the VSV tag was included in the primers for producing PCR products of the Plexin-B1 cDNA. The PCR product was then cloned into the original plasmid pcDNA3plexinB1. The insertion of VSV sequence was confirmed by sequencing (Fig. 3.1B). The expression construct for VSV-Plexin-B1 was named pVSVplexinB1. A similar expression construct for VSV-Plexin-B1 was also obtained from Dr. Tamagnone.

3.2.2 In vitro mutagenesis of VSV tagged WT Plexin-B1

A5359G, A5653G and T5714C mutations were introduced into pVSVplexinB1 by *in vitro* mutagenesis. Three colonies were picked from each plate and expanded into 2ml LB culture for screening. DNA Minipreps were done on the bacteria culture and the plasmid obtained was subjected to SfiI and KpnI digestion screening. All

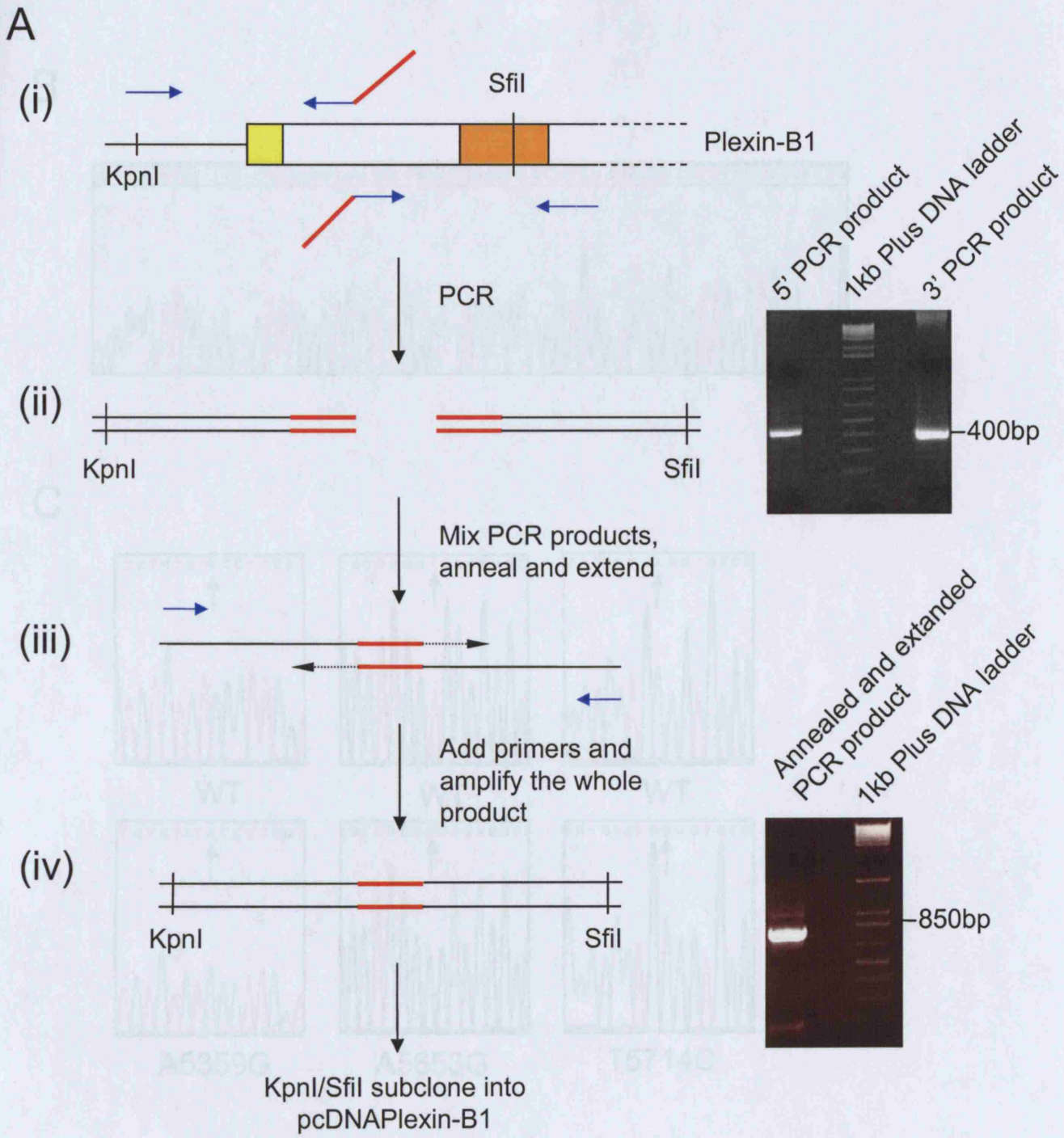

Figure 3.1 Cloning and expression of VSV-Plexin-B1. (A) Schematic representation of the cloning strategy of pVSVplexinB1. (i) Parts of the Plexin-B1 cDNA flanking the desired VSV tag insertion site were amplified by PCR from pcDNA3plexinB1. (ii) The two PCR products were then mixed, annealed and extended. (iii) Primers at the two ends were then added to amplify the whole product. (iv) The resultant PCR product was subcloned back into pcDNA3plexinB1 to yield pVSVplexinB1.The corresponding PCR products were shown on the right. Red: VSV tag sequence; Blue: Primers; Yellow: part of Plexin-B1 cDNA coding for membrane signal; Orange: part of Plexin-B1 cDNA encoding the Sema domain.

B

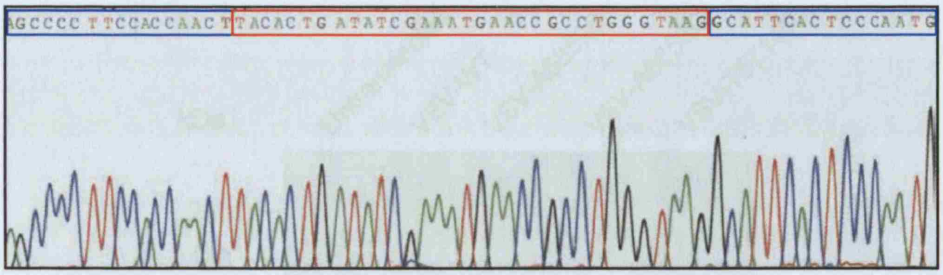

C

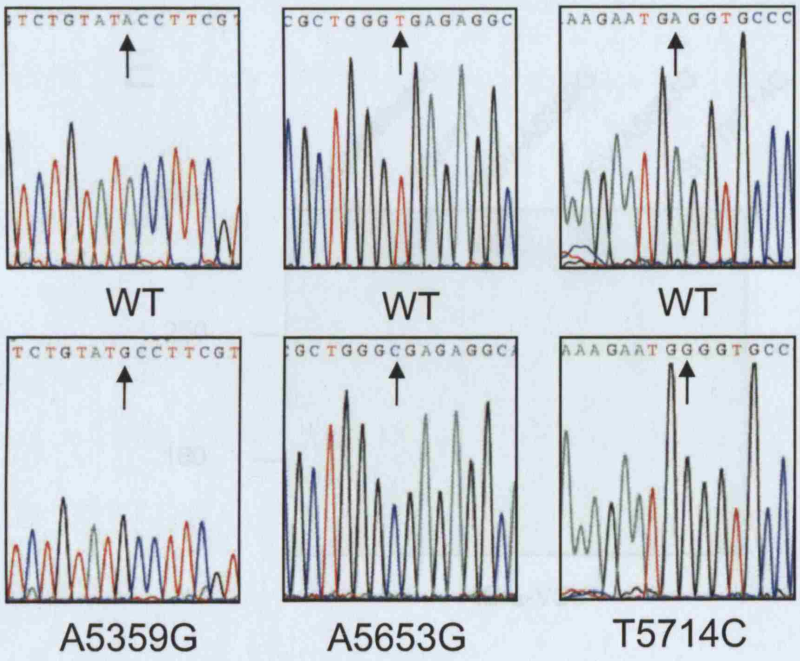

Figure 3.1 Cloning and expression of VSV-Plexin-B1. (B) Confirmation of the VSV sequence insertion by sequencing. Sequences in blue frame: Plexin-B1 sequence; sequence in red frame: VSV tag sequence. (C) Sequencing confirmation of mutagenesis. Mutations were introduced into pVSVplexinB1 by *in vitro* mutagenesis. Arrows indicate nucleotides mutated. The reverse complementary strands were shown for A5653G and T5714C mutations.

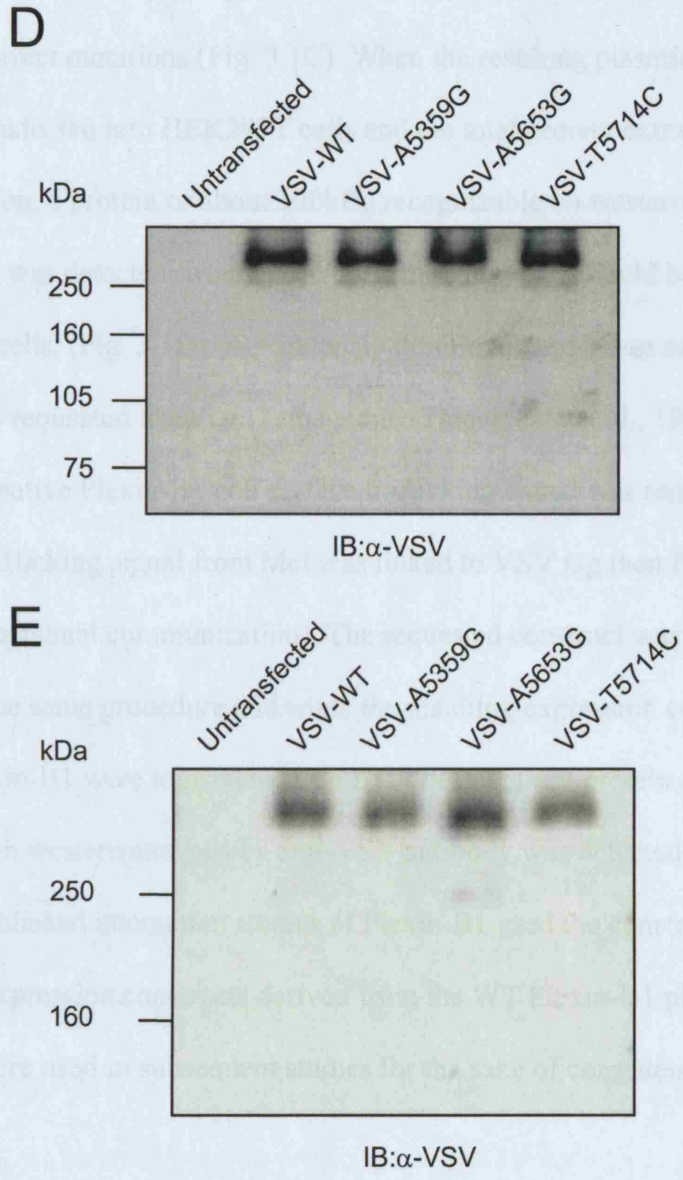

Figure 3.1 Cloning and expression of VSV-Plexin-B1. (D) Expression of VSV-Plexin-B1 in HEK293T transfected with pVSVPlexin-B1 was verified by western blotting analysis with anti-VSV antibody. (E) pVSVPlexin-B1 from Dr. Tamagnone expressed proteins of the same size.

clones gave the same restriction digestion fragments of expected sizes. Sequencing amplified products encompassing the mutations confirmed that all the clones picked harbour the correct mutations (Fig. 3.1C). When the resulting plasmids were transiently transfected into HEK293T cells and the total protein extracted one day after transfection, a protein of about 300kDa recognizable on western analysis by anti-VSV antibody was detected; whereas no corresponding band could be observed in untransfected cells. (Fig. 3.1D). A previously described expression construct of VSV-Plexin-B1 was requested from Dr. Tamagnone (Tamagnone et al., 1999). In their construct, the native Plexin-B1 cell surface trafficking signal was removed and the cell surface trafficking signal from Met was linked to VSV tag then Plexin-B1 (Tamagnone, personal communication). The requested construct was mutated according to the same procedure and when the resulting expression constructs for WT or mutant Plexin-B1 were transfected into HEK293T cells, a protein of about 300kDa recognizable on western analysis by anti-VSV antibody was detected (Fig. 3.1E). Since most published interaction studies of Plexin-B1 used the construct from Dr. Tamagnone, expression constructs derived from the WT Plexin-B1 plasmid from Dr. Tamagnone were used in subsequent studies for the sake of consistency with other studies.

3.2.3 Expression and purification of Sema4D-AP

To assay the binding of WT/Mutant Plexin-B1 to Sema4D, I sought to purify a Sema4D-alkaline phosphatase (AP) fusion protein. The alkaline phosphatase enable easy and quantitative detection of the ligand (Flanagan and Cheng, 2000; Flanagan et al., 2000). The fusion protein also contains the glutathione S-transferase (GST) tag to facilitate purification. The GST-Sema4D-AP construct used in this study has been

previously described (Tamagnone et al., 1999). A similar approach was successful in characterizing binding of c-kit ligand to its receptor (Flanagan and Leder, 1990).

When transfected into COS cells, the GST-Sema4D-AP construct directs the secretion of GST-Sema4D-AP protein into the culture supernatant. The fusion protein was then purified from the harvested supernatant with a glutathione column. The expected size of GST-Sema4D-AP is (27+120+67) = 214kDa.

In the earliest attempt to purify Sema4D-AP, COS-1 cells, the only COS cell line available in our laboratory at the time, were transfected with the Sema4D expression plasmid (24μg per 10 cm dish). Two 10 cm culture dishes were seeded with COS-1 cells at density of 3×10^6 cell per dish one day before transfection. Culture supernatant was collected (30ml from two 10cm dishes) and 0.2μm filtered 3 days after transfection. 700μl Glutathione-Sephraose4B was added into the supernatant and incubated overnight to let Sema4D-AP bind to the beads. Then supernatant with the beads were poured down an empty column and the supernatant was left to drain. The retained beads were washed with 10 bed volumes of PBS and the bound Sema4D-AP was eluted with free glutathione. When fractions were resolved on SDS-PAGE and stained with coomassie blue, no protein could be detected (figure 3.2A, upper panel). However Alkaline Phosphatase activity assay suggested that the protein product was indeed present in fractions F2 and F3 (figure 3.2A, lower panel). To visualize the protein, fractions were resolved again on SDS-PAGE and stained by silver staining method which is a more sensitive protein staining. However, the amount of protein was still below the detection limit of the method (figure 3.2B, upper panel). Attempt was made to concentrate the product with ultracentrifugation method, but the final product was still too diluted to show the desired product on silver stained SDS-PAGE gel (figure 3.2B, lower panel.)

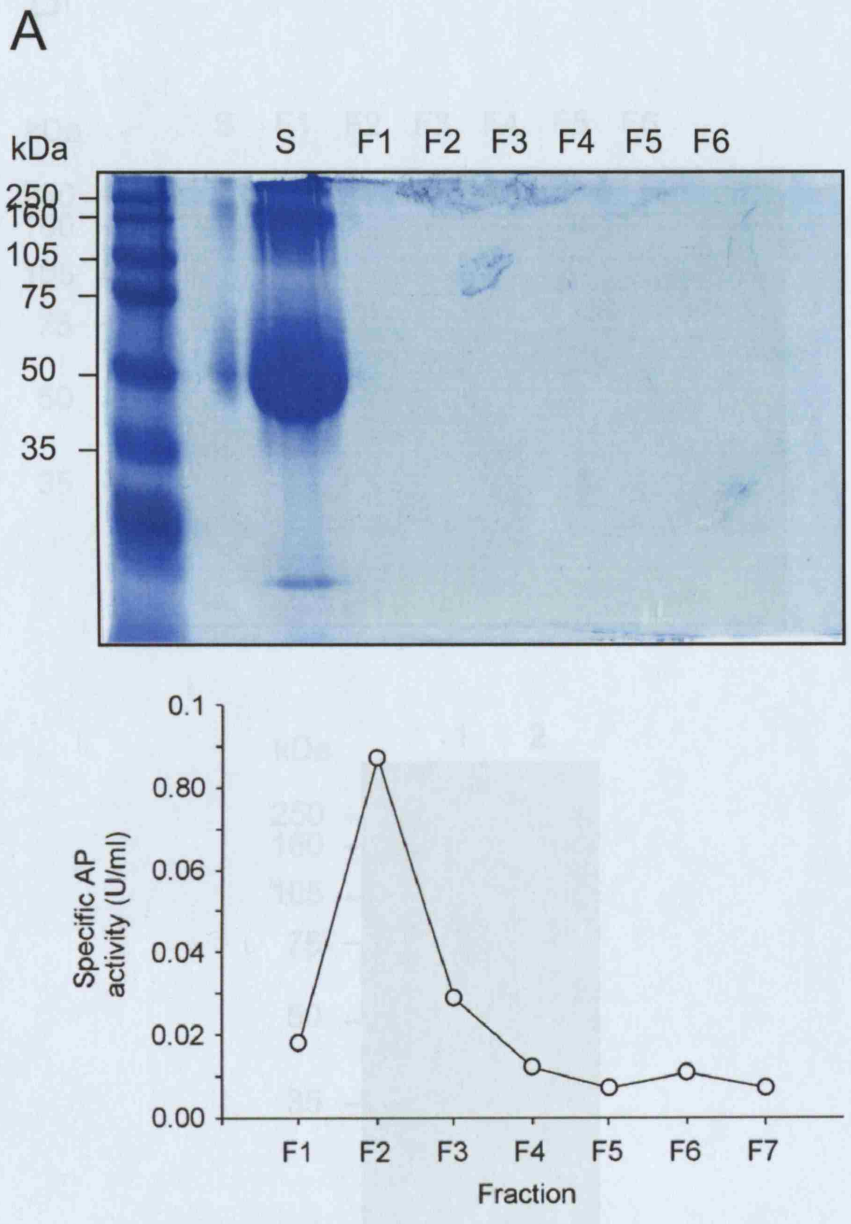

Figure 3.2 Preparation of Plexin-B1 ligand. GST-Sema4D-AP was expressed in COS cells. The culture supernatant was passed through a Glutathione-Sepharose4B column. The bound GST-Sema4D-AP was eluted with 10mM glutathione (pH8) and the fractions were resolved on SDS-PAGE gel. (A) Upper panel: Coomassie blue staining of fractions from first purification. F1-F7: fraction 1 to fraction 7. Each fraction was eluted with 1.5ml of glutathione. Lower panel: Alkaline Phosphatase activity test of the elutes.

B

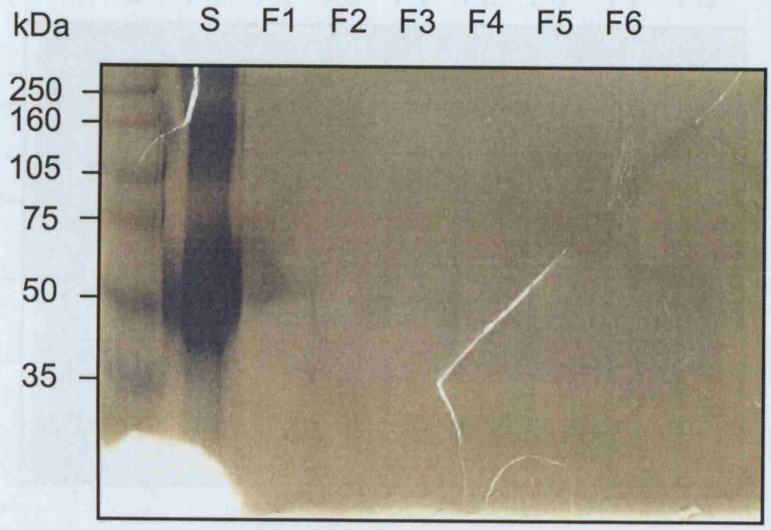

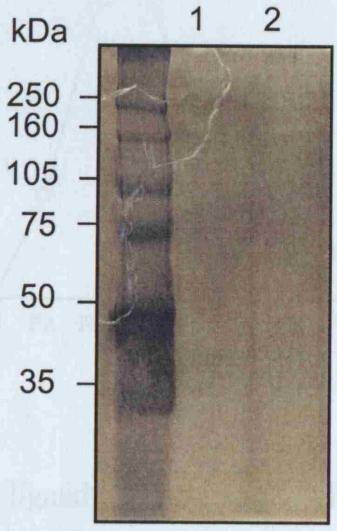

Figure 3.2 Preparation of Plexin-B1 ligand. GST-Sema4D-AP was expressed in COS cells. (B) Upper panel: Silver staining of fractions from first purification. Lower panel: silver staining of fractions concentrated with centricon.

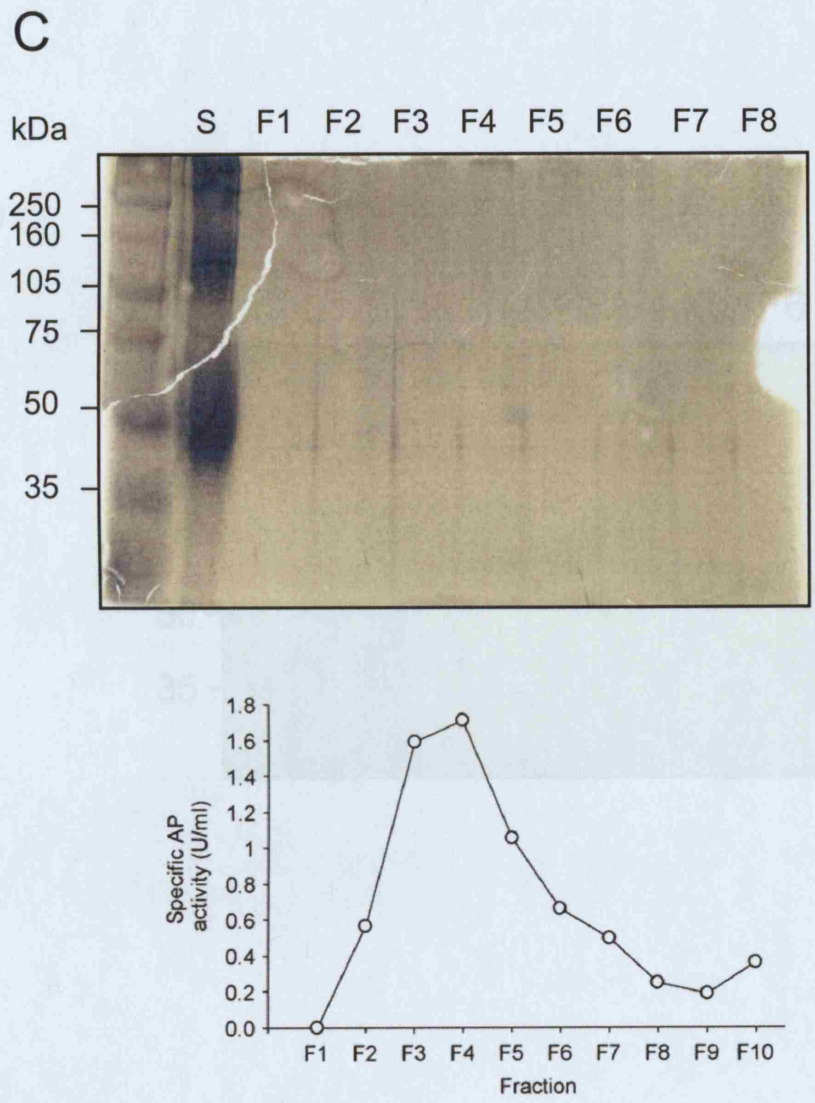

Figure 3.2 Preparation of Plexin-B1 ligand. GST-Sema4D-AP was expressed in COS cells. (C) Upper panel: Silver staining of fractions from purification using supernatant from three 10cm dishes as starting material. Lower panel: Alkaline Phosphatase activity test of the fractions.

D

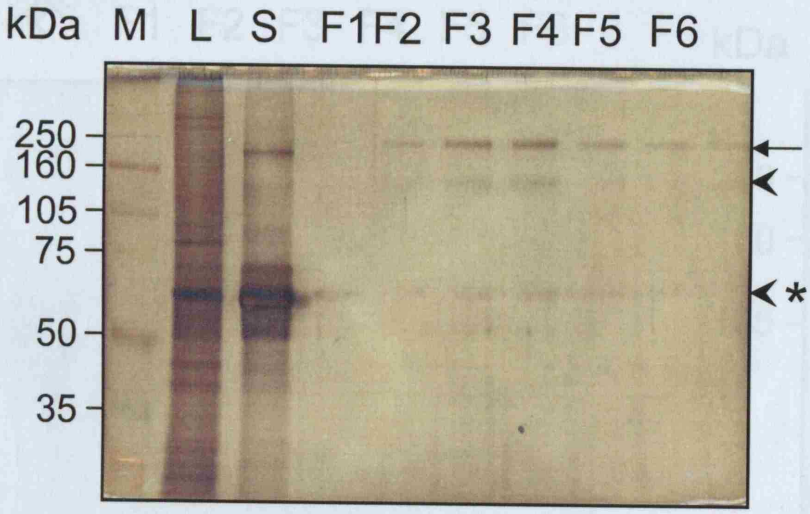

Figure 3.2 Preparation of Plexin-B1 ligand. GST-Sema4D-AP was expressed in COS cells. (D) Silver staining of fractions when using four T180 flasks as starting material.

Figure 3.2 Preparation of Plexin-B1 ligand. GST-Sema4D-AP was expressed in COS cells. (E) Purification using supernatant from four T180 flasks as starting material. Left panel: Coomassie blue stain; Right panel: Western blot with anti-GST. M: protein size marker; S: supernatant; Flow: flowthrough; Arrow: GST-Sema4D-AP

To increase the amount of desired protein product, I doubled the starting material (60 ml culture supernatant) and increased the amount of Glutathione Sepharose4B to 1500μl. Alkaline Phosphatase activity assay indicated a remarkable increase of the protein product (figure 3.2C, lower panel). The peak specific AP activity (1.7113 U/ml) was significantly higher than that of the earliest attempt (0.087 U/ml). However the protein preparation was still too dilute for the product to be stained on silver stained SDS-PAGE gel (figure 3.2C, upper panel).

It was suggested that among the sublines of COS cell, COS-7 is more suitable than COS-1 for protein expression and purification purpose, because of the ability of COS-7 to maintain more copies of exogeneously introduced plasmids (Aruffo, 1998). Therefore, COS-7 was acquired from ATCC for my purpose of Sema4D-AP purification. To increase the amount of final protein product, four T180 flasks of COS-7 cells were transfected (seeded 6×10^6 per flask one day before) with 48μg of Sema4D-AP expressing plasmid per flask. 120ml culture supernatant was used as starting material 3 days after transfection. As shown in figure 3.2D, the fractions from Glutathione-Sepharose4B beads contains the protein product of expected size under silver staining.

Further increase of purification product was achieved when the Glutathione-Sepharose4B beads were replaced by prepacked Glutathione-Sepharose4B column (Amersham). As shown in figure 3.2E, a major band of approximately 215kDa was observed when the column eluted fractions were run on SDS-PAGE and the proteins visualized by coomassie blue staining. Most of the GST-fusion protein consistently eluted at fraction 2 to 3. By comparison with known amount of BSA loaded together onto the gel, the concentration of purified Sema4D was estimated to be approximately 25ng/μl to 150ng/μl. Two smaller, fainter bands were observed consistently. Their

sizes are about 150kDa (arrow head, figure 3.2E left panel) and 70kDa (arrow head with asterisk, figure 3.2E left panel). The 150kDa band was recognizable by anti-GST antibody in western blot but the 70kDa one was not (Figure 3.2E right panel). From the coomassie blue staining, the major band can account for more than 90% of the protein present in the sample. Therefore, I have expressed and purified Sema4D which can be used in subsequent assays.

3.2.4 In situ binding

To monitor the binding of Sema4D to Plexin-B1 *in situ*, Plexin-B1 WT/mutant was expressed in COS-7 cells. Sema4D-AP protein was then allowed to bind with the Plexin-B1 expressed, and the bound protein was visualized by BCIP/NIP staining for AP activity. As shown in figure 3.3, untransfected COS-7 cells do not bind to Sema4D-AP, nor do COS-7 cells transfected with the vector pcDNA3. When Plexin-B1 WT is expressed, the Sema4D-AP binds to the COS-7 cells (figure 3.3A). This happens also when the expressed Plexin-B1 harbour the A5359G/A5653G/T5714C mutations (figure 3.3A). While the protein expression was similar for all the mutants (indicated by western blot shown in figure 5.3), the staining intensity is comparable, suggesting that qualitatively the mutant Plexin-B1 proteins bind to Sema4D with a similar affinity to WT Plexin-B1. The binding was quantified by substituting BCIP/NIP with p-Nitrophenyl Phosphate and the AP activity was measured by spectrophotometry. The amount of Sema4D-AP binding to COS-7 cells transfected with same amount of Plexin-B1 WT/mutant constructs was similar (Fig. 3.3B). Taken together, all three mutants showed binding to Sema4D therefore the mutations do not inhibit ligand binding. Some differences were seen between binding of the mutants

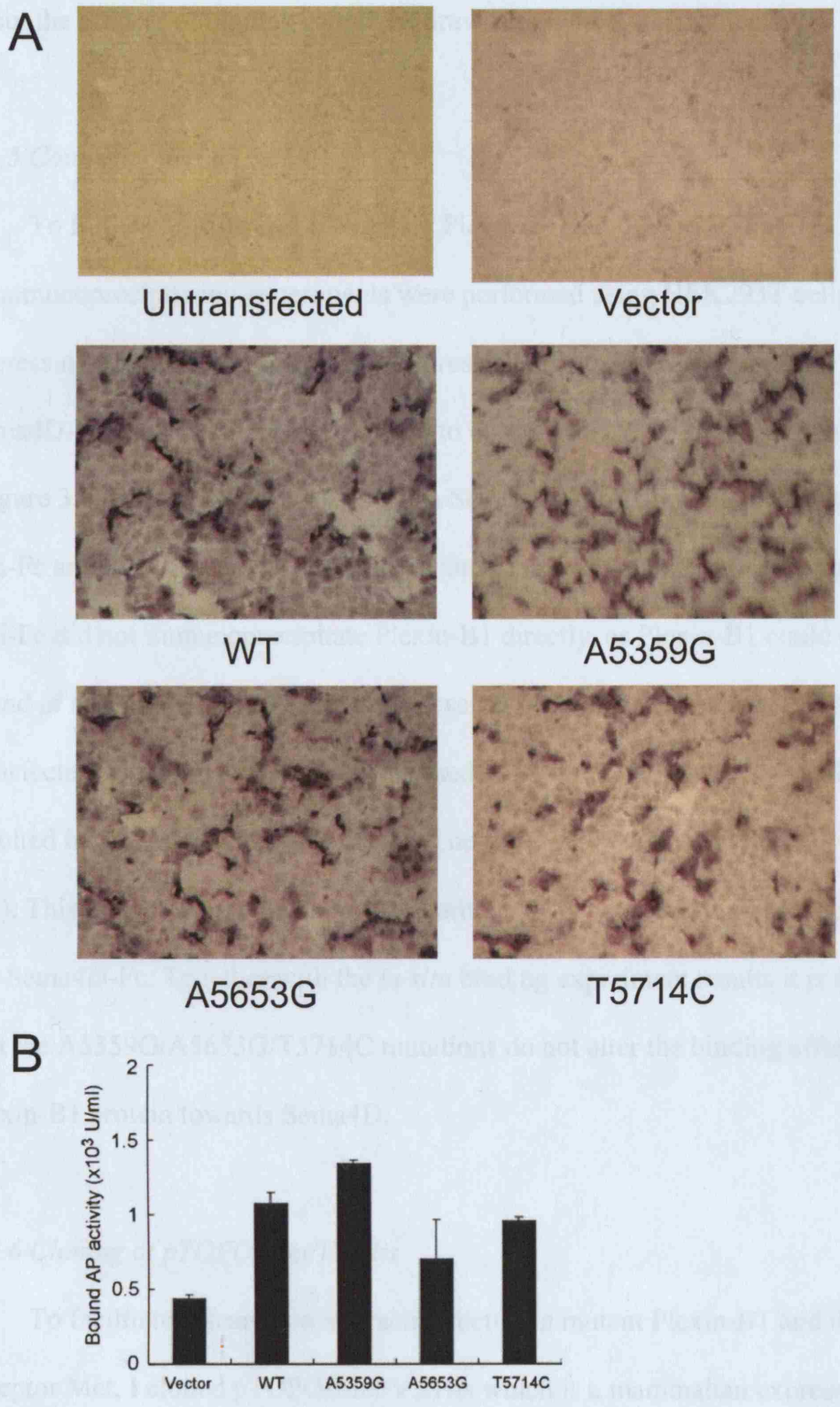

Figure 3.3 Plexin-B1 mutants can bind to Sema4D. (A) Wild type or mutant Plexin-B1 was expressed in COS-7 cells. Two days after transfection the cells were treated with Sema4D-AP, fixed and stained with BCIP/NBT.Photos were taken under 30X magnification. (B) Bound AP was assayed by lysing the cells and used p-Nitrophenyl Phosphate as AP substrate. Results were calculated from data of three independent experiments. Error bar = SEM.

and WT to Sema4D, but these methods are not quantitatively accurate, so conclusions about the affinity of binding cannot be drawn from these experiments.

3.2.5 Coimmunoprecipitation

To further confirm that the mutant Plexin-B1 can bind to Sema4D, coimmunoprecipitation experiments were performed using HEK293T cells co-expressing Plexin-B1 and Sema4D. Expression of Plexin-B1 WT/mutants and Sema4D-Fc were confirmed and shown to be at similar level by western blot analysis (figure 3.4 the two lower panels). When Sema4D-Fc was immunoprecipitated with anti-Fc antibody, Plexin-B1 WT and mutants could all be coimmuprecipitated. The anti-Fc did not immunoprecipitate Plexin-B1 directly, as Plexin-B1 could not be found in the immunoprecipitate in the absence of Sema4D. When the lysate from cells transfected with Sema4D-Fc only was used to immunoprecipitate Sema4D-FC, the resulted immunoprecipitate complex did not react with anti-VSV antibody (figure 3.4). This indicated that the anti-VSV antibody does not react non-specifically with the Sema4D-Fc. Together with the *in situ* binding experiment results it is suggested that the A5359G/A5653G/T5714C mutations do not alter the binding affinity of Plexin-B1 protein towards Sema4D.

3.2.6 Cloning of pTOPO-Met/V5/His

To facilitate research on interaction between mutant Plexin-B1 and the HGF receptor Met, I cloned pTOPO-Met/V5/His which is a mammalian expression construct for C-terminally V5/His tagged-Met. The coding region of human Met cDNA was amplified by PCR, then cloned into pcDNA3.1D/V5-His-TOPO by TOPO cloning method (Invitrogen). The presence of Met insert was checked with PCR with

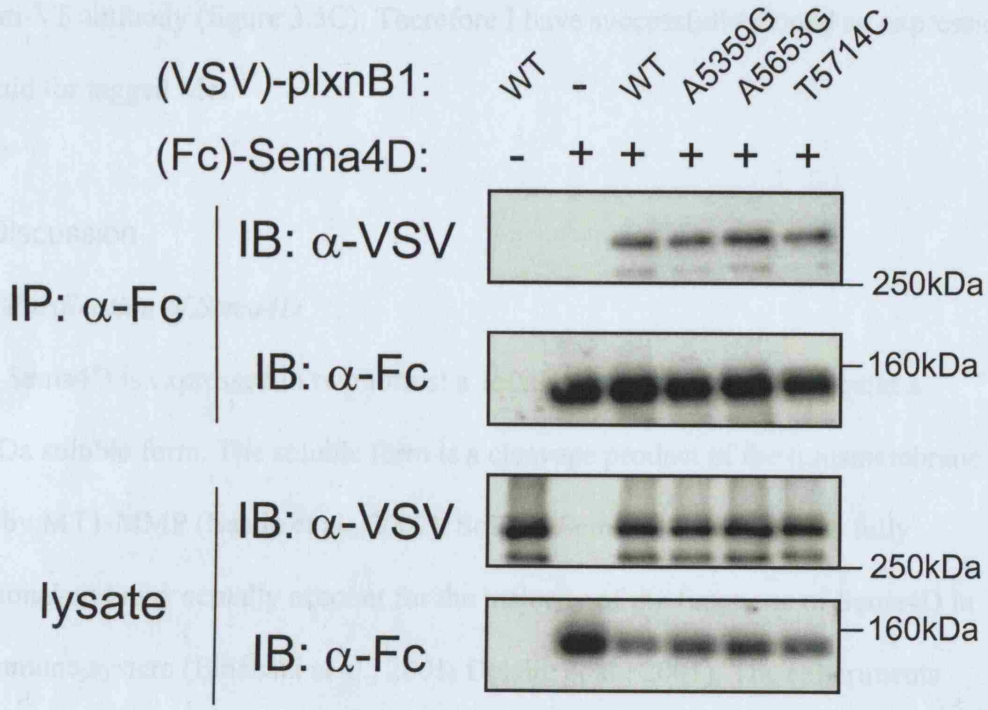

Figure 3.4 Plexin-B1 mutants can be coimmunoprecipitated with Sema4D. Plexin-B1 and Sema4D-Fc was coexpressed in HEK293T cells. Proteins were immunoprecipitated from the cell lysate with anti-Fc antibody two days after transfection.

primers flanking the the TOPO cloning site (figure 3.5A). The direction of the insert was checked by sequencing (figure 3.5B). And finally when the construct was transfected into HEK293T at different amount, a protein product recognised by anti-Met antibody and slighter larger than the endogeneous Met could be detected. The amount of the exogeneous protein varied according to the amount of pTOPO-Met/V5/His transfected (figure 3.5C). The protein product could also be recognised by anti-V5 antibody (figure 3.5C). Therefore I have successfully cloned an expression plasmid for tagged Met.

3.3 Discussion

3.3.1 Purification of Sema4D

Sema4D is expressed in two forms: a 150kDa transmembrane form and a 120kDa soluble form. The soluble form is a cleavage product of the transmembrane form by MT1-MMP (Basile et al., 2007). Soluble Sema4D (sSema4D) is fully functional and may actually account for the majority of the functions of Sema4D in the immune system (Elhabazi et al., 2001; Delaire et al., 2001). The experiments carried out in this study utilized an expression construct for GST-Sema4D-AP which has been described previously. It expresses the extracellular domain of Sema4D when transfected into mammalian cells. The protein purified was proved to be functional in binding to and stimulating Plexin-B1 (Giordano et al., 2002; Tamagnone et al., 1999).

In the current procedure for purifying the fusion protein, the supernatant was harvested four days after transfection. I found that the yield of Sema4D production was higher compared with harvesting at day 3 after transfection. This may be because the plasmid has a SV40 replication origin so it replicates as the cells divide and COS-

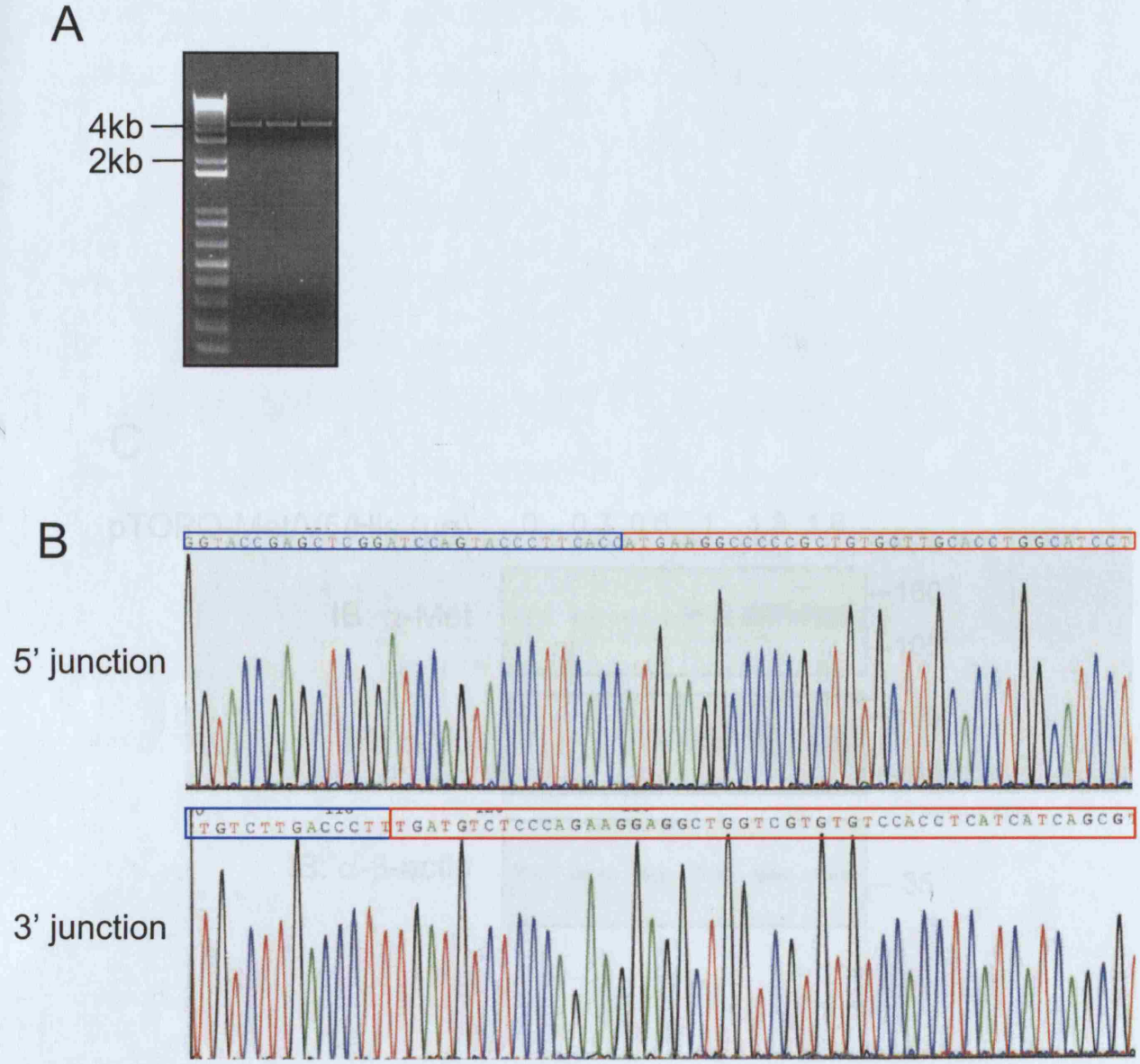

Figure 3.5 Verification of Met expressing plasmid. (A) Three clones of pTOPO-Met/V5/His was subjected to PCR with primers flanking the multiple cloning site of pTOPO. (B) the 5' and 3' junctions of the insert was checked by sequencing. Blue frames: sequences belonging to pTOPO. Red frames: sequences belonging to Met cDNA.

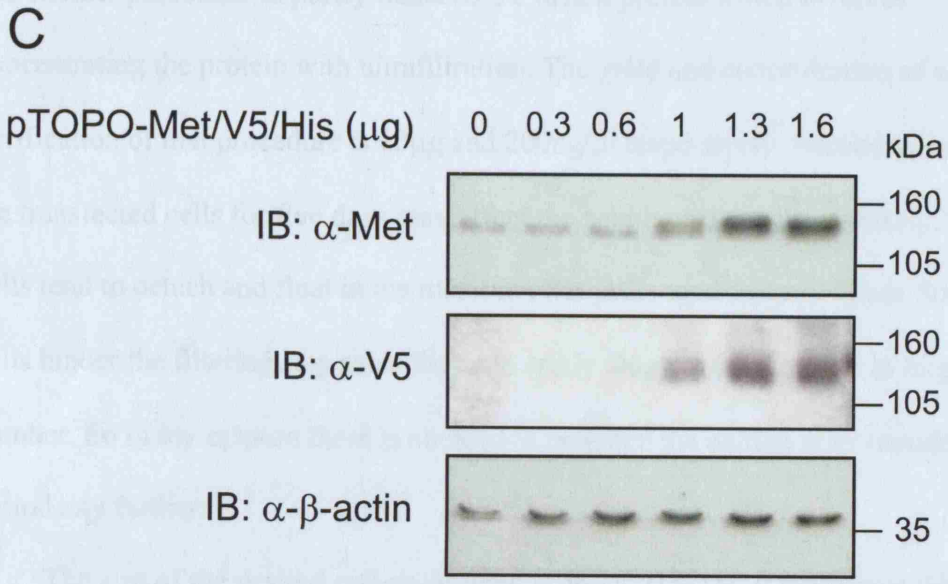

Figure 3.5 Verification of Met expressing plasmid. (C) Lysate of HEK293T cells transfected with indicated amount of pTOPO-Met/V5/His was resolved on SDS-PAGE and subjected to western blot using anti-Met antibody.

7 cells were engineered to express the SV40 T antigen. Therefore the copy number per cell did not get diluted over the culture period. Theoretically, the yield of culturing 5 days should be higher, however the yield at 4 days was sufficient for the planned experiments. The typical yield per purification is about 100μg with a concentration about 100ng/μl without further concentration procedures. This amount can be used in about eight *in situ* binding experiments with 10 wells per experiment. Our laboratory has another procedure to purify Sema4D-Fc fusion protein which involves concentrating the protein with ultrafiltration. The yield and concentration of a typical purification of that procedure is 10μg and 200ng/μl respectively. Secondly, culturing the transfected cells for five days may affect the health of the cells adversely. The cells tend to detach and float in the medium after prolonged culture. These floating cells hinder the filtering step since they can easily clog the 0.2μm filter in large number. So in my opinion there is no need to lengthen the culture after transfection period any further.

The size of the desired protein product is about 215kDa. It represents the majority of the protein species in my purified product (~90%). Nonetheless, I observed two minor products with sizes about 150kDa and 70kDa. Because the 150kDa product was detectable by GST antibody in western blotting analysis, I propose it is a degradation product of the GST-Sema4D-AP fusion protein. The AP domain of the fusion protein may be easily cleaved to give a protein of size around 150kDa (215-68 = 147). In support of this, a faint band at about 70kDa is actually barely visible in the purification product. This band is not detectable by GST antibody so it is likely to be the AP domain. A western blotting analysis using an antibody against the extracellular domain of Sema4D would provide information regarding the identities of these protein species. However currently all the commercially available

Sema4D antibodies recognize the intracellular domain of Sema4D. Anyway, the purified GST-Sema4D-AP showed good purity and is in convenient concentration. Therefore good purification of GST-Sema4D-AP has been achieved.

3.3.2 In situ binding

The aim of this study is to investigate whether those mutations on Plexin-B1 discovered in prostate cancers affect one particular function of Plexin-B1, which is the binding to Sema4D. *In situ* binding is the direct method to assess this. The experiment involves expressing the protein to be tested in a selected cell type and treating the cells with labelled ligand. The advantage of using COS-7 cells in this experiment is that COS-7 has undetectable basal expression level of Plexin-B1. Therefore any binding of the ligand can be attributed to the exogenously expressed protein, and hence any effect on the binding can be ascribed to the mutation introduced into the expressed protein.

Although by staining intensity it is quite obvious that the mutations have no effect on the ligand binding capacity, the comparison was not quantitative. A more meticulous approach to determine the affinity of the Plexin-B1 mutants towards Sema4D would be measuring the concentration of bound and unbound ligand over a range of added ligand concentration. The data is then analysed by Scatchard plot to determine the dissociation constant for each Plexin-B1 mutant (Tamagnone et al., 1999). However this was not done due to equipment and time constraint. It is planned for more detailed analyses of the interaction between mutant Plexin-B1 proteins and Sema4D in the future. For the purpose of testing qualitatively whether there is an obvious difference in the binding capacity, the current method is sufficient. Attempts were made to quantify the staining intensity with spectrophotometer, (Fig. 3.3B).

The conclusion that approximately equal staining is observed and that the mutations have no big impact on the ligand binding capacity is based on the assumption that the mutations do not affect the cell surface expression (cell trafficking) of the proteins, and the assumption that the plasmids were transfected into cells at similar transfection efficiency. Althought I did not directly assay the transfection efficiency of the plasmids quantitatively, two pieces of information suggested the plamids were transfected and expressed at similar level. First of all, the overall Plexin-B1 protein expression levels are the same for WT and mutant proteins as shown by western blotting figure 5.3B. Secondly, in immunofluorescent staining experiments in which cells transfected with Plexin-B1 were stained by anti-Plexin-b1, no obvious difference in the number and density of Plexin-B1 positive cell was observed.

3.3.3 Coimmunoprecipitation

As a confirmation of the *in situ* staining results I also tried to coimmunoprecipitate Plexin-B1 mutants with Sema4D. I found that Plexin-B1 mutants are capable of interacting with Sema4D, in agreement with the results obtained from *in situ* staining experiments. Coimmunoprecipitation was used as a secondary method for investigating the Sema4D binding capacity of the Plexin-B1 mutants. For this purpose it has several limitations compared with *in situ* staining. First of all, since both Plexin-B1 and Sema4D proteins were expressed in the cells by transfection of expression plasmids, the interaction between Plexin-B1 and Sema4D observed was likely to be happening in the cytoplasm. That means some of the Plexin-B1 and Sema4D might not have interacted in the physiological, extracellular environment. Nonetheless, given the facts that significant amount of Plexin-B1 can be

found on cell surface (from *in situ* binding experiments) and the Sema4D constructs were engineered to express secretory Sema4D protein, it is reasonable to assume that most of the interaction observed occurs extracellularly. Another limitation of using coimmunoprecipitation to investigate receptor ligand binding is that there is no good way to quantify the results. The band intensities in a western analysis could be compared semi-quantitatively, however. Despite these limitations, the coimmunoprecipitation results supported the finding that the mutations do not affect the Sema4D binding capacity of Plexin-B1.

Chapter 4

Effects of Plexin-B1 mutations on Rho regulating activity of Plexin-B1

4.1 Introduction

There is a plethora of evidence suggesting that the Rho small GTPase is important for Plexin-B1 function. In Drosophila Plexin-B directly interacts with RhoA and enhances RhoA activity (Hu et al., 2001), thereby regulates motor, sensory and CNS axon pathfinding in developing embryos (Ayoob et al., 2006; Bates and Whitington, 2007). Plexin-B1 activation leads to axonal growth cone collapse in rat primary hippocampal neurons (Swiercz et al., 2002). This phenomenon is dependent on RhoA. Although Plexin-B1 does not directly interact with RhoA in mammalian cells, it interacts with and regulate at least two Rho specific Guanine exchange factor (GEF), PDZ-RhoGEF and LARG (Perrot et al., 2002; Aurandt et al., 2002; Hirotani et al., 2002; Driessens et al., 2002; Oinuma et al., 2003). The general picture from these studies is that Plexin-B1 activates RhoA upon Sema4D stimulation through the action of associated Rho GEFs PDZ-RhoGEF and LARG. RhoA-GTP binds to and activate Rho-dependent kinase (ROCK) which phosphorylate Myosin Light Chain (MLC) and enhances the actomyosin contractility. Contraction of actin-myosin microfilaments generates the contractile force for growth cone retraction in neuronal cells, or the formation of stress fibres in non-neuronal cells (Kruger et al., 2005).

However, there were reports of results against this general picture. Cell collapse is morphologically defined as disassembly of focal adhesion over large area of a cell and shrinkage of the cell's surface area. Cell collapse has many features in common to axonal growth cone collapse, including the disassembly of focal adhesion, reduction of lamellipodia and shrinkage due to traction force exerted by microtubule cytoskeleton. Therefore cell collapse induced in epithelial cells has become a convenient model for Plexin mediated growth cone collapse (Turner and Hall, 2006). Barberis et al. showed, in their mouse fibroblast cell collapse model, that Plexin-B1

mediated cell collapse is not dependent on ROCK, and is actually inhibited by activation of RhoA by LPA (Barberis et al., 2004). They further demonstrated that this negative regulation of Rho by Plexin-B1 is mediated by p190-RhoGAP, a GTPase activating protein physically interacting with Plexin-B1 (Barberis et al., 2005).

RhoA is important for cell migration since it controls the retraction of the cell rear during cell migration. Therefore I am interested in whether mutated Plexin-B1 has altered regulation on Rho. To this end two sets of experiments were done to see whether mutated Plexin-B1 can still physically interact with PDZ-RhoGEF, and whether the mutations affect Plexin-B1 function on Rho activation/inactivation.

4.2 Results

4.2.1 Coimmunoprecipitation of Plexin-B1 and PDZ-RhoGEF

There is a PDZ-binding motif at the very C-terminal end of Plexin-B1. Although the mutations do not fall into this motif, it is of interest to test whether the three mutations affect PDZ-RhoGEF binding. To this end I expressed VSV-Plexin-B1 WT or mutant and myc-PDZ-RhoGEF in HEK293T cells and immunoprecipitated Plexin-B1. The immunoprecipitates were probed with anti-VSV and anti-myc in western blot analysis for the detection of Plexin-B1 and PDZ-RhoGEF protein respectively. The coimmunoprecipitation of PDZ-RhoGEF with WT Plexin-B1 was observed (Figure 4.1), as reported previously (Hirotani et al., 2002; Perrot et al., 2002; Swiercz et al., 2002). A5359G, A5653G and T5714C mutants could all coimmunoprecipiate with PDZ-RhoGEF, at similar levels to WT Plexin-B1. This indicated that the mutations do not affect the interaction between Plexin-B1 and PDZ-RhoGEF (Figure 4.1).

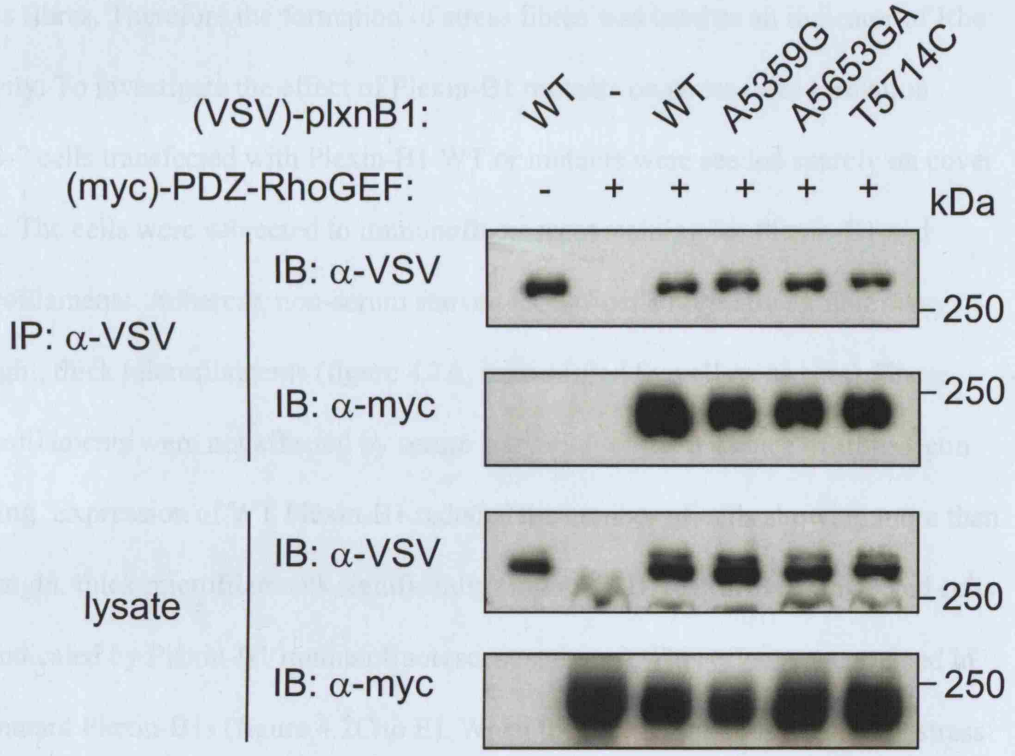

Figure 4.1 Plexin-B1 mutations do not affect PDZ-RhoGEF binding. Lysates from HEK293T cells transfected with Plexin-B1 and PDZ-RhoGEF were immunoprecipitated with anti-VSV and bound proteins detected by immunoblotting.

4.2.2 Stress fiber formation assay

Stress fibres are long bundles of microfilaments made up of actin subunits and myosin-II. They are involved in the attachment of cultured cells to a substratum, and in the determination of cell shape and cellular mobility. They are found in most cells and attach to the cell membrane at focal adhesions.

Rho activation was shown to be sufficient and necessary for the formation of stress fibres. Therefore the formation of stress fibres was used as an indicator of Rho activity. To investigate the effect of Plexin-B1 mutants on stress fibre formation, COS-7 cells transfected with Plexin-B1 WT or mutants were seeded sparely on cover slips. The cells were subjected to immunofluorescent staining for Plexin-B1 and microfilaments. Adherent, non-serum starved COS-7 cells normally exhibit many straight, thick microfilaments (figure 4.2A, exemplified by yellow arrows). These microfilaments were not affected by serum starvation or the presence of fibronectin coating. Expression of WT Plexin-B1 reduced the number of cells showing more than 3 straight, thick microfilaments significantly (figure 4.2B, Plexin-B1 transfected cells are indicated by Plexin-B1 immunofluorescent staining). This effect was retained in the mutant Plexin-B1s (figure 4.2C to E). When the number of cells exhibiting stress fibers was counted for each group of transfected cells, no difference in the percentage of Plexin-B1 expressing cells showing stress fiber was detected (figure 4.3). So in terms of regulating stress fibre formation, the mutations do not affect Plexin-B1 function. This indirectly suggests that the Rho regulation function of Plexin-B1 is not affected by the mutations.

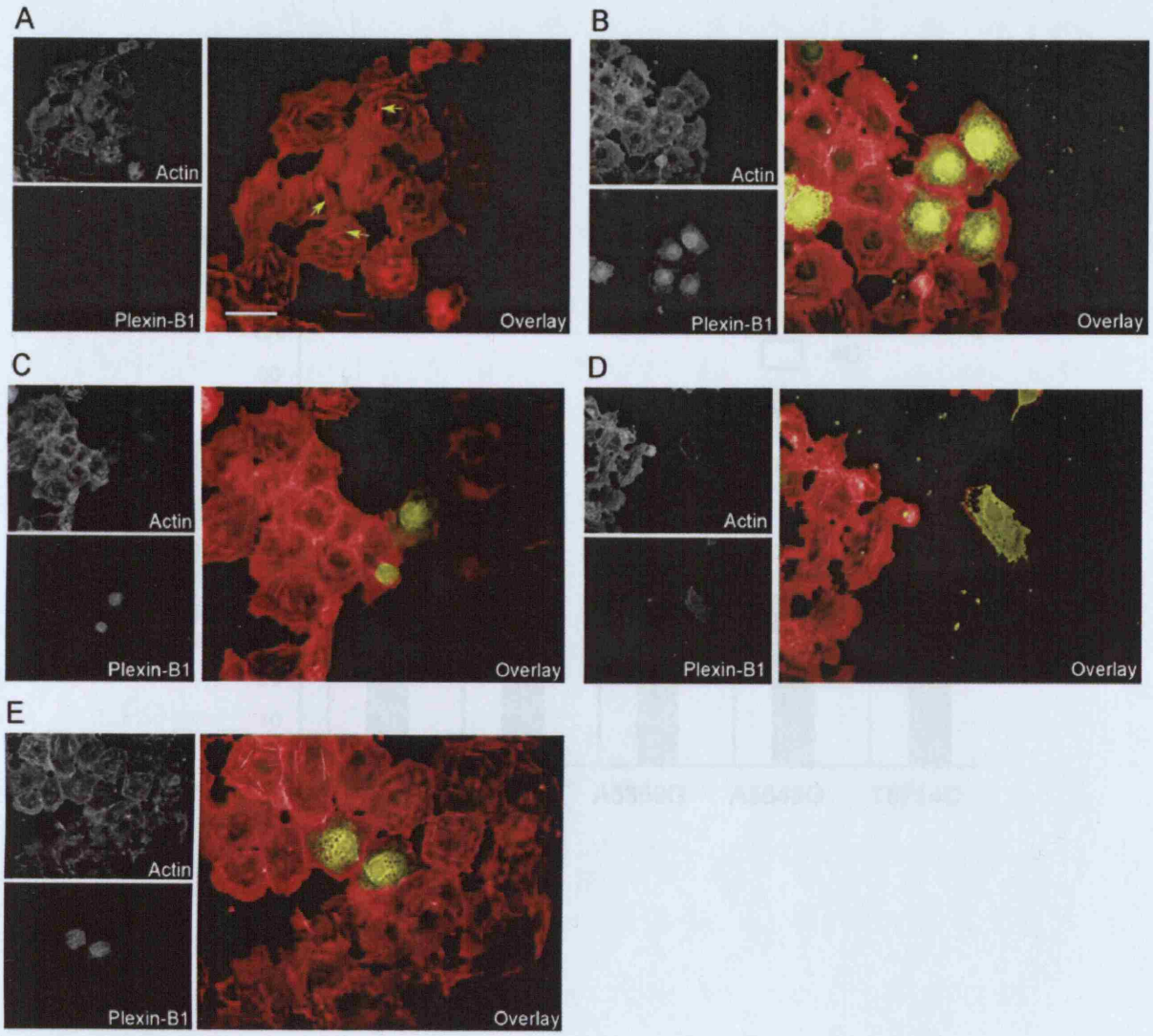

Figure 4.2 Overexpression of Plexin-B1 inhibits stress fiber formation. COS-7 cells were seeded onto coverslips without fibronectin coating before being transfected with (A) Vector; (B) Plexin-B1 WT; (C) Plexin-B1 A5359G; (D) Plexin-B1 A5653G; or (E) Plexin-B1 T5714C. One day after transfection, the cells were fixed in 4% paraformaldehyde in PBS, permeabilized with 0.1% Triton-X 100 in PBS and then blocked with 2% BSA in PBS. Fixed cells were stained with anti-Plexin-B1 or Phallodin for actin. Scale bar = 50μm.

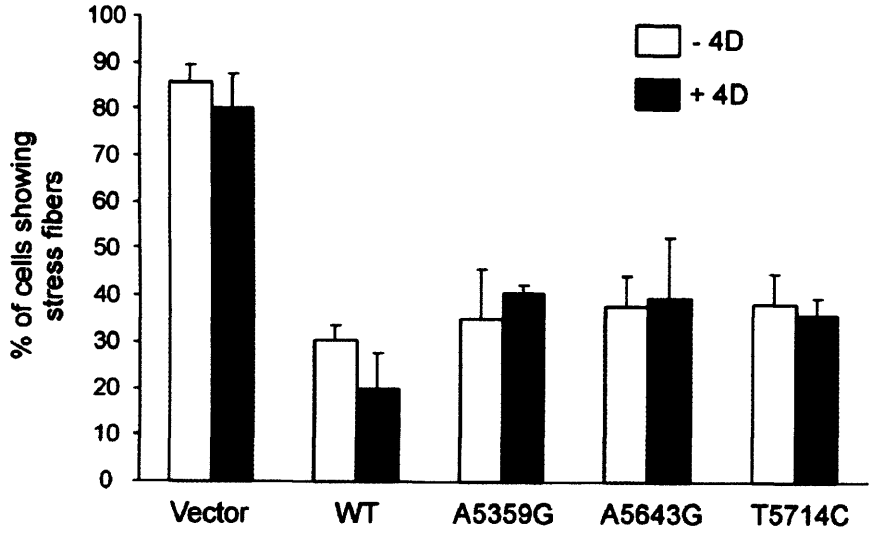

Figure 4.3 Plexin-B1 mutations do not affect RhoA regulation function. The number of cells possessing more than three straight actin bundles of at least 5μm long was counted. The identities of the slides counted were blinded to the researcher. At least 50 cells were counted per slides. Error bars = SEM, n =3

4.2.3 Plexin-B1 has no effect on endogeneous ErbB-2 phosphorylation status in HEK293T cells

It has been suggested that Plexin-B1 transduces Sema4D signalling to RhoGEFs through the actions of receptor tyrosine kinases Met and ErbB-2 (Swiercz et al., 2004; Swiercz et al., 2007). Thus, ErbB-2 constitutatively interacts with Plexin-B1. Stimulation of Plexin-B1 with Sema4D induces the phosphorylation of both Plexin-B1 and ErbB-2 but not PDZ-RhoGEF. Although little is known about the events immediately downstream of these tyrosine phosphorylations, studies using si-RNA mediated ErbB-2 knock-out, pharmacological ErbB-2 inhibitors, or dominant negative ErbB-2 constructs clearly established that phosphorylation by ErbB-2 is a pre-requesite for Plexin-B1 to activate RhoA (Swiercz et al., 2004). I therefore was interested in probing the possible influence of the mutations on ErbB-2 phosphorylation status. I expressed Plexin-B1 in HEK293T cells and stimulated the transfected cells with Sema4D after six hours of serum starving. The phosphorylation status of endogeneous ErbB-2 was monitoried by western analysis using anti-phospho-ErbB-2(Y1248) antibody. Interestingly, in HEK293T cells, ErbB-2 is constitutatively phosphorylated, regardless of the expression of Plexin-B1 or stimulation of Sema4D (figure 4.4A). Longer serum starvation (24 hours) did not reduce the phosphorylation level of ErbB-2 (figure 4.4B). So the results suggested that HEK293T is not a suitable cell line for studying the problem.

4.3 Discussion

In this part of the study I explored the possibility that the mutations may affect Rho signalling by Plexin-B1. Since in mammalian cells Plexin-B1 does not interact directly with Rho, its interaction with the two Rho GEFs, PDZ-RhoGEF and LARG,

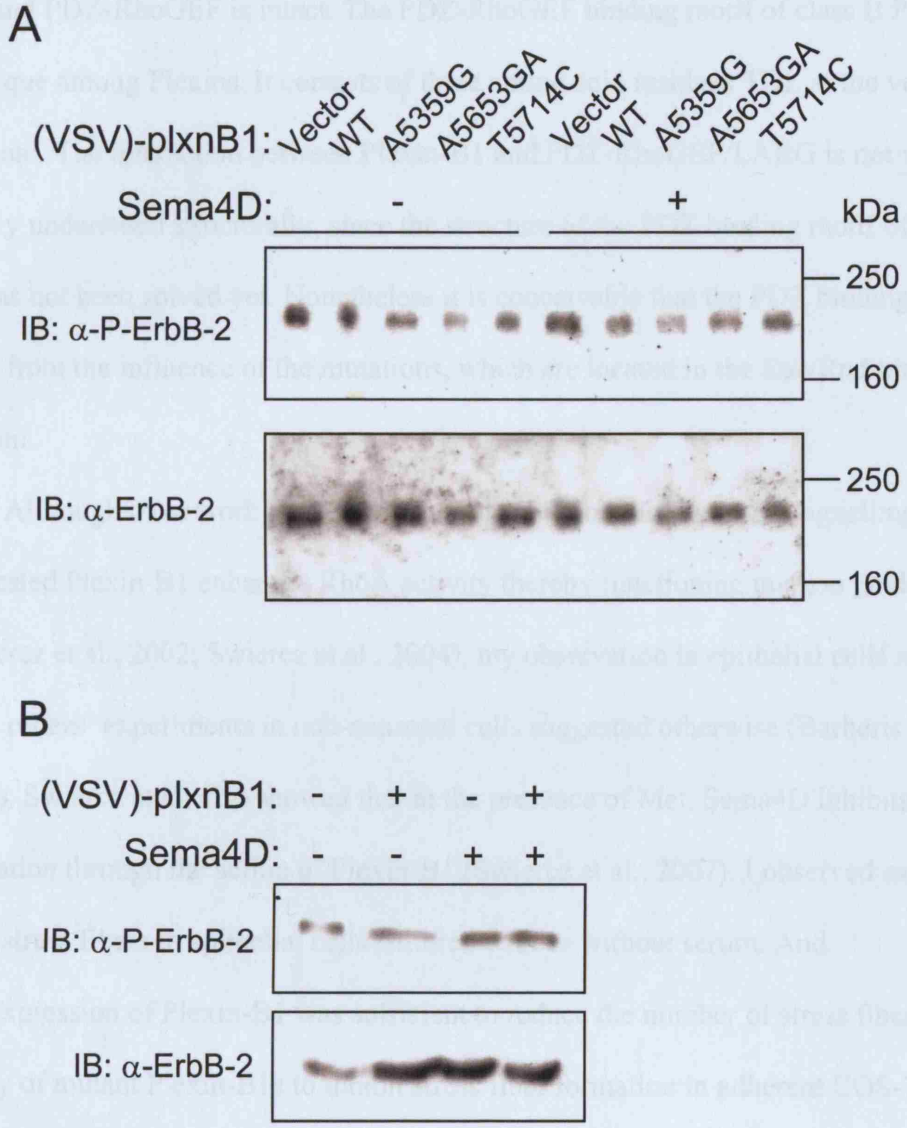

Figure 4.4 ErbB-2 is constitutively phosphorylated in HEK293T cells. (A) HEK293T cells were transfected with indicated Plexin-B1. The cells were serum starved two days after transfection for six hours. 1000ng/ml Sema4D-AP was used to stimulate the cells for 15 minutes, before the cells were lysed with RIPA. The lysate was analysed by western analysis with anti-P-ErbB-2 and anti-ErbB-2 antibody. (B) ErbB-2 phosphorylation persisted after 24 hours of serum starvation.

is of great importance for Rho-dependent Plexin-B1 functions. Coimmuno-precipitation experiments clearly demonstrated the interaction between mutant Plexin-B1s and PDZ-RhoGEF is intact. The PDZ-RhoGEF binding motif of class B Plexins is unique among Plexins. It consists of three amino acid residues TDL at the very C-terminal. The interaction between Plexin-B1 and PDZ-RhoGEF/LARG is not very clearly understood structurally, since the structure of the PDZ binding motif of plexin-B1 has not been solved yet. Nonetheless it is conceivable that the PDZ binding motif is far from the influence of the mutations, which are located in the Rac/Rnd binding domain.

Although most work concerning the role of RhoA in Plexin-B1 signalling suggested Plexin-B1 enhances RhoA activity thereby functioning in axon guidance (Swiercz et al., 2002; Swiercz et al., 2004), my observation in epithelial cells and some others' experiments in non-neuronal cells suggested otherwise (Barberis et al., 2004). Swiercz et al. also showed that in the presence of Met, Sema4D inhibits Rho activation through the action of Plexin-B1 (Swiercz et al., 2007). I observed extensive actin stress fibers in epithelial cells cultured with or without serum. And overexpression of Plexin-B1 was sufficient to reduce the number of stress fibers. The ability of mutant Plexin-B1s to inhibit stress fiber formation in adherent COS-7 cells provided cellular functional evidence that the mutations do not affect Rho signalling. I acknowledge that RhoA activity should be directly estimated by Rhotekin Rho binding domain (GST-RBD) pull-down assay (Swiercz et al., 2002). I tried to use the assay to assess the RhoA activity in Plexin-B1 transfected COS-7 cells. Although an inhibition of RhoA could be observed when Plexin-B1 WT was expressed (figure. 4.5), the result was unfortunately not reliably reproducible. We are going to repeat this experiment, for it is a crucial evidence for our claim. But since the cost of the Rho

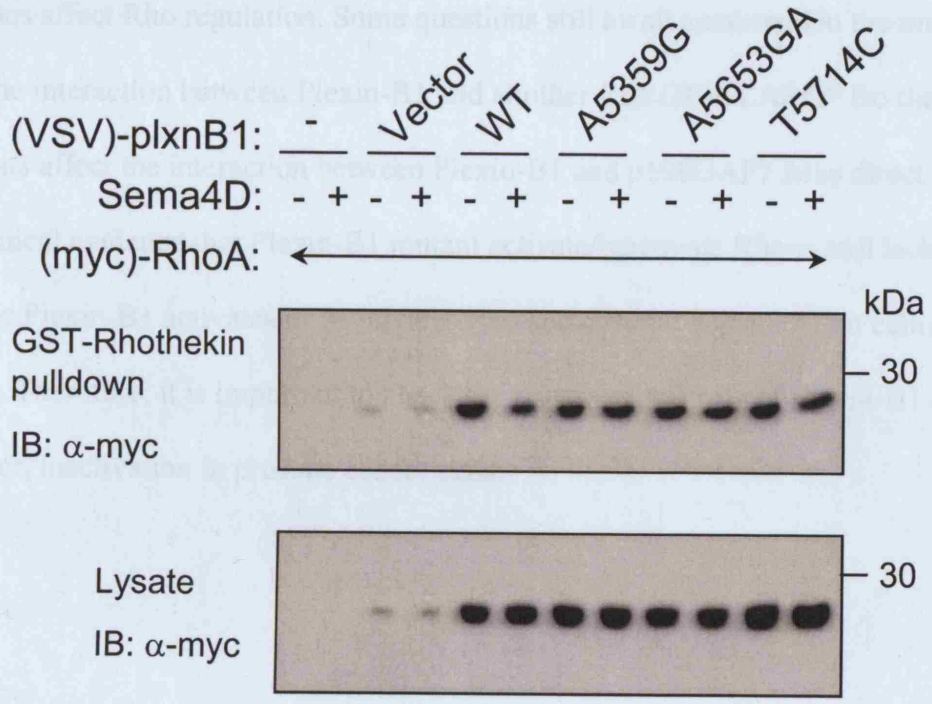

Figure 4.5 GST-Rhotekin RBD pulldown assay for Rho activity. Plexin-B1 and RhoA were expressed in COS-7 cells. The cells were serum starved for 24 hours before treatment with Sema4D-AP for 15 minutes. The cells were then lysed and the activated RhoA was pulled down with GST-Rhothekin RBD and analysed by western blotting using anti-myc antibody.

assay kit is rather high, we are now trying to make in-house made GST-Rhotekin. When GST-Rhotekin of satisfactory quality is made, more GST-Rhotekin and larger amounts of starting material can be used in the future Rho activity assay experiments. Taken together, my results provided important information regarding the effects of the mutations on Rho-regulation function of Plexin-B1, suggesting that the mutations are very unlikely to affect Rho signalling.

Nonetheless, the results are insufficient to exclude the possibility that the mutations affect Rho regulation. Some questions still await answers. Do the mutations affect the interaction between Plexin-B1 and another Rho GEF, LARG? Do the mutations affect the interaction between Plexin-B1 and p190GAP? Also direct biochemical evidence that Plexin-B1 mutant activate/inactivate Rho is still lacking. Whether Plexin-B1 activates or inactivates Rho seems to be dependent on cellular context. Therefore, it is important to check the physiological role of Plexin-B1 on Rho activation/inactivation in prostate cancer cells.

Chapter 5

Effects of Plexin-B1 mutations on Rac1 regulating activity of Plexin-B1

5.1 Introduction

The regulation of Rac proteins is an important means for Plexin-B1 to perform its functions. The small GTPase Rac1 directly binds to the cytoplasmic domain of Plexin-B1 (Driessens et al., 2001; Vikis et al., 2000). Like other p21 GTPases, Rac1 cycles between the inactive GDP-bound form and the active GTP-bound form under the influence of guanine exchange factors (GEFs) or GTPase activating proteins (GAPs). Thus, the activity of GEFs stimulates the exchange of GDP for GTP bound by Rac1 and hence leads to the binding and activation of downstream effectors like p21-activated kinase (Pak). Rac1 binds to Plexin-B1 only in its GTP-bound form and is essential for the cytoskeleton changes mediated by Plexin-B1 clustering (Driessens et al., 2001; Vikis et al., 2000). Plexin-B1 was suggested to inhibit Rac1 (Vikis et al., 2002). However no Rac-GAP activity could be demonstrated on Plexin-B1. Instead, it was suggested that Plexin-B1 inhibts Rac1 by sequestering it and therefore preventing it from interacting with its downstream effectors. Moreover, the signalling between Plexin-B1 and Rac was proposed to be bidirectional, thus Rac-GTP binding enhances the cell surface localization of Plexin-B1 (Vikis et al., 2002). The exact significance of the Rac-mediated enhancement of Plexin-B1 cell surface localization is currently not known. But it was suggested that it may represent a crosstalk opportunity for some G-protein coupled receptors which regulate Rac to interact with the Plexin-B1 pathway (Vikis et al., 2002).

Given the importance of Rac on Plexin-B1 functions, it is interesting to test whether any of the mutants affect Plexin-B1 and Rac interaction. In this chapter, this question was first answered by GST-pulldown technique and then the consequence of the affected interaction between Rac and Plexin-B1 T5714C mutant was investigated.

5.2 Results

5.2.1 Anti-B1cyto antibody optimisation

Antibody raised against the cytoplasmic domain of Plexin-B1 was previously described (Vikis et al., 2002). I acquired this antibody from Dr. KL Guan. An experiment was done to determine the specificity and suitable working dilution for western blotting. Different amount of Plexin-B1 expression plasmid was transfected into HEK293T cells. Two days later the cells were lysed and the lysate was resolved on SDS-PAGE, blotted onto PVDF membrane, and probed with anti-B1cyto at different dilution. I found that unlike anti-VSV antibody, anti-B1cyto detected the ~300kDa and the ~100kDa forms of Plexin-B1 (figure 5.1). It also gives a major band which is not specific since it also appeared in lane of lysate without Plexin-B1. From the result I concluded that a dilution of 1/4000 to 1/5000 is the best working dilution for western blotting experiments. Although different amount of Plexin-B1 plasmid was transfected, the differences of Plexin-B1 band intensity were not obvious.

5.2.2 GST-pulldown of Rac1

To assess the interaction between mutant Plexin-B1 and Rac1, a fusion protein with GST-tag and the cytoplasmic domain of Plexin-B1 was used to pull-down exogeneously expressed Rac1 in HEK293T cell lysate. To clone the expression plasmid of GST-B1cyto, the region of Plexin-B1 cDNA encoding the cytoplasmic domain was amplified by PCR and cloned into the vector pGEX-4T-3. Mutations were introduced by *in vitro* mutagenesis to the plasmids. And the presence of the correct sequence changes was confirmed by sequencing. The fusion proteins were expressed in *E.coli* and purified by glutathione sepharose-4B. The expressed and purified fusion proteins were resolved in SDS-PAGE gel followed with coomassie

Figure 5.1 Testing of anti-B1cyto antibody. A antibody raised against the cytoplasmic domain of Plexin-B1 was acquired from Dr. KL Guan. It was used to detect proteins in HEK293T lysate from cells transfected with the indicated amount of Plexin-B1 plasmid. Different dilution were used to determine the best operational dilution. M = Protein size markers.

blue staining. The constructs expressed a protein of about 100kDa which is the expected size (figure 5.2A, left panel, arrowhead), together with GST (figure 5.2A, left panel, arrow) and some other impurity. The 100kDa protein could be detected by anti-B1cyto and anti-GST (figure 5.2A), suggesting that it is the protein I expected. The levels of the purified proteins were similar suggesting that the mutations exert no effect on the expression of the proteins in *E.coli* (figure 5.2A, left panel).

The fusion proteins were used to pull down either Rac1L61 or RacN17 expressed in the lysate of transfected HEK293T cells, which were expressed at similar level (figure 5.2B). The pulled down proteins were resolved in SDS-PAGE and detected with anti-myc antibody in western blotting. As shown in Figure 5.2C, GST-B1cytoWT interacts with RacL61 but not RacN17, consistent with previous reports (Vikis et al., 2000; Vikis et al., 2002). GST-B1cytoA5359G and GST-B1cytoA5653G interact with RacL61 too. GST-B1cytoA5359G may bind with lower affinity. GST-B1cytoT5715C, on the other hand, has lost the ability to interact with RacL61. This experiment suggested that the T5714C mutation abolishes the interaction between Plexin-B1 and Rac.

5.2.3 The T5714C mutation in Plexin-B1 inhibits Rac-dependent trafficking of Plexin-B1 to the cell surface

It has been reported that Rac1-GTP binds and facilitates the cell surface expression of Plexin-B1. I hypothesized that since the T5714C mutant has loss the ability to bind Rac1L61, coexpressing Rac1L61 with the mutant will not enhance the cell surface expression of the mutant Plexin-B1. To test this hypothesis, I coexpressed Plexin-B1 with or without the mutations and RacL61 in COS-7 and treated the cells with Sema4D-AP fusion protein. The Sema4D-AP binds to the Plexin-B1 on the cell

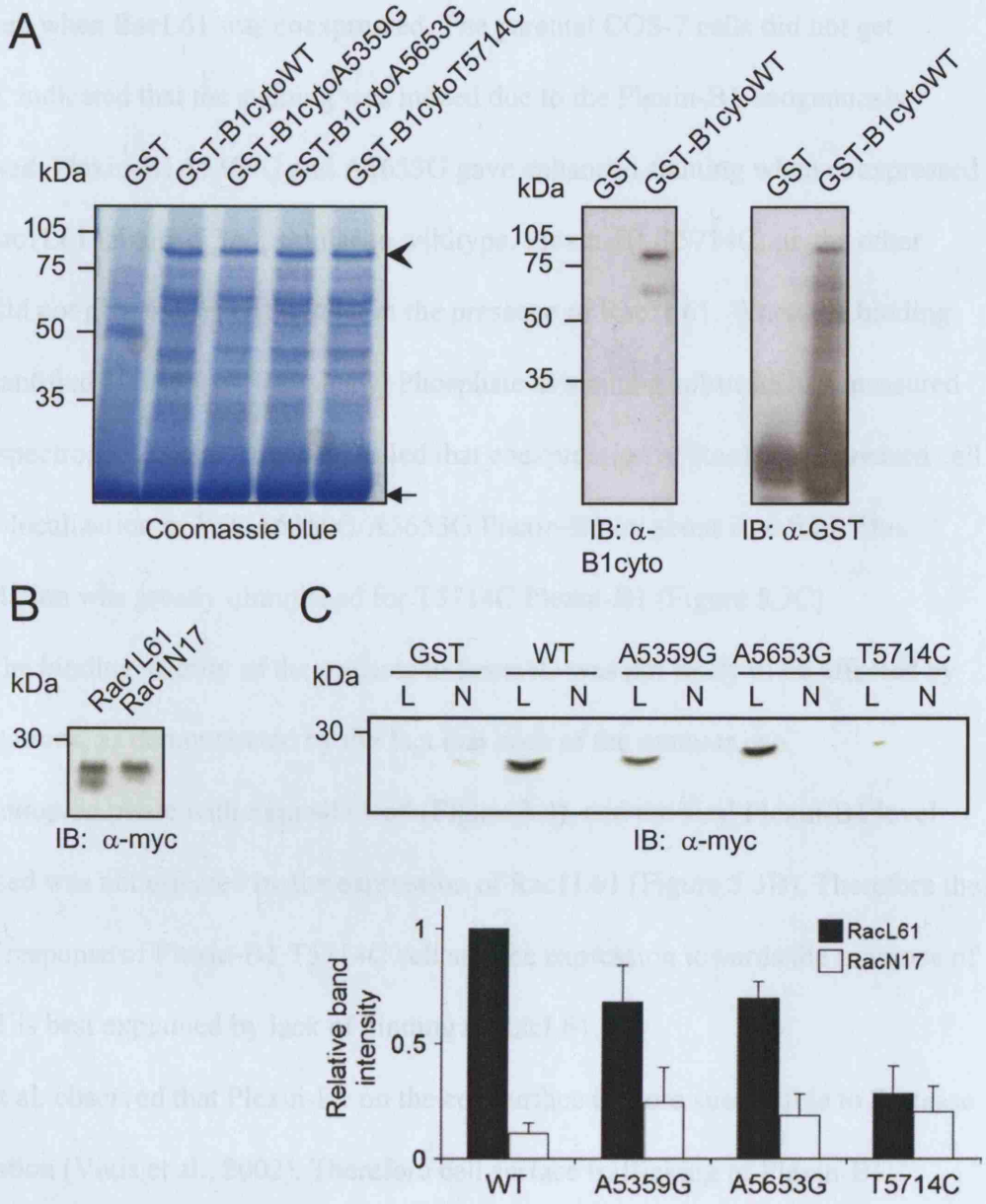

Figure 5.2 Plexin-B1 T5714C mutant does not bind Rac1L61. (A) GST fusion protein of Plexin-B1 cytoplasmic domain with or without the mutations were expressed and purified from E.coli. (left panel). GST-B1cyto was probed with anti-B1cyto or anti-GST in western blot analysis (right panel). (B) Constitutive active or dominant negative Rac1 protein expressed in HEK293T lysate. (C) 50μg of GST fusion protein was incubated with 0.5mg of total cell lysate from cell transfected with indicated Rac mutants (L: Rac1L61; N:Rac1N17). The bound protein was resolved on SDS-PAGE and the presence of Rac1 protein was detected by Western blotting using anti-myc. Relative band intensity was measured from five repeats of the experiment and expressed in lower panel. Error bar = SEM.

surface and this was revealed by staining with BCIP/NBT. As shown in Figure 5.3A, COS-7 cells expressing wildtype Plexin-B1 were stained blue, and this staining was enhanced when RacL61 was coexpressed. The parental COS-7 cells did not get stained, indicated that the staining was indeed due to the Plexin-B1 exogenously expressed. Plexin-B1A5359G and A5653G gave enhanced staining when coexpressed with Rac1L61 (figure 5.3A), similar to wildtype. Plexin-B1 T5714C, on the other hand, did not give enhanced staining in the presence of Rac1L61. When the binding was quantified by using p-Nitrophenyl Phosphate as staining substrate and measured with a spectrophotometer, it was revealed that coexpression of Rac1L61 increased cell surface localization of WT/A5359G/A5653G Plexin-B1 by about five-fold. This upregulation was greatly diminished for T5714C Plexin-B1 (Figure 5.3C).

The binding affinity of the mutants to Sema4D was not likely to be affected by the mutations, as demonstrated by the fact that each of the mutants can coimmunoprecipitate with Sema4D well (Figure 3.4), and the total Plexin-B1 level expressed was not affected by the expression of Rac1L61 (Figure 5.3B). Therefore the lack of response of Plexin-B1 T5714C cell surface expression towards the presence of RacL61 is best explained by lack of binding to RacL61.

Vikis et al. observed that Plexin-B1 on the cell surface is more susceptible to Protease K digestion (Vikis et al., 2002). Therefore cell surface trafficking of Plexin-B1 mediated by RacL61 would increase the susceptibility of Plexin-B1 towards Protease K (Vikis et al., 2002). I tried to adapt their assay to test the Plexin-B1 mutants. WT or mutant Plexin-B1 was transfected into HEK293T cells. The cells were subjected to protease K treatment two days after transfection and then the cell lysate was probed with anti-B1cyto in western analysis. Without Protease K treatment, anti-B1cyto detected two specific Plexin-B1 bands: one of about 300kDa

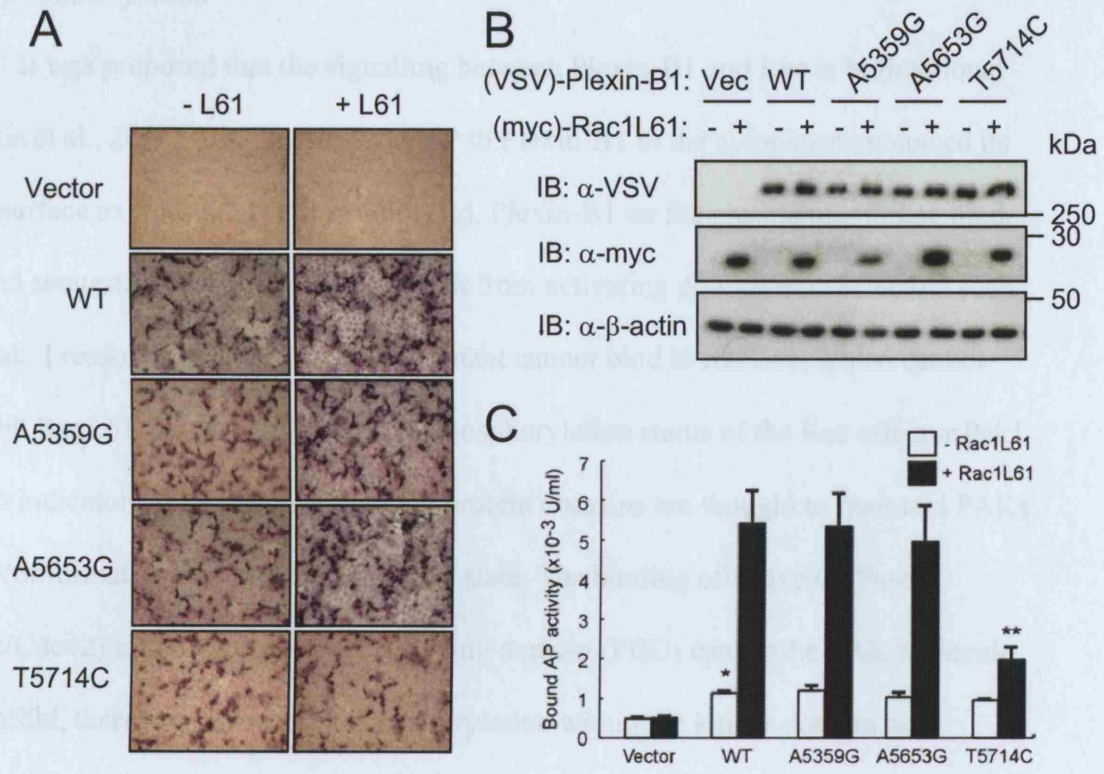

Figure 5.3 Plexin-B1 T5714C mutant is unresponsive to Rac1L61 mediated increase in cell surface expression. (A) Plexin-B1 WT, A5359G, A5653G and T5714C cell surface expression in the presence of Rac1L61 was detected by staining with Sema4D-AP followed by BCIP/NBT. (B) The total Plexin-B1 level in the cells was detected by western blotting using anti-VSV. (C) The amount of bound Sema4D-AP was quantified by substituting BCIP/NBT with p-Nitrophenyl Phosphate and measured the bound specific AP activity by spectrophotometry. *$p<0.01$ versus vector without L61; **$p<0.01$ versus WT with L61, one tail t-test.

and one of about 100kDa (Figure 5.4). I found that Protease K treatment digested the 100kDa protein into fragment of about 50kDa. However I could not detect any difference in the presence or absence of RacL61.

5.2.4 T5714C and A653G mutant forms of Plexin-B1 do not inhibit RacL61-dependent Pak phosphorylation

It was proposed that the signalling between Plexin-B1 and Rac is bidirectional (Vikis et al., 2002). Binding of Rac-GTP to Plexin-B1 in the cytoplasm enhanced its cell surface expression. On the other hand, Plexin-B1 on the plasma membrane binds to and sequesters Rac-GTP and inhibits it from activating downstream effectors such as Pak. I reasoned that since T5714C mutant cannot bind to RacL61, it also cannot inhibit RacL61. To test this I used the phosphorylation status of the Rac effector Pak1 as an indicator of Rac activity. Internal protein domains are thought to maintain PAKs in a conformationally restricted, inactive state. The binding of active GTPase (Rac/Cdc42) to the N-terminal p21-binding domain (PBD) causes the PAK molecule to unfold, thereby allowing autophosphorylation within the kinase domain and regulatory N-terminus and subsequently promoting substrate phosphorylation (Zhao and Manser, 2005).

Plexin-B1, RacL61 and Pak1 were coexpressed in COS-7 cells. The phosphorylation status of Pak1 was monitored by western blot using Anti-Phospho-Pak1(Thr423) antibody. Coexpression of Rac1L61 and Pak1 stimulated the autophosphorylation of Pak1 (figure 5.5A, second lane). WT Plexin-B1 was able to inhibit this Pak activation. A5359G also inhibited Pak phosphorylation. T5714C Plexin-B1 failed to inhibit Pak activation mediated by RacL61 (figure 5.5A, sixth lane). To our surprise, although Plexin-B1 A5653G only showed a reduced binding

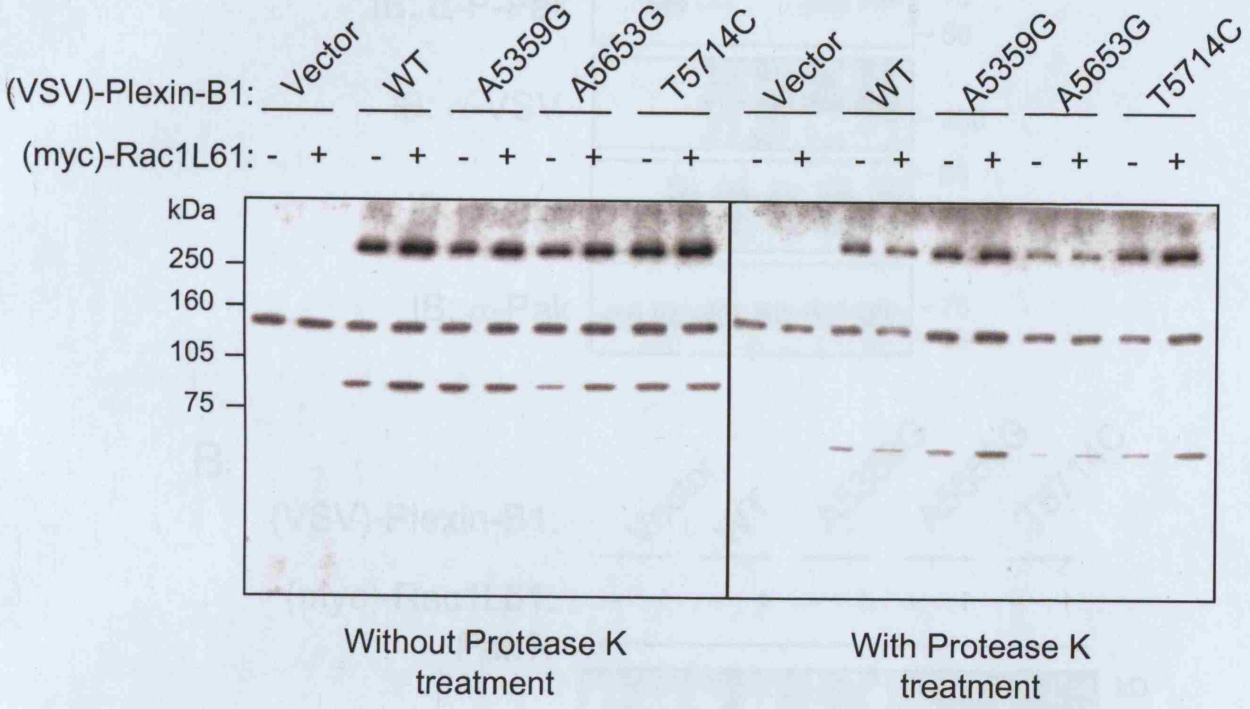

Figure 5.4 Protease K treatment of Plexin-B1 transfected HEK293T cells. Transfected cells were subjected to 0.02mg/ml protease K treatment for 30 minutes. Lysate was analysed with western blotting using anti-B1cyto antibody.

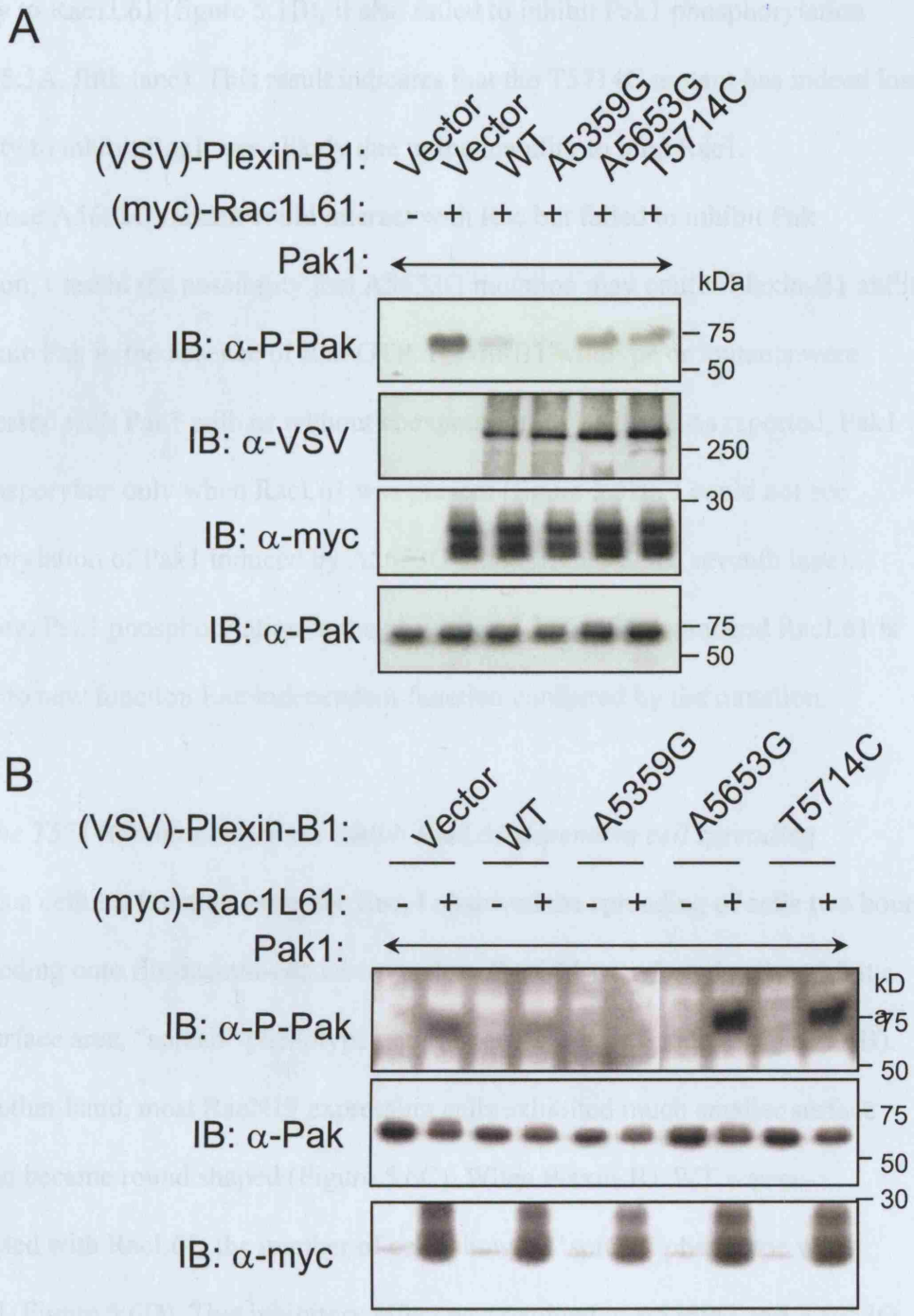

Figure 5.5 Plexin-B1 T5714C mutant cannot inhibit Rac1. Plexin-B1 and Pak1 was coexpressed with (A) or without (B) Rac1L61 in COS-7 cells. The phosphorylation state of transfected Pak1 was monitored by western blot with anti-P(423)-Pak1 antibody.

capacity to Rac1L61 (figure 5.1B), it also failed to inhibit Pak1 phosphorylation (figure 5.5A, fifth lane). This result indicates that the T5714C mutant has indeed lost its ability to inhibit Rac1, very likely due to the inability to bind Rac1.

Since A5653G mutant could interact with Rac but failed to inhibit Pak activation, I tested the possibility that A5653G mutation may confer Plexin-B1 ability to activate Pak in the absence of Rac-GTP. Plexin-B1 wildtype or mutants were coexpressed with Pak1 with or without coexpression of RacL61. As reported, Pak1 autophosporylate only when RacL61 was present (figure 5.5B). I could not see phosphorylation of Pak1 induced by A5653G alone (figure 5.5B, seventh lane). Therefore, Pak1 phosphorylation in the presence of A5653G mutant and RacL61 is not due to new function Rac independent function conferred by the mutation.

5.2.5 The T5714C mutant does not inhibit RacL61-dependent cell spreading

As a cellular function assay for Rac, I observed the spreading of cells two hours after seeding onto fibronectin-coated coverslips. RacL61 transfected cells exhibit a large surface area, "spread" phenotype with discernable lamelipodia (Figure 5.6B). On the other hand, most RacN17 expressing cells exhibited much smaller surface area, and became round shaped (Figure 5.6C). When Plexin-B1 WT was co-transfected with RacL61, the number of cells showing 'spread' phenotype was reduced (Figure 5.6D). This inhibitory effect was retained in A5359G and A5653G Plexin-B1, but on the other hand was lost in T5714C Plexin-B1 (Figure 5.6E). Taken together, the T5714C mutation abolishes Rac1 binding to Plexin-B1 and renders Plexin-B1 less effective in inhibiting Rac1 activity.

5.3 Discussion

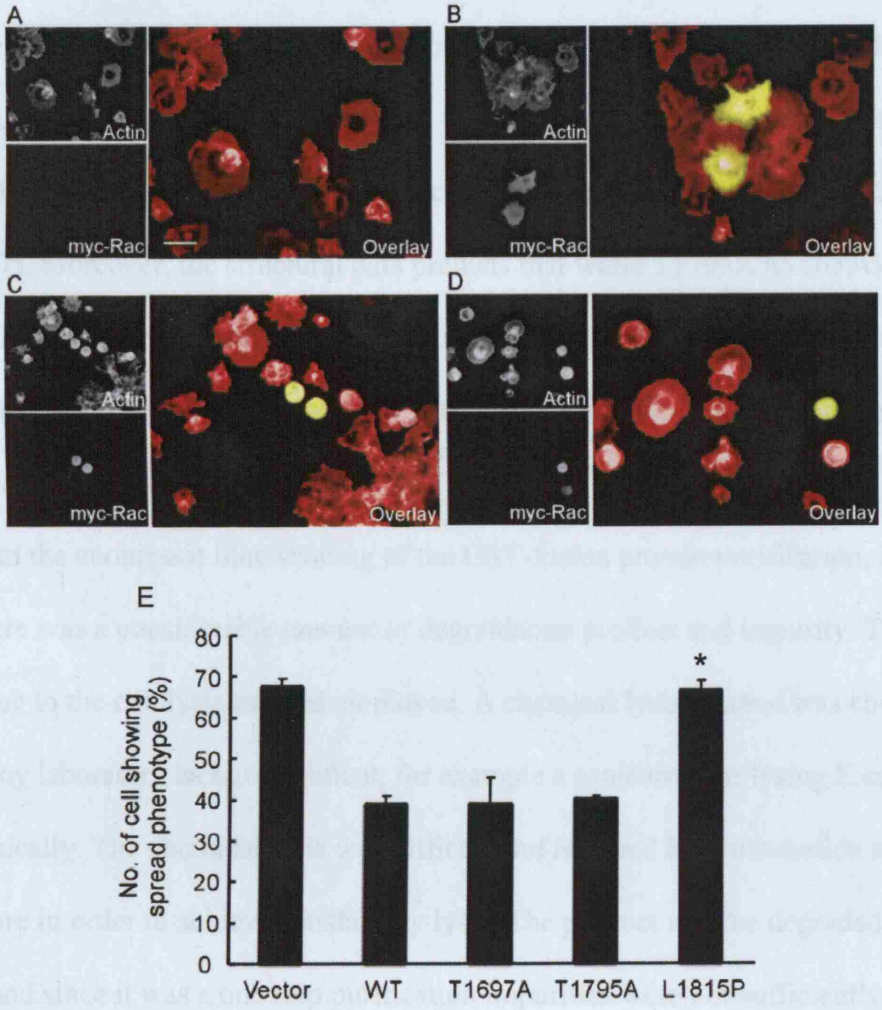

Figure 5.6 Plexin-B1 T5714C mutant cannot inhibit Rac1. COS-7 The cells were trypsinized two days after transfection of (A) Vectors; (B) RacL61; (C) RacN17; or (D) RacL61+Plexin-B1 WT, and seeded onto fibronectin-coated coverslips for two hours. The attached cells were stained by anti-myc (green) or phallodin (red). (E) The number of cell showing spread morphology was counted. The identity of the slides were blinded to the reseaercher. *$p<0.05$ versus L61 + WT, one tail t-test.

In this chapter, the effects of A5359G, A5653G and T5714C mutations on the interaction between Plexin-B1 and Rac were investigated. By GST-pulldown technique I showed that T5714C mutation abolishes the binding of Plexin-B1 to Rac-GTP. Interestingly, a recent structurally study reveals that L1815P (T5714C) mutation will perturb the structure of the putative Rho GTPase binding domain (RBD) (Tong et al., 2007), which agrees with my finding. In fact, L1815 is at the binding interface, and it is therefore expected to have a significant effect on binding (Tong et al., 2008) (figure 5.7). Moreover, the structural data predicts that while T1795A (A5653G) mutation has no effect on Rho GTPase binding affinity, it does perturb the average structure locally. This structural data may shed light on why the A5653G mutant failed to inhibit Pak1 phosphorylation.

From the coomassie blue staining of the GST-fusion protein purification, it seems there was a considerable amount of degratdation product and impurity. This may be due to the cell lysis method employed. A chemical lysis method was chosen because my laboratory lacks equipment, for example a sonicator, for lysing E.coli cells physically. The chemical lysis was difficult and required long incubation at room temperature in order to achieve satisfactory lysis. The product may be degraded in the process, and since it was a one step purification impurities were not sufficiently removed. Nonetheless, since resumably the same impurities were present in all of the GST fusion preparation they should not be responsible for the difference in Rac binding ability I observed.

T5714C mutant lost its ability to inhibit Rac. This led us to predict that it would positively regulate cell migration. Recent experiments in our laboratory supported this prediction. In time lapse microscopy assays, the chemokinesis of cells induced by Sema4D increased with the expression of mutant Plexin-B1 (Wong et al., 2007). And

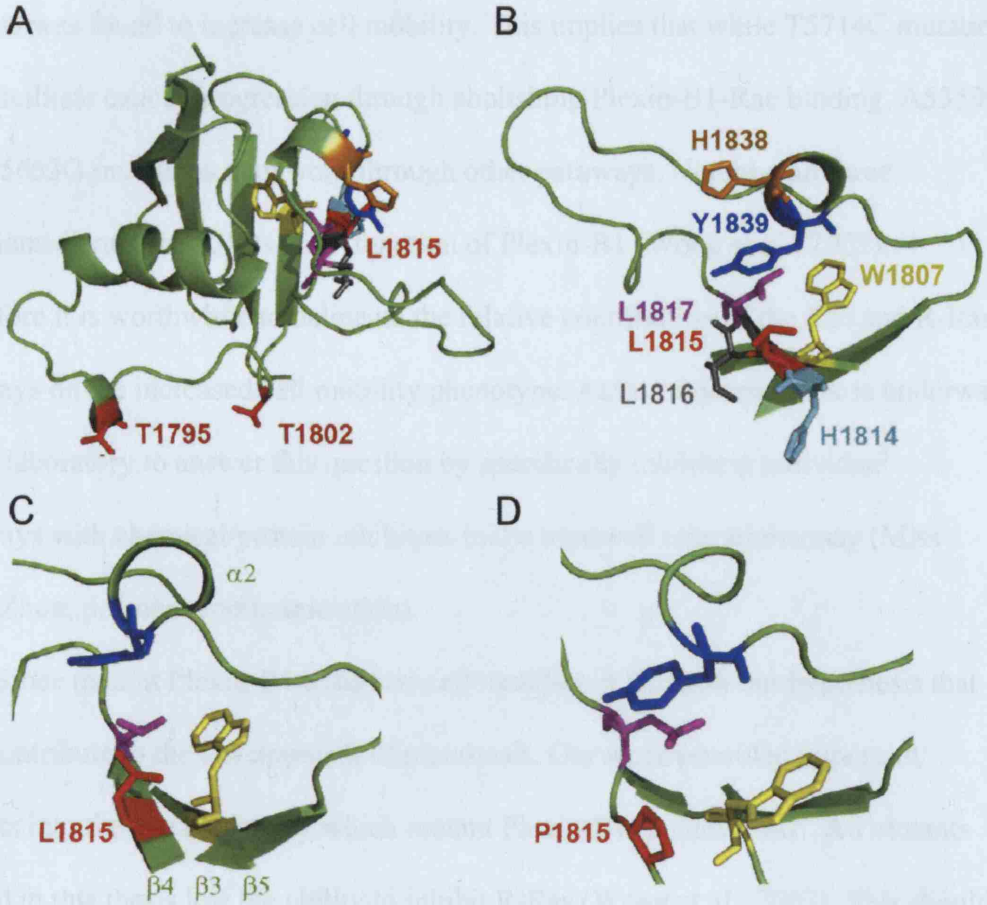

Figure 5.7 Conformational changes in L1815P mutant. (A) The Rho GTPase binding domain (RBD) of Plexin-B1 is shown. (B) Binding site for Rho GTPases viewed from a different angle (as seen from the back of the structure in [A]). Snap-shots of the structure models after 5ns of MD at 300K. Region around residue 1815: (C) wild type; and (D) L1815P. Adapted and modified from Tong et al., 2008.

in transwell migration assays, WT Plexin-B1 inhibits cell migration towards fibronectin by about two fold. Mutant Plexin-B1 on the other hand increased cell mobility by about two to three fold (Miss Chun Zhou, personal communiciation). Although only T5714C mutant lost the ability to interact with Rac1, all three of the mutants was found to increase cell mobility. This implies that while T5714C mutation may facilitate cancer progression through abolishing Plexin-B1-Rac binding, A5359G and A5653G mutations may work through other pathways. Notably, all three mutations disrupt the R-Ras GAP function of Plexin-B1 (Wong et al., 2007). Therefore it is worthwhile to delineate the relative contribution of the Rac and R-Ras pathways on the increased cell mobility phenotype. At this moment work is underway in our laboratory to answer this question by specifically inhibiting individual pathways with chemical/protein inhibitors in the transwell migration assay (Miss Chun Zhou, personal communiciation).

Since mutant Plexin-B1 enhances cell mobility, it fits with our hypothesis that they contribute to the development of metastasis. Our work provided important insights into the mechanism by which mutant Plexin-B1s achieve this. All mutants studied in this thesis lost the ability to inhibit R-Ras (Wong et al., 2007). This should have important implications on cell migration since the R-Ras GAP activity of Plexin-B1 inhibits cell migration by regulating β1 integrin activity (Oinuma et al., 2006). Rac activation leads to the formation of lamellipodia and membrane ruffling. I showed that the T5714C mutant has lost the ability to inhibit formation of lamelliopidia (figure 5.6) and to inhibit activation of Pak1 (figure 5.5). These results shed light on the reason of increased migration ability of cells expressing the mutant Plexin-B1. If these signalling pathways were established as the main pathways for mutant Plexin-

B1-mediated metastases, it would be of interest to design therapeutic strategies to interfere with these pathways.

Given the GST-pulldown results (figure 5.1), it was expected that A5359G and A5653G mutations would not interfere with the ability of Plexin-B1 to regulate Rac1. In fact, the cell spreading assay results (figure 5.3B) suggested that both A5359G and A5653G mutants can inhibit Rac as WT Plexin-B1 does. Intriguingly, when the phosphorylation status of the Rac effector Pak1 was checked, it was found that A5653G mutants could not efficiently inhibit Rac. This suggested the current model of Rac inhibition by Plexin-B1 through sequestration may be too simplified, since A5653G mutant provided an example of a Plexin-B1 capable of binding to but not able to inhibit Rac. Of course, to substantiate this notion more experiments needed to be done to answer more detailed questions regarding the mechanism of lost of Rac inhibition by A5653G Plexin-B1. First of all, a direct observation of Rac activation state upon expression of A5653G Plexin-B1 would be a more conclusive piece of evidence about the ability of A5653G Plexin-B1 to inhibit Rac. This would be done in our laboratory by Rac-GTP pulldown assay with non-mutated Rac in the future. Secondly, when the results of the GST-pulldown experiments were analysed quantitatively, a slight descrease in Rac binding was suggested for T5653G mutant (figure 5.2C lower panel). So it is possible that a certain amount of Rac1L61 was available for activating Pak1 upon A5653G Plexin-B1 expression. It is noteworthy that although A5359G mutant showed a similar decrease in Rac binding (figure 5.2C lower panel), it retained the ability to inhibit Pak1 phosphorylation (figure 5.5). This may suggest the qualitative nature of the GST-pulldown assay does not allow us to differentiate the mutants' ability to inhibit Pak1 phosphorylation based on their Rac binding ability. In order to obtain a more accurate comparison of binding affinity

surface plasmon resonance (SPR) based technology may be employed (Toyofuku et al., 2007).

Chapter 6

Discussion

6.1 Significance of this study

Previous work in our laboratory (Wong et al., 2007) was the first report of the involvement of Plexin-B1 in the progression of cancer. The work presented in this thesis is the molecular characterization of three of the mutations identified. We have found that the loss of Rac binding caused by mutations in the Plexin-B1 gene affect cell function. The T5714C mutation, which inhibits RacGTP binding to Plexin-B1, results in a defect in Rac-induced cell surface trafficking of Plexin-B1. The T5714C mutant form of Plexin-B1 is also defective in sequestration and inhibition of Rac downstream of Plexin-B1 and has lost the inhibitory effect of WT Plexin-B1 on Rac – induced lamellipodia formation and PAK activation. The A5653G mutation reduces binding of Rac-GTP to Plexin-B1 and A5653G mutant form of Plexin-B1 no longer inhibits Rac-induced Pak activation. Mutations in Plexin-B1 therefore affect both upstream and downstream signalling of Plexin-B1. We have also found that the 3 mutations tested have little effect on sema4D binding or PDZRhoGEF binding.

The T5714C therefore has several effects on cell function. Loss of Rac-dependent cell surface trafficking will result in the mutant form being less accessible to activation by Sema4D at the cell surface. Cells expressing the T5714C form will have lost Plexin-B1 dependent ability to sequester and inhibit Rac resulting in enhanced lamellipodia formation and Pak activation. The cytoplasmic domain of Plexin-B1 exists as an inactive dimer which is disrupted upon Rnd, Rac or RhoD binding (Tong et al., 2007). Mutant forms of Plexin-B1 with a loss of Rac binding may be more likely to exist in their inactive conformation. The T5714C mutation lies within the Rac binding domain (Tong et al., 2007) and so would be predicted to affect Rac binding directly. The A5359G and A5653G mutations fall outside this region and may affect the conformation of Plexin-B1 resulting in a reduction in binding.

We found that mutations in Plexin-B1 abolish Rac1 binding and hence affects Plexin-B1 and cell function, most significantly by rendering Plexin-B1 ineffective in inhibiting Rac1. Our results shed light on one of the mechanisms by which Plexin-B1 mutations found in prostate cancer may contribute to tumour progression. The work would facilitate the understanding of the exact role of Plexin-B1 in the progression of prostate cancer, or in other types of cancers.

Together with our collaborator's work, we now have a clearer picture about the functional consequences of Plexin-B1 mutations (figure 6.1). Since all three of the mutations abolish R-Ras binding, the mutant Plexin-B1 could no longer inhibit R-Ras by acting as R-Ras GAP (Wong et al., 2007). This directly leads to a loss of inhibition of integrin, particularly β1 integrins which R-Ras regulates (Oinuma et al., 2006). Since R-Ras mediated integrin activation was implicated in inhibition of cell migratioin (Oinuma et al., 2006), abolishment of Plexin-B1's R-Ras GAP activity is predicted to positively regulate cell migration. This prediction was verified in our time lapse experiments (Wong et al., 2007) and Boyden chamber cell migration experiments (Miss Chun Zhou, personal communication). T5714C mutation render Plexin-B1 unable to inhibit Rac. Since Rac activation on the leading edge of a migrating cell is important for the formation of membrane ruffle which is crucial structure for cell migration. It is also predicted that T5714C mutant will have positive effect on cell migration. While these proposed mechanisms are plausible explanation for the enhanced cell migration phenotype we observed in mutant expressing cells, we do not know which pathway is more important. Moreover, the roles of receptor kinases such as Met or ErbB-2 are not clear. Therefore one of the current goals in our laboratory is to delineate the mechanism by which the mutations affect cell migration.

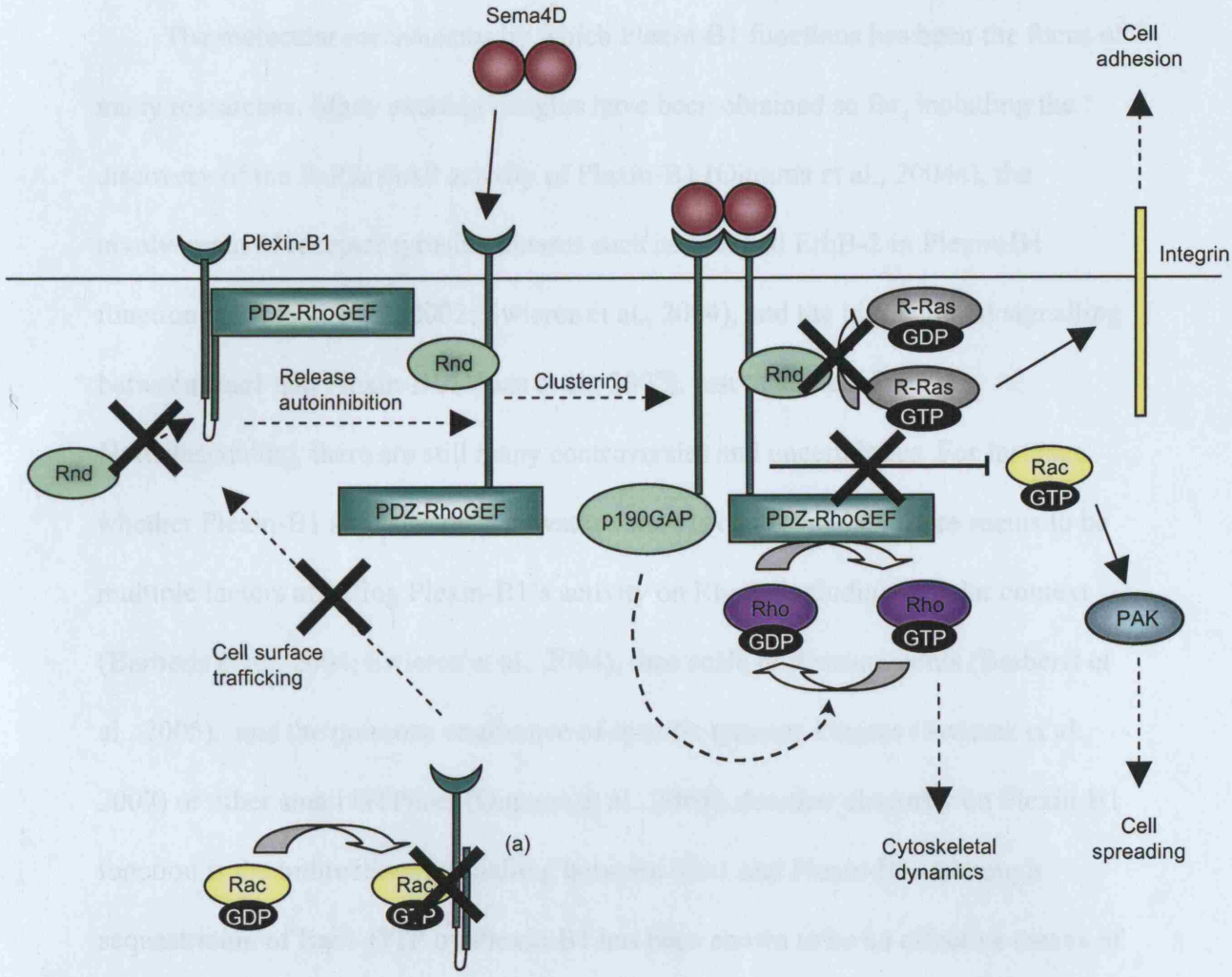

Figure 6.1 Signalling processes of Plexin-B1 affected by the mutations. T5714C mutation abolish interaction with Rac-GTP and Rnd. A5359G, A5653G and T5714C mutations abolish R-Ras interaction. Therefore, the cell surface trafficking of Plexin-B1 and Rac inhibition was affected. Through Pak, the cell spreading was affected by T5714C mutant. Since all mutants cannot inactivate R-Ras, cell adhesion was increased.

6.2 Cell surface trafficking of Plexin-B1

The molecular mechanisms by which Plexin-B1 functions has been the focus of many researches. Many exciting insights have been obtained so far, including the discovery of the R-Ras GAP activity of Plexin-B1 (Oinuma et al., 2004a), the involvement of receptor tyrosine kinases such as Met and ErbB-2 in Plexin-B1 function (Giordano et al., 2002; Swiercz et al., 2004), and the bidirectional signalling between Rac1 and Plexin-B1 (Vikis et al., 2002), just to name a few. Notwithstanding, there are still many controversies and uncertainties. For instance, whether Plexin-B1 activates or inactivates RhoA is controversial. There seems to be multiple factors affecting Plexin-B1's activity on RhoA, including cellular context (Barberis et al., 2004; Swiercz et al., 2004), time scale of measurements (Barberis et al., 2005), and the presence or absence of specific tyrosine kinases (Swiercz et al., 2007) or other small GTPases (Oinuma et al., 2003). Another obscurity on Plexin-B1 function is the bidirectional signalling between Rac1 and Plexin-B1. Although sequestration of Rac1-GTP by Plexin-B1 has been shown to be an effective means of inhibiting signalling downstream of Rac1, little is known about the significance of Plexin-B1 cell surface trafficking promoted by Rac1.

It is of worth to note that our understanding of the mutations depends very much on our understanding on the molecular mechanisms of WT Plexin-B1 functioning. In this study, instead of trying to elucidate the molecular mechanisms of Plexin-B1 function, we identified cancer-related Plexin-B1 mutations and tried to derive and test hypothesises of the effects of the mutations based on the knowledge already obtained on the functioning of Plexin-B1. Since I demonstrated that T5714C mutation abolishes Rac1 binding, and further demonstrated that T5714C mutant is thus unable to inhibit Rac1, I hypothesized it would affect the cell migration ability and partially

tested that hypothesis by showing that the mutant affects lamellipodia formation. However on the other hand I observed T5714C mutation abolished the cell surface trafficking of Plexin-B1 promoted by Rac1, and this observation called for a better understanding about this process. What is the physiological function of this phenomenon? What initiated the activation of Rac1? Does this phenomenon control the sensitivity of the cell towards Sema4D? Does this happen locally within a cell? Does this phenomenon have any bearing on cell migration? Does it affect Plexin-B1 interaction with Met or ErbB-2? These are just few questions need to be answered before we could have a better evaluation on the effect of T5714C mutation.

6.3 Effect of Met/ErbB2 on Plexin-B1 mediated Rho activation/inactivation

The effect of Plexin-B1 on RhoA has been controversial. In Drosophila Plexin-B directly interacts with RhoA and enhances RhoA activity (Hu et al., 2001), thereby regulates motor, sensory and CNS axon pathfinding in developing embryos (Ayoob et al., 2006; Bates and Whitington, 2007). In rat primary hippocampal neurons Plexin-B1 activation leads to RhoA activation which in turn leads to axonal growth cone collapse (Swiercz et al., 2002). Moreover, Plexin-B1 directly interacts with and regulates two Rho specific Guanine exchange factor (GEF), PDZ-RhoGEF and LARG (Perrot et al., 2002; Aurandt et al., 2002; Hirotani et al., 2002; Driessens et al., 2002; Oinuma et al., 2003). However, Barberis et al. showed, in their mouse fibroblast cell collapse model, that Plexin-B1 mediated cell collapse is not dependent on ROCK, and is actually inhibited by activation of RhoA (Barberis et al., 2004). They further demonstrated that this negative regulation of Rho by Plexin-B1 is mediated by p190-RhoGAP, a Rho-specific GTPase activating protein physically interacting with Plexin-B1 (Barberis et al., 2005).

Recently a report shed light on this issue by suggesting that the Met and ErbB2 compete for Plexin-B1 binding and affect the outcome of RhoA activation/inactivation (Swiercz et al., 2007). It seems that if the stoichiometry of Plexin-B1, ErbB-2 and Met favours Met-Plexin-B1 interaction, RhoA inactivation would be the result of Sema4D stimulation. It would lead to RhoA activation if more ErbB-2 is present, on the other hand.

In my attempts to test whether Plexin-B1 mutations affect RhoA regulating function, I used non-serum starved COS-7 cells. I observed inactivation of RhoA when Plexin-B1 is present even with or without the stimulation of Sema4D. In a previous experiement I have shown the expression of Met in COS-7. But the expression level of ErbB-2 in COS-7 is not clear. So it remains to be determined whether the interaction between Plexin-B1 and ErbB-2 or Met would be favoured. Therefore it is interesting to investigate in COS-7 system the relative expression levels of the two receptor tyrosine kinases. The evidence I have got so far suggested that the mutations bear no effect on RhoA inactivation or activation. It therefore implies that the mutations do not affect Met or ErbB-2 binding. We have already got direct evidence on the binding between mutant Plexin-B1 and ErbB-2 (Zhou, personal communication). And the interaction between Plexin-B1 and Met in COS-7 await confirmation. It is interesting to note that the presence of Met or ErbB-2 bears little consequence on the interaction between Plexin-B1 and Rac (Swiercz et al., 2007), so the conclusions about the effects of the mutations on Rac-regulating function of Plexin-B1 could be attributable to the direct effects of those mutations on Rac interaction.

6.4 Diagnostic value of Plexin-B1 mutations

Plexin-B1 mutants losing Rac1 binding capability have been generated by other researchers, and it was pointed out that those mutants failed to translocate to the cell surface (Giordano, personal communication). This observation matched our result on the prostate cancer-related mutation T5714C, which failed to bind Rac1-GTP and defective in expressing on the cell surface. Giordano's observation, together with the results reported in this thesis, predicted that tumour cells harbouring T5714C mutant Plexin-B1 would express the receptor mainly in the cytoplasm. Question regarding the specific cellular location of those Plexin-B1 failed to be trafficked to the cell surface could be answered by confocal microscopy. Should there be an easily detectable cellular spatial expression pattern under immunohistological observation, it might be a marker of clinical interest.

Tissue microarray data suggested that Plexin-B1 is overexpressed in most (>90%) prostate cancer (Wong et al., 2007). Therefore it has good potential to be a diagnostic marker. Our work on the molecular action of three of the mutations (A5359G, A5653G, and T5714C) implied that the importance of the mutations towards cancer progression varies. For instance, T5714C may result in a more severe phenotype. Combination of expressing and mutation data may thus provide a better picture of how a particular cancer would progress.

6.5 Future work

Although high frequency of mutations in Plexin-B1 gene has been found in prostate cancer metastasis, there was no decisive answer to the question whether mutated Plexin-B1 does indeed instrumental to cancer progression, or more precisely, the cancer metastasis process. The effect of the mutations on the metastasis of tumour animal models should be tested. Current murine models which best captured the

clinical features of prostate cancer include conditional *PTEN* knock-out or Myc knock-in in prostate (Wang et al., 2003; Ellwood-Yen et al., 2003). Transgenic coexpression of mutant Plexin-B1 in these models should provide insight on the effects of the mutant Plexin-B1 on the metastasis of the cancer.

T5714C mutant abolish both R-Ras GAP activity and Rac binding ability of Plexin-B1 (Wong et al., 2007). Therefore it is conceivable that it may more severely affect the function of Plexin-B1 then do the other two mutations studied. It would be interesting to generate transgenic mice with knock-in Plexin-B1 T5714C and see whether they are more susceptible to sporadic cancers or induced cancer.

Based on what I have found on the T5714C mutation, I believe it is a loss-of-function mutation. A simple model of the action of Plexin-B1 T5714C mutant protein in cancer based on this knowledge would be that Plexin-B1 normally acts as 'brake' of cell migration. T5714C mutation may render the cells expressing the mutant protein more easily migrate. We have already some preliminary evidence supporting cells expressing mutant Plexin-B1 are more tend to migrate (Nitkunan T. and Zhou C., personal communication). Nonetheless, we also obtained experimental results disagreeing with this model (Dr. Magali Willamson, personal communication). Recently, there is indication that action of Plexin-B1 on Rho is cellular context dependent, so that whether Plexin-B1 activates or inactivates Rho depends on the presence of either ErbB2 or Met, respectively (Swiercz et al., 2007). It is therefore prudent to consider the receptor tyrosine kinases context in the tumour cells when judging whether the Plexin-B1 mutations would impede or facilitate cancer progression.

The cytoskeleton changes which bring about cell migration require very delicate, localized regulation of Rho-like small GTPases (Ridley et al., 2003). In

migrating cells, Rac is mainly activated in the leading edges, resulting in the formation of lammelipodia. According to the current model, Plexin-B1 interacts with and inhibits Rac and thereby exerting a negative effect on cell migration (Vikis et al., 2002). However it should be pointed out that so far the regulation of Rac by Plexin-B1 has only been shown biochemically *in vitro* and a demonstration of Rac spatial regulation by Plexin-B1 would further establish the role of Plexin-B1 in cell migration. To this end, fluorescence resonance energy transfer (FRET) based Rac activation probe might prove instrumental (Gardiner et al., 2002).

Taken together, my results suggested that among A5359G, A5653G and T5714C mutations of Plexin-B1 found in metastatic prostate cancers, while all of them abolish R-RasGAP activity of Plexin-B1, T5714C particularly affect Rac1 signalling through Plexin-B1.

Reference List

Adachi,T., Flaswinkel,H., Yakura,H., Reth,M., and Tsubata,T. (1998). The B cell surface protein CD72 recruits the tyrosine phosphatase SHP-1 upon tyrosine phosphorylation. J. Immunol. *160*, 4662-4665.

Adams,R.H., Lohrum,M., Klostermann,A., Betz,H., and Puschel,A.W. (1997). The chemorepulsive activity of secreted semaphorins is regulated by furin-dependent proteolytic processing. EMBO J. *16*, 6077-6086.

Aizawa,H., Wakatsuki,S., Ishii,A., Moriyama,K., Sasaki,Y., Ohashi,K., Sekine-Aizawa,Y., Sehara-Fujisawa,A., Mizuno,K., Goshima,Y., and Yahara,I. (2001). Phosphorylation of cofilin by LIM-kinase is necessary for semaphorin 3A-induced growth cone collapse. Nat. Neurosci. *4*, 367-373.

Arnold,J.T. and Isaacs,J.T. (2002). Mechanisms involved in the progression of androgen-independent prostate cancers: it is not only the cancer cell's fault. Endocr. Relat Cancer *9*, 61-73.

Aruffo,A. (1998). Transient Expression of Proteins Using COS Cells. In Current Protocols in Molecular Biology, John Wiley & Sons Inc.), p. 16.12.1-16.12.7.

Aurandt,J., Vikis,H.G., Gutkind,J.S., Ahn,N., and Guan,K.L. (2002). The semaphorin receptor plexin-B1 signals through a direct interaction with the Rho-specific nucleotide exchange factor, LARG. Proc. Natl. Acad. Sci. U. S. A *99*, 12085-12090.

Avraham,H., Park,S.Y., Schinkmann,K., and Avraham,S. (2000). RAFTK/Pyk2-mediated cellular signalling. Cell Signal. *12*, 123-133.

Ayoob,J.C., Terman,J.R., and Kolodkin,A.L. (2006). Drosophila Plexin B is a Sema-2a receptor required for axon guidance. Development. *133*, 2125-2135.

Bagnard,D., Lohrum,M., Uziel,D., Puschel,A.W., and Bolz,J. (1998). Semaphorins act as attractive and repulsive guidance signals during the development of cortical projections. Development *125*, 5043-5053.

Barberis,D., Artigiani,S., Casazza,A., Corso,S., Giordano,S., Love,C.A., Jones,E.Y., Comoglio,P.M., and Tamagnone,L. (2004). Plexin signaling hampers integrin-based adhesion, leading to Rho-kinase independent cell rounding, and inhibiting lamellipodia extension and cell motility. FASEB J. *18*, 592-594.

Barberis,D., Casazza,A., Sordella,R., Corso,S., Artigiani,S., Settleman,J., Comoglio,P.M., and Tamagnone,L. (2005). p190 Rho-GTPase activating protein associates with plexins and it is required for semaphorin signalling. J. Cell Sci. *118*, 4689-4700.

Barisani,D., Meneveri,R., Ginelli,E., Cassani,C., and Conte,D. (2000). Iron overload and gene expression in HepG2 cells: analysis by differential display. FEBS Lett. *469*, 208-212.

Basile,J.R., Afkhami,T., and Gutkind,J.S. (2005). Semaphorin 4D/plexin-B1 induces endothelial cell migration through the activation of PYK2, Src, and the phosphatidylinositol 3-kinase-Akt pathway. Mol. Cell Biol. *25*, 6889-6898.

Basile,J.R., Barac,A., Zhu,T., Guan,K.L., and Gutkind,J.S. (2004). Class IV semaphorins promote angiogenesis by stimulating Rho-initiated pathways through plexin-B. Cancer Res. *64*, 5212-5224.

Basile,J.R., Holmbeck,K., Bugge,T.H., and Gutkind,J.S. (2007). MT1-MMP controls tumor-induced angiogenesis through the release of semaphorin 4D. J. Biol. Chem. *282*, 6899-6905.

Bates,K.E. and Whitington,P.M. (2007). Semaphorin 2a secreted by oenocytes signals through plexin B and plexin A to guide sensory axons in the Drosophila embryo. Dev. Biol. *302*, 522-535.

Billard,C., Delaire,S., Raffoux,E., Bensussan,A., and Boumsell,L. (2000). Switch in the protein tyrosine phosphatase associated with human CD100 semaphorin at terminal B-cell differentiation stage. Blood *95*, 965-972.

Birchmeier,C., Birchmeier,W., Gherardi,E., and Vande Woude,G.F. (2003). Met, metastasis, motility and more. Nat. Rev. Mol. Cell Biol. *4*, 915-925.

Bougeret,C., Mansur,I.G., Dastot,H., Schmid,M., Mahouy,G., Bensussan,A., and Boumsell,L. (1992). Increased surface expression of a newly identified 150-kDa dimer early after human T lymphocyte activation. J. Immunol. *148*, 318-323.

Burbelo,P.D., Finegold,A.A., Kozak,C.A., Yamada,Y., and Takami,H. (1998). Cloning, genomic organization and chromosomal assignment of the mouse p190-B gene. Biochim. Biophys. Acta. *1443*, 203-210.

Chambers,A.F., Groom,A.C., and MacDonald,I.C. (2002). Dissemination and growth of cancer cells in metastatic sites. Nat. Rev. Cancer *2*, 563-572.

Chedotal,A., Del Rio,J.A., Ruiz,M., He,Z., Borrell,V., de Castro,F., Ezan,F., Goodman,C.S., Tessier-Lavigne,M., Sotelo,C., and Soriano,E. (1998). Semaphorins III and IV repel hippocampal axons via two distinct receptors. Development *125*, 4313-4323.

Cheung,E., Wadhera,P., Dorff,T., and Pinski,J. (2008). Diet and prostate cancer risk reduction. Expert. Rev. Anticancer Ther. *8*, 43-50.

Christensen,C., Ambartsumian,N., Gilestro,G., Thomsen,B., Comoglio,P., Tamagnone,L., Guldberg,P., and Lukanidin,E. (2005). Proteolytic processing converts the repelling signal Sema3E into an inducer of invasive growth and lung metastasis. Cancer Res. *65*, 6167-6177.

Christensen,C.R., Klingelhofer,J., Tarabykina,S., Hulgaard,E.F., Kramerov,D., and Lukanidin,E. (1998). Transcription of a novel mouse semaphorin gene, M-semaH, correlates with the metastatic ability of mouse tumor cell lines. Cancer Res. *58*, 1238-1244.

Comeau,M.R., Johnson,R., DuBose,R.F., Petersen,M., Gearing,P., VandenBos,T., Park,L., Farrah,T., Buller,R.M., Cohen,J.I., Strockbine,L.D., Rauch,C., and Spriggs,M.K. (1998). A poxvirus-encoded semaphorin induces cytokine production from monocytes and binds to a novel cellular semaphorin receptor, VESPR. Immunity. *8*, 473-482.

Comoglio,P.M., Tamagnone,L., and Giordano,S. (2004). Invasive growth: a two-way street for semaphorin signalling. Nat. Cell Biol. *6*, 1155-1157.

Conrotto,P., Corso,S., Gamberini,S., Comoglio,P.M., and Giordano,S. (2004). Interplay between scatter factor receptors and B plexins controls invasive growth. Oncogene ..

Conrotto,P., Valdembri,D., Corso,S., Serini,G., Tamagnone,L., Comoglio,P.M., Bussolino,F., and Giordano,S. (2005). Sema4D induces angiogenesis through Met recruitment by Plexin B1. Blood ..

De Marzo,A.M., Nakai,Y., and Nelson,W.G. (2007). Inflammation, atrophy, and prostate carcinogenesis. Urol. Oncol. *25*, 398-400.

de Winter,F., Holtmaat,A.J., and Verhaagen,J. (2002a). Neuropilin and class 3 semaphorins in nervous system regeneration. Adv. Exp. Med. Biol. *515:115-39.*, 115-139.

de Winter,F., Oudega,M., Lankhorst,A.J., Hamers,F.P., Blits,B., Ruitenberg,M.J., Pasterkamp,R.J., Gispen,W.H., and Verhaagen,J. (2002b). Injury-induced class 3 semaphorin expression in the rat spinal cord. Exp. Neurol. *175*, 61-75.

Delaire,S., Billard,C., Tordjman,R., Chedotal,A., Elhabazi,A., Bensussan,A., and Boumsell,L. (2001). Biological activity of soluble CD100. II. Soluble CD100, similarly to H-SemaIII, inhibits immune cell migration. J. Immunol. *166*, 4348-4354.

DeMarzo,A.M., Nelson,W.G., Isaacs,W.B., and Epstein,J.I. (2003). Pathological and molecular aspects of prostate cancer. Lancet *361*, 955-964.

Deng,S., Hirschberg,A., Worzfeld,T., Penachioni,J.Y., Korostylev,A., Swiercz,J.M., Vodrazka,P., Mauti,O., Stoeckli,E.T., Tamagnone,L., Offermanns,S., and Kuner,R. (2007). Plexin-B2, but not Plexin-B1, critically modulates neuronal migration and patterning of the developing nervous system in vivo. J. Neurosci. *27*, 6333-6347.

Dickson,B.J. (2002). Molecular mechanisms of axon guidance. Science *298*, 1959-1964.

Driessens,M.H., Hu,H., Nobes,C.D., Self,A., Jordens,I., Goodman,C.S., and Hall,A. (2001). Plexin-B semaphorin receptors interact directly with active Rac and regulate the actin cytoskeleton by activating Rho. Curr. Biol. *11*, 339-344.

Driessens,M.H., Olivo,C., Nagata,K., Inagaki,M., and Collard,J.G. (2002). B plexins activate Rho through PDZ-RhoGEF. FEBS Lett. *529*, 168-172.

Eickholt,B.J., Mackenzie,S.L., Graham,A., Walsh,F.S., and Doherty,P. (1999). Evidence for collapsin-1 functioning in the control of neural crest migration in both trunk and hindbrain regions. Development *126*, 2181-2189.

Eickholt,B.J., Walsh,F.S., and Doherty,P. (2002). An inactive pool of GSK-3 at the leading edge of growth cones is implicated in Semaphorin 3A signaling. J. Cell Biol. *157*, 211-217.

Elhabazi,A., Delaire,S., Bensussan,A., Boumsell,L., and Bismuth,G. (2001). Biological activity of soluble CD100. I. The extracellular region of CD100 is released from the surface of T lymphocytes by regulated proteolysis. J. Immunol. *166*, 4341-4347.

Elhabazi,A., Lang,V., Herold,C., Freeman,G.J., Bensussan,A., Boumsell,L., and Bismuth,G. (1997). The human semaphorin-like leukocyte cell surface molecule CD100 associates with a serine kinase activity. J. Biol. Chem. *19;272*, 23515-23520.

Ellwood-Yen,K., Graeber,T.G., Wongvipat,J., Iruela-Arispe,M.L., Zhang,J., Matusik,R., Thomas,G.V., and Sawyers,C.L. (2003). Myc-driven murine prostate cancer shares molecular features with human prostate tumors. Cancer Cell. *4*, 223-238.

Fan,J., Mansfield,S.G., Redmond,T., Gordon-Weeks,P.R., and Raper,J.A. (1993). The organization of F-actin and microtubules in growth cones exposed to a brain-derived collapsing factor. J. Cell Biol. *121*, 867-878.

Fazzari,P., Penachioni,J., Gianola,S., Rossi,F., Eickholt,B.J., Maina,F., Alexopoulou,L., Sottile,A., Comoglio,P.M., Flavell,R.A., and Tamagnone,L. (2007). Plexin-B1 plays a redundant role during mouse development and in tumour angiogenesis. BMC. Dev. Biol. *7:55.*, 55.

Flanagan,J.G. and Cheng,H.J. (2000). Alkaline phosphatase fusion proteins for molecular characterization and cloning of receptors and their ligands. Methods Enzymol. *327:198-210.*, 198-210.

Flanagan,J.G., Cheng,H.J., Feldheim,D.A., Hattori,M., Lu,Q., and Vanderhaeghen,P. (2000). Alkaline phosphatase fusions of ligands or receptors as in situ probes for staining of cells, tissues, and embryos. Methods Enzymol. *327:19-35.*, 19-35.

Flanagan,J.G. and Leder,P. (1990). The kit ligand: a cell surface molecule altered in steel mutant fibroblasts. Cell. *63*, 185-194.

Foster,R., Hu,K.Q., Lu,Y., Nolan,K.M., Thissen,J., and Settleman,J. (1996). Identification of a novel human Rho protein with unusual properties: GTPase deficiency and in vivo farnesylation. Mol. Cell Biol. *16*, 2689-2699.

Fournier,A.E., Nakamura,F., Kawamoto,S., Goshima,Y., Kalb,R.G., and Strittmatter,S.M. (2000). Semaphorin3A enhances endocytosis at sites of receptor-F-actin colocalization during growth cone collapse. J. Cell Biol. *149*, 411-422.

Fujioka,S., Masuda,K., Toguchi,M., Ohoka,Y., Sakai,T., Furuyama,T., and Inagaki,S. (2003). Neurotrophic effect of Semaphorin 4D in PC12 cells. Biochem. Biophys. Res. Commun. *301*, 304-310.

Fukuhara,S., Chikumi,H., and Gutkind,J.S. (2000). Leukemia-associated Rho guanine nucleotide exchange factor (LARG) links heterotrimeric G proteins of the G(12) family to Rho. FEBS Lett. *485*, 183-188.

Fukuhara,S., Murga,C., Zohar,M., Igishi,T., and Gutkind,J.S. (1999). A novel PDZ domain containing guanine nucleotide exchange factor links heterotrimeric G proteins to Rho. J. Biol. Chem. *274*, 5868-5879.

Furuyama,T., Inagaki,S., Kosugi,A., Noda,S., Saitoh,S., Ogata,M., Iwahashi,Y., Miyazaki,N., Hamaoka,T., and Tohyama,M. (1996). Identification of a novel transmembrane semaphorin expressed on lymphocytes. J. Biol. Chem. *271*, 33376-33381.

Futamura,M., Kamino,H., Miyamoto,Y., Kitamura,N., Nakamura,Y., Ohnishi,S., Masuda,Y., and Arakawa,H. (2007). Possible role of semaphorin 3F, a candidate tumor suppressor gene at 3p21.3, in p53-regulated tumor angiogenesis suppression. Cancer Res. *67*, 1451-1460.

Gardiner,E.M., Pestonjamasp,K.N., Bohl,B.P., Chamberlain,C., Hahn,K.M., and Bokoch,G.M. (2002). Spatial and temporal analysis of Rac activation during live neutrophil chemotaxis. Curr. Biol. *12*, 2029-2034.

Gentile,A. and Comoglio,P.M. (2004). Invasive growth: a genetic program. Int. J. Dev. Biol. *48*, 451-456.

Gherardi,E., Love,C.A., Esnouf,R.M., and Jones,E.Y. (2004). The sema domain. Curr. Opin. Struct. Biol. *14*, 669-678.

Giordano,S., Corso,S., Conrotto,P., Artigiani,S., Gilestro,G., Barberis,D., Tamagnone,L., and Comoglio,P.M. (2002). The semaphorin 4D receptor controls invasive growth by coupling with Met. Nat. Cell Biol. *4*, 720-724.

Giraudon,P., Vincent,P., Vuaillat,C., Verlaeten,O., Cartier,L., Marie-Cardine,A., Mutin,M., Bensussan,A., Belin,M.F., and Boumsell,L. (2004). Semaphorin CD100 from activated T lymphocytes induces process extension collapse in oligodendrocytes and death of immature neural cells. J. Immunol. *172*, 1246-1255.

Gitler,A.D., Lu,M.M., and Epstein,J.A. (2004). PlexinD1 and semaphorin signaling are required in endothelial cells for cardiovascular development. Dev. Cell *7*, 107-116.

Gonzalgo,M.L. and Isaacs,W.B. (2003). Molecular pathways to prostate cancer. J. Urol. *170*, 2444-2452.

Goshima,Y., Nakamura,F., Strittmatter,P., and Strittmatter,S.M. (1995). Collapsin-induced growth cone collapse mediated by an intracellular protein related to UNC-33. Nature *376*, 509-514.

Gronberg,H. (2003). Prostate cancer epidemiology. Lancet *361*, 859-864.

Guasch,R.M., Scambler,P., Jones,G.E., and Ridley,A.J. (1998). RhoE regulates actin cytoskeleton organization and cell migration. Mol. Cell Biol. *18*, 4761-4771.

Hall,A. (1998). Rho GTPases and the actin cytoskeleton. Science *279*, 509-514.

Hall,K.T., Boumsell,L., Schultze,J.L., Boussiotis,V.A., Dorfman,D.M., Cardoso,A.A., Bensussan,A., Nadler,L.M., and Freeman,G.J. (1996). Human CD100, a novel leukocyte semaphorin that promotes B-cell aggregation and differentiation. Proc. Natl. Acad. Sci. U. S. A *93*, 11780-11785.

Hancock,J.F. (2003). Ras proteins: different signals from different locations. Nat. Rev. Mol. Cell Biol. *4*, 373-384.

He,Z., Wang,K.C., Koprivica,V., Ming,G., and Song,H.J. (2002). Knowing how to navigate: mechanisms of semaphorin signaling in the nervous system. Sci. STKE. *2002*, RE1.

Herold,C., Elhabazi,A., Bismuth,G., Bensussan,A., and Boumsell,L. (1996). CD100 is associated with CD45 at the surface of human T lymphocytes. Role in T cell homotypic adhesion. J. Immunol. *157*, 5262-5268.

Hirotani,M., Ohoka,Y., Yamamoto,T., Nirasawa,H., Furuyama,T., Kogo,M., Matsuya,T., and Inagaki,S. (2002). Interaction of plexin-B1 with PDZ domain-containing Rho guanine nucleotide exchange factors. Biochem. Biophys. Res. Commun. *297*, 32-37.

Holly,S.P., Larson,M.K., and Parise,L.V. (2005). The unique N-terminus of R-ras is required for rac activation and precise regulation of cell migration. Mol. Biol. Cell *16*, 2458-2469.

Hu,H., Marton,T.F., and Goodman,C.S. (2001). Plexin B mediates axon guidance in Drosophila by simultaneously inhibiting active Rac and enhancing RhoA signaling. Neuron *32*, 39-51.

Ito,T., Kagoshima,M., Sasaki,Y., Li,C., Udaka,N., Kitsukawa,T., Fujisawa,H., Taniguchi,M., Yagi,T., Kitamura,H., and Goshima,Y. (2000). Repulsive axon guidance molecule Sema3A inhibits branching morphogenesis of fetal mouse lung. Mech. Dev. *97*, 35-45.

Jin,Z. and Strittmatter,S.M. (1997). Rac1 mediates collapsin-1-induced growth cone collapse. J. Neurosci. *17*, 6256-6263.

Kagoshima,M. and Ito,T. (2001). Diverse gene expression and function of semaphorins in developing lung: positive and negative regulatory roles of semaphorins in lung branching morphogenesis. Genes Cells *6*, 559-571.

Kameyama,T., Murakami,Y., Suto,F., Kawakami,A., Takagi,S., Hirata,T., and Fujisawa,H. (1996a). Identification of a neuronal cell surface molecule, plexin, in mice. Biochem. Biophys. Res. Commun. *226*, 524-529.

Kameyama,T., Murakami,Y., Suto,F., Kawakami,A., Takagi,S., Hirata,T., and Fujisawa,H. (1996b). Identification of plexin family molecules in mice. Biochem. Biophys. Res. Commun. *226*, 396-402.

Keely,P.J., Rusyn,E.V., Cox,A.D., and Parise,L.V. (1999). R-Ras signals through specific integrin alpha cytoplasmic domains to promote migration and invasion of breast epithelial cells. J. Cell Biol. *145*, 1077-1088.

Kikutani,H. and Kumanogoh,A. (2003). Semaphorins in interactions between T cells and antigen-presenting cells. Nat. Rev. Immunol. *3*, 159-167.

Kinbara,K., Goldfinger,L.E., Hansen,M., Chou,F.L., and Ginsberg,M.H. (2003). Ras GTPases: integrins' friends or foes? Nat. Rev. Mol. Cell Biol. *4*, 767-776.

Kirby,r. (2002). An Illustrated Pocketbook of Prostatic Diseases. The Parthenon Publishing Group).

Kitsukawa,T., Shimizu,M., Sanbo,M., Hirata,T., Taniguchi,M., Bekku,Y., Yagi,T., and Fujisawa,H. (1997). Neuropilin-semaphorin III/D-mediated chemorepulsive signals play a crucial role in peripheral nerve projection in mice. Neuron *19*, 995-1005.

Kobayashi,H., Koppel,A.M., Luo,Y., and Raper,J.A. (1997). A role for collapsin-1 in olfactory and cranial sensory axon guidance. J. Neurosci. *17*, 8339-8352.

Kolodkin,A.L., Matthes,D.J., O'Connor,T.P., Patel,N.H., Admon,A., Bentley,D., and Goodman,C.S. (1992). Fasciclin IV: sequence, expression, and function during growth cone guidance in the grasshopper embryo. Neuron *9*, 831-845.

Kourlas,P.J., Strout,M.P., Becknell,B., Veronese,M.L., Croce,C.M., Theil,K.S., Krahe,R., Ruutu,T., Knuutila,S., Bloomfield,C.D., and Caligiuri,M.A. (2000). Identification of a gene at 11q23 encoding a guanine nucleotide exchange factor: evidence for its fusion with MLL in acute myeloid leukemia. Proc. Natl. Acad. Sci. U. S. A *97*, 2145-2150.

Kruger,R.P., Aurandt,J., and Guan,K.L. (2005). Semaphorins command cells to move. Nat. Rev. Mol. Cell Biol. *6*, 789-800.

Kuhn,T.B., Brown,M.D., Wilcox,C.L., Raper,J.A., and Bamburg,J.R. (1999). Myelin and collapsin-1 induce motor neuron growth cone collapse through different pathways: inhibition of collapse by opposing mutants of rac1. J. Neurosci. *19*, 1965-1975.

Kumanogoh,A., Marukawa,S., Suzuki,K., Takegahara,N., Watanabe,C., Ch'ng,E., Ishida,I., Fujimura,H., Sakoda,S., Yoshida,K., and Kikutani,H. (2002). Class IV semaphorin Sema4A enhances T-cell activation and interacts with Tim-2. Nature *419*, 629-633.

Kumanogoh,A., Watanabe,C., Lee,I., Wang,X., Shi,W., Araki,H., Hirata,H., Iwahori,K., Uchida,J., Yasui,T., Matsumoto,M., Yoshida,K., Yakura,H., Pan,C., Parnes,J.R., and Kikutani,H. (2000). Identification of CD72 as a lymphocyte receptor

for the class IV semaphorin CD100: a novel mechanism for regulating B cell signaling. Immunity. *13*, 621-631.

Love,C.A., Harlos,K., Mavaddat,N., Davis,S.J., Stuart,D.I., Jones,E.Y., and Esnouf,R.M. (2003). The ligand-binding face of the semaphorins revealed by the high-resolution crystal structure of SEMA4D. Nat. Struct. Biol. *10*, 843-848.

Luo,Y., Raible,D., and Raper,J.A. (1993). Collapsin: a protein in brain that induces the collapse and paralysis of neuronal growth cones. Cell *75*, 217-227.

Lyons,G.E. (1996). Vertebrate heart development. Curr. Opin. Genet. Dev. *6*, 454-460.

Maestrini,E., Tamagnone,L., Longati,P., Cremona,O., Gulisano,M., Bione,S., Tamanini,F., Neel,B.G., Toniolo,D., and Comoglio,P.M. (1996b). A family of transmembrane proteins with homology to the MET-hepatocyte growth factor receptor. Proc. Natl. Acad. Sci. U. S. A *93*, 674-678.

Maestrini,E., Tamagnone,L., Longati,P., Cremona,O., Gulisano,M., Bione,S., Tamanini,F., Neel,B.G., Toniolo,D., and Comoglio,P.M. (1996a). A family of transmembrane proteins with homology to the MET-hepatocyte growth factor receptor. Proc. Natl. Acad. Sci. U. S. A *93*, 674-678.

Masuda,K., Furuyama,T., Takahara,M., Fujioka,S., Kurinami,H., and Inagaki,S. (2004). Sema4D stimulates axonal outgrowth of embryonic DRG sensory neurones. Genes Cells *9*, 821-829.

McNeal,J.E., Redwine,E.A., Freiha,F.S., and Stamey,T.A. (1988). Zonal distribution of prostatic adenocarcinoma. Correlation with histologic pattern and direction of spread. Am. J. Surg. Pathol. *12*, 897-906.

Miao,H.Q., Lee,P., Lin,H., Soker,S., and Klagsbrun,M. (2000). Neuropilin-1 expression by tumor cells promotes tumor angiogenesis and progression. FASEB J. *14*, 2532-2539.

Mitsui,N., Inatome,R., Takahashi,S., Goshima,Y., Yamamura,H., and Yanagi,S. (2002). Involvement of Fes/Fps tyrosine kinase in semaphorin3A signaling. EMBO J. *21*, 3274-3285.

Monti,S., Proietti-Pannunzi,L., Sciarra,A., Lolli,F., Falasca,P., Poggi,M., Celi,F.S., and Toscano,V. (2007). The IGF axis in prostate cancer. Curr. Pharm. Des. *13*, 719-727.

Muller,M.W., Giese,N.A., Swiercz,J.M., Ceyhan,G.O., Esposito,I., Hinz,U., Buchler,P., Giese,T., Buchler,M.W., Offermanns,S., and Friess,H. (2007). Association of axon guidance factor Semaphorin 3A with poor outcome in pancreatic cancer. Int. J. Cancer. ..

Nair,P.N., McArdle,L., Cornell,J., Cohn,S.L., and Stallings,R.L. (2007). High-resolution analysis of 3p deletion in neuroblastoma and differential methylation of the SEMA3B tumor suppressor gene. Cancer Genet. Cytogenet. *174*, 100-110.

Nobes,C.D., Lauritzen,I., Mattei,M.G., Paris,S., Hall,A., and Chardin,P. (1998). A new member of the Rho family, Rnd1, promotes disassembly of actin filament structures and loss of cell adhesion. J. Cell Biol. *141*, 187-197.

Ohta,K., Mizutani,A., Kawakami,A., Murakami,Y., Kasuya,Y., Takagi,S., Tanaka,H., and Fujisawa,H. (1995). Plexin: a novel neuronal cell surface molecule that mediates cell adhesion via a homophilic binding mechanism in the presence of calcium ions. Neuron *14*, 1189-1199.

Oinuma,I., Ishikawa,Y., Katoh,H., and Negishi,M. (2004a). The Semaphorin 4D receptor Plexin-B1 is a GTPase activating protein for R-Ras. Science *305*, 862-865.

Oinuma,I., Katoh,H., Harada,A., and Negishi,M. (2003). Direct interaction of Rnd1 with Plexin-B1 regulates PDZ-RhoGEF-mediated Rho activation by Plexin-B1 and induces cell contraction in COS-7 cells. J. Biol. Chem. *278*, 25671-25677.

Oinuma,I., Katoh,H., and Negishi,M. (2004b). Molecular dissection of the semaphorin 4D receptor plexin-B1-stimulated R-Ras GTPase-activating protein activity and neurite remodeling in hippocampal neurons. J. Neurosci. *24*, 11473-11480.

Oinuma,I., Katoh,H., and Negishi,M. (2006). Semaphorin 4D/Plexin-B1-mediated R-Ras GAP activity inhibits cell migration by regulating beta(1) integrin activity. J. Cell Biol. *173*, 601-613.

Perrot,V., Vazquez-Prado,J., and Gutkind,J.S. (2002). Plexin B regulates Rho through the guanine nucleotide exchange factors leukemia-associated Rho GEF (LARG) and PDZ-RhoGEF. J. Biol. Chem. *277*, 43115-43120.

Polleux,F., Morrow,T., and Ghosh,A. (2000). Semaphorin 3A is a chemoattractant for cortical apical dendrites. Nature *404*, 567-573.

Qi,L., Robinson,W.A., Brady,B.M., and Glode,L.M. (2003). Migration and invasion of human prostate cancer cells is related to expression of VEGF and its receptors. Anticancer Res. *23*, 3917-3922.

Rabacchi,S.A., Solowska,J.M., Kruk,B., Luo,Y., Raper,J.A., and Baird,D.H. (1999). Collapsin-1/semaphorin-III/D is regulated developmentally in Purkinje cells and collapses pontocerebellar mossy fiber neuronal growth cones. J. Neurosci. *19*, 4437-4448.

Ridley,A.J., Schwartz,M.A., Burridge,K., Firtel,R.A., Ginsberg,M.H., Borisy,G., Parsons,J.T., and Horwitz,A.R. (2003). Cell migration: integrating signals from front to back. Science. *302*, 1704-1709.

Ridley,A.J., Self,A.J., Kasmi,F., Paterson,H.F., Hall,A., Marshall,C.J., and Ellis,C. (1993). rho family GTPase activating proteins p190, bcr and rhoGAP show distinct specificities in vitro and in vivo. EMBO J. *12*, 5151-5160.

Roche,J., Drabkin,H., and Brambilla,E. (2002). Neuropilin and its ligands in normal lung and cancer. Adv. Exp. Med. Biol. *515:103-14.*, 103-114.

Rohm,B., Rahim,B., Kleiber,B., Hovatta,I., and Puschel,A.W. (2000). The semaphorin 3A receptor may directly regulate the activity of small GTPases. FEBS Lett. *486*, 68-72.

Sahai,E. and Marshall,C.J. (2002). RHO-GTPases and cancer. Nat. Rev. Cancer *2*, 133-142.

Sakr,W.A., Haas,G.P., Cassin,B.F., Pontes,J.E., and Crissman,J.D. (1993). The frequency of carcinoma and intraepithelial neoplasia of the prostate in young male patients. J. Urol. *150*, 379-385.

Sasaki,Y., Cheng,C., Uchida,Y., Nakajima,O., Ohshima,T., Yagi,T., Taniguchi,M., Nakayama,T., Kishida,R., Kudo,Y., Ohno,S., Nakamura,F., and Goshima,Y. (2002). Fyn and Cdk5 mediate semaphorin-3A signaling, which is involved in regulation of dendrite orientation in cerebral cortex. Neuron *35*, 907-920.

Sekido,Y., Bader,S., Latif,F., Chen,J.Y., Duh,F.M., Wei,M.H., Albanesi,J.P., Lee,C.C., Lerman,M.I., and Minna,J.D. (1996). Human semaphorins A(V) and IV reside in the 3p21.3 small cell lung cancer deletion region and demonstrate distinct expression patterns. Proc. Natl. Acad. Sci. U. S. A *93*, 4120-4125.

Semaphorin Nomenclature Committee (1999). Unified nomenclature for the semaphorins/collapsins. Cell *97*, 551-552.

Sethi,T., Ginsberg,M.H., Downward,J., and Hughes,P.E. (1999). The small GTP-binding protein R-Ras can influence integrin activation by antagonizing a Ras/Raf-initiated integrin suppression pathway. Mol. Biol. Cell *10*, 1799-1809.

Shepherd,I., Luo,Y., Raper,J.A., and Chang,S. (1996). The distribution of collapsin-1 mRNA in the developing chick nervous system. Dev. Biol. *173*, 185-199.

Shi,W., Kumanogoh,A., Watanabe,C., Uchida,J., Wang,X., Yasui,T., Yukawa,K., Ikawa,M., Okabe,M., Parnes,J.R., Yoshida,K., and Kikutani,H. (2000). The class IV semaphorin CD100 plays nonredundant roles in the immune system: defective B and T cell activation in CD100-deficient mice. Immunity. *13*, 633-642.

Song,H., Ming,G., He,Z., Lehmann,M., McKerracher,L., Tessier-Lavigne,M., and Poo,M. (1998). Conversion of neuronal growth cone responses from repulsion to attraction by cyclic nucleotides. Science *281*, 1515-1518.

Spassky,N., de Castro,F., Le Bras,B., Heydon,K., Queraud-LeSaux,F., Bloch-Gallego,E., Chedotal,A., Zalc,B., and Thomas,J.L. (2002). Directional guidance of oligodendroglial migration by class 3 semaphorins and netrin-1. J. Neurosci. *22*, 5992-6004.

Steinberg,G.D., Carter,B.S., Beaty,T.H., Childs,B., and Walsh,P.C. (1990). Family history and the risk of prostate cancer. Prostate *17*, 337-347.

Steup,A., Ninnemann,O., Savaskan,N.E., Nitsch,R., Puschel,A.W., and Skutella,T. (1999). Semaphorin D acts as a repulsive factor for entorhinal and hippocampal neurons. Eur. J. Neurosci. *11*, 729-734.

Sugimoto,Y., Taniguchi,M., Yagi,T., Akagi,Y., Nojyo,Y., and Tamamaki,N. (2001). Guidance of glial precursor cell migration by secreted cues in the developing optic nerve. Development *128*, 3321-3330.

Swiercz,J.M., Kuner,R., Behrens,J., and Offermanns,S. (2002). Plexin-B1 directly interacts with PDZ-RhoGEF/LARG to regulate RhoA and growth cone morphology. Neuron *35*, 51-63.

Swiercz,J.M., Kuner,R., and Offermanns,S. (2004). Plexin-B1/RhoGEF-mediated RhoA activation involves the receptor tyrosine kinase ErbB-2. J. Cell Biol. *165*, 869-880.

Swiercz,J.M., Worzfeld,T., and Offermanns,S. (2007). ERBB-2 and met reciprocally regulate cellular signaling via plexin-B1. J. Biol. Chem. *%19;*..

Takagi,S., Tsuji,T., Amagai,T., Takamatsu,T., and Fujisawa,H. (1987). Specific cell surface labels in the visual centers of Xenopus laevis tadpole identified using monoclonal antibodies. Dev. Biol. *122*, 90-100.

Tamagnone,L., Artigiani,S., Chen,H., He,Z., Ming,G.I., Song,H., Chedotal,A., Winberg,M.L., Goodman,C.S., Poo,M., Tessier-Lavigne,M., and Comoglio,P.M. (1999). Plexins are a large family of receptors for transmembrane, secreted, and GPI-anchored semaphorins in vertebrates. Cell *99*, 71-80.

Tamamaki,N., Fujimori,K., Nojyo,Y., Kaneko,T., and Takauji,R. (2003). Evidence that Sema3A and Sema3F regulate the migration of GABAergic neurons in the developing neocortex. J. Comp Neurol. *455*, 238-248.

Taniguchi,M., Yuasa,S., Fujisawa,H., Naruse,I., Saga,S., Mishina,M., and Yagi,T. (1997). Disruption of semaphorin III/D gene causes severe abnormality in peripheral nerve projection. Neuron *19*, 519-530.

Tong,Y., Chugha,P., Hota,P.K., Alviani,R.S., Li,M., Tempel,W., Shen,L., Park,H.W., and Buck,M. (2007). Binding of Rac1, Rnd1 and RhoD to a novel Rho GTPase interaction motif destabilizes dimerization of the plexin-B1 Effector domain. J. Biol. Chem. ..

Tong,Y., Hota,P.K., Hamaneh,M.B., and Buck,M. (2008). Insights into oncogenic mutations of plexin-B1 based on the solution structure of the Rho GTPase binding domain. Structure. *16*, 246-258.

Torres-Vazquez,J., Gitler,A.D., Fraser,S.D., Berk,J.D., Van,N.P., Fishman,M.C., Childs,S., Epstein,J.A., and Weinstein,B.M. (2004). Semaphorin-plexin signaling guides patterning of the developing vasculature. Dev. Cell *7*, 117-123.

Toyofuku,T., Yabuki,M., Kamei,J., Kamei,M., Makino,N., Kumanogoh,A., and Hori,M. (2007). Semaphorin-4A, an activator for T-cell-mediated immunity, suppresses angiogenesis via Plexin-D1. EMBO J. *26*, 1373-1384.

Toyofuku,T., Zhang,H., Kumanogoh,A., Takegahara,N., Suto,F., Kamei,J., Aoki,K., Yabuki,M., Hori,M., Fujisawa,H., and Kikutani,H. (2004a). Dual roles of Sema6D in cardiac morphogenesis through region-specific association of its receptor, Plexin-A1,

with off-track and vascular endothelial growth factor receptor type 2. Genes Dev. *18*, 435-447.

Toyofuku,T., Zhang,H., Kumanogoh,A., Takegahara,N., Yabuki,M., Harada,K., Hori,M., and Kikutani,H. (2004b). Guidance of myocardial patterning in cardiac development by Sema6D reverse signalling. Nat. Cell Biol. *6*, 1204-1211.

Tsai,H.H. and Miller,R.H. (2002). Glial cell migration directed by axon guidance cues. Trends Neurosci. *25*, 173-175.

Turner,L.J. and Hall,A. (2006). Plexin-induced collapse assay in COS cells. Methods Enzymol. *406:665-76.*, 665-676.

Uzgare,A.R., Xu,Y., and Isaacs,J.T. (2004). In vitro culturing and characteristics of transit amplifying epithelial cells from human prostate tissue. J. Cell Biochem. *91*, 196-205.

van der,Z.B., Hellemons,A.J., Leenders,W.P., Burbach,J.P., Brunner,H.G., Padberg,G.W., and van Bokhoven,H. (2002). PLEXIN-D1, a novel plexin family member, is expressed in vascular endothelium and the central nervous system during mouse embryogenesis. Dev. Dyn. *225*, 336-343.

Varela-Echavarria,A., Tucker,A., Puschel,A.W., and Guthrie,S. (1997). Motor axon subpopulations respond differentially to the chemorepellents netrin-1 and semaphorin D. Neuron *18*, 193-207.

Vastrik,I., Eickholt,B.J., Walsh,F.S., Ridley,A., and Doherty,P. (1999). Sema3A-induced growth-cone collapse is mediated by Rac1 amino acids 17-32. Curr. Biol. *9*, 991-998.

Vikis,H.G., Li,W., and Guan,K.L. (2002). The plexin-B1/Rac interaction inhibits PAK activation and enhances Sema4D ligand binding. Genes Dev. *16*, 836-845.

Vikis,H.G., Li,W., He,Z., and Guan,K.L. (2000). The semaphorin receptor plexin-B1 specifically interacts with active Rac in a ligand-dependent manner. Proc. Natl. Acad. Sci. U. S. A *97*, 12457-12462.

Walzer,T., Galibert,L., Comeau,M.R., and De Smedt,T. (2005a). Plexin C1 engagement on mouse dendritic cells by viral semaphorin A39R induces actin cytoskeleton rearrangement and inhibits integrin-mediated adhesion and chemokine-induced migration. J. Immunol. *174*, 51-59.

Walzer,T., Galibert,L., and De Smedt,T. (2005b). Poxvirus semaphorin A39R inhibits phagocytosis by dendritic cells and neutrophils. Eur. J. Immunol. *35*, 391-398.

Wang,S., Gao,J., Lei,Q., Rozengurt,N., Pritchard,C., Jiao,J., Thomas,G.V., Li,G., Roy-Burman,P., Nelson,P.S., Liu,X., and Wu,H. (2003). Prostate-specific deletion of the murine Pten tumor suppressor gene leads to metastatic prostate cancer. Cancer Cell. *4*, 209-221.

Wang,X., Kumanogoh,A., Watanabe,C., Shi,W., Yoshida,K., and Kikutani,H. (2001). Functional soluble CD100/Sema4D released from activated lymphocytes: possible role in normal and pathologic immune responses. Blood *97*, 3498-3504.

Watanabe,C., Kumanogoh,A., Shi,W., Suzuki,K., Yamada,S., Okabe,M., Yoshida,K., and Kikutani,H. (2001). Enhanced immune responses in transgenic mice expressing a truncated form of the lymphocyte semaphorin CD100. J. Immunol. *167*, 4321-4328.

Wong,O.G., Nitkunan,T., Oinuma,I., Zhou,C., Blanc,V., Brown,R.S., Bott,S.R., Nariculam,J., Box,G., Munson,P., Constantinou,J., Feneley,M.R., Klocker,H., Eccles,S.A., Negishi,M., Freeman,A., Masters,J.R., and Williamson,M. (2007). Plexin-B1 mutations in prostate cancer. Proc. Natl. Acad. Sci. U. S. A. *104*, 19040-19045.

Worzfeld,T., Puschel,A.W., Offermanns,S., and Kuner,R. (2004). Plexin-B family members demonstrate non-redundant expression patterns in the developing mouse nervous system: an anatomical basis for morphogenetic effects of Sema4D during development. Eur. J. Neurosci. *19*, 2622-2632.

Xiang,R.H., Hensel,C.H., Garcia,D.K., Carlson,H.C., Kok,K., Daly,M.C., Kerbacher,K., van den,B.A., Veldhuis,P., Buys,C.H., and Naylor,S.L. (1996). Isolation of the human semaphorin III/F gene (SEMA3F) at chromosome 3p21, a region deleted in lung cancer. Genomics *32*, 39-48.

Yamada,T., Endo,R., Gotoh,M., and Hirohashi,S. (1997). Identification of semaphorin E as a non-MDR drug resistance gene of human cancers. Proc. Natl. Acad. Sci. U. S. A *94*, 14713-14718.

Yarden,Y. and Sliwkowski,M.X. (2001). Untangling the ErbB signalling network. Nat. Rev. Mol. Cell Biol. *2*, 127-137.

Zhang,Z., Vuori,K., Wang,H., Reed,J.C., and Ruoslahti,E. (1996). Integrin activation by R-ras. Cell *85*, 61-69.

Zhao,Z.S. and Manser,E. (2005). PAK and other Rho-associated kinases--effectors with surprisingly diverse mechanisms of regulation. Biochem. J. *386*, 201-214.

Publication

Wong,O.G., Nitkunan,T., Oinuma,I., Zhou,C., Blanc,V., Brown,R.S., Bott,S.R., Nariculam,J., Box,G., Munson,P., Constantinou,J., Feneley,M.R., Klocker,H., Eccles,S.A., Negishi,M., Freeman,A., Masters,J.R., and Williamson,M. (2007). Plexin-B1 mutations in prostate cancer. Proc. Natl. Acad. Sci. U. S. A. 104, 19040-19045.